

RPPR submitted to the US DOE NETL  
DE-FE0010799

**Small Molecular Associative Carbon Dioxide (CO<sub>2</sub>) Thickeners for Improved Mobility Control**

Final Research Performance Report

Start date: 1/1/13

End date: 9/30/17

Principal Author: Robert Enick PI  
Bayer Professor of Chemical and Petroleum Engineering  
(412)624-9649 or (412)277-0154

Dec. 31, 2017

DUNS Number DUNS: 00-451-4360

Department of Chemical and Petroleum Engineering  
940 Benedum Engineering Hall  
University of Pittsburgh, Pittsburgh PA 15261

A handwritten signature in black ink, appearing to read "Robert M. Enick", with a small, separate, handwritten "S" underneath.

## **DISCLAIMER**

This report was prepared as an account of work sponsored by an agency of the United States Government. Neither the United States Government nor any agency thereof, nor any of their employees, makes any warranty, express or implied, or assumes any legal liability or responsibility for the accuracy, completeness, or usefulness of any information, apparatus, product, or process disclosed, or represents that its use would not infringe privately owned rights. Reference herein to any specific commercial product, process, or service by trade name, trademark, manufacturer, or otherwise does not necessarily constitute or imply its endorsement, recommendation, or favoring by the United States Government or any agency thereof. The views and opinions of authors expressed herein do not necessarily state or reflect those of the United States Government or any agency thereof.

## Table of contents

Table of contents	3
List of figures	4
List of tables	8
List of acronyms and abbreviations	9
1. Executive summary	11
2. Accomplishments	14
3. Products	18
4. Participants and other collaborating organizations	19
5. Impact	21
6. Changes/problems	22
7. Special reporting requirements	23
8. Budgetary information	23
9. Training and professional development	23
10. Project results	30
10.1 ARPA-E-funded efforts to design a small molecule CO <sub>2</sub> thickener	31
10.2 High molecular weight polyfluoroacrylate (PFA) as a CO <sub>2</sub> -soluble thickener that does not require a co-solvent	35
10.3 Cores for the flow-through-porous-media studies	46
10.4 Core floods: Thickened CO <sub>2</sub> displacing CO <sub>2</sub>	47
10.5 Core floods: CO <sub>2</sub> or thickened CO <sub>2</sub> displacing crude oil	59
10.6 Core floods: CO <sub>2</sub> or thickened CO <sub>2</sub> displacing brine	63
10.7 Dual parallel core floods; Thickened CO <sub>2</sub> displacing brine for mobility control or conformance control	77
10.8 Improved wellbore integrity via sealing small cracks with CO <sub>2</sub> -soluble polymers that block water, oil and gas	96
11.0 References	110

## List of figures

### Chapter 10.1

Figure 10.1.1 Type 1 compound benzene tris[ {tris(trimethylsiloxy)silyl}propyl urea], designated as 2300-10. This small molecule was the most effective ARPA-e-funded small molecule thickener for CO<sub>2</sub>. Unfortunately this molecule required substantial amounts of organic co-solvents for dissolution in CO<sub>2</sub>. 31

Figure 10.1.2 Type 2 compound, a silicone-amide-anthraquinone compound, designated as 2008-90. This small molecule was the most effective Type 2 ARPA-e-funded small molecule thickener for CO<sub>2</sub>. Unfortunately this molecule required substantial amounts of organic co-solvents for dissolution in CO<sub>2</sub>. 32

Figure 10.1.3 Transparent rigid gel formed by adding 10wt% 2008-90 to hexane, gently heating, and cooling 32

Figure 10.1.4 Relative viscosity of solutions of (CO<sub>2</sub> + co-solvent + thickener) at ~22-25 °C, average shear rate = 9000 s<sup>-1</sup>/(relative viscosity). The best Type 1 thickener 2300-10 corresponds to the red triangle data; the best Type 2 thickener 2008-90 corresponds to the yellow diamonds. (The PDMS curves correspond to high molecular weight silicone oil data which was used for comparison with the small molecule data.) 33

### Chapter 10.2

Figure 10.2.1 Chemical structure, appearance and description of high molecular weight PFA 38

Figure 10.2.2 Pressure required at 24 °C to dissolve PFA in CO<sub>2</sub> as a function of PFA concentration for three batches of PFA. (The higher pressure data for one batch is likely due to an impurity in the sample.) 39

Figure 10.2.3 Relative Viscosity of CO<sub>2</sub> + PFA solutions at 0.5%, 1.0 and 5.0wt% concentrations of PFA in CO<sub>2</sub> at 25°C and 5000 psi. No co-solvent was required. 41

Figure 10.2.4 The ability of PFA to increase the viscosity of CO<sub>2</sub> at 24 °C. Falling ball viscometry results. The average shear rate on the falling ball is in the 1000 – 10000 s<sup>-1</sup> range. 42

Figure 10.2.5 Falling cylinder viscometry results for single-phase solutions of 1wt% PFA in CO<sub>2</sub> at 25 °C and 3000 psi, PFA batch PD1C. Each data point corresponds to a different aluminum cylinder. 43

### Chapter 10.4

Figure 10.4.1 Pressure drop as a function of time for the displacement of pure CO<sub>2</sub> from a 125 mD Berea core by a solution of 1wt% PFA in CO<sub>2</sub> at the same T and P. The initial increase in viscosity was commensurate with that expected from thickening, however the subsequent increase in pressure drop was attributed to PFA adsorption. 47

Figure 10.4.2 Pressure drop as a function of time for the displacement of pure CO<sub>2</sub> from a 285 mD Berea core by a solution of 1wt% PFA in CO<sub>2</sub> at the same T and P. The initial increase in viscosity was commensurate with that expected from thickening, however the subsequent increase in pressure drop was attributed to PFA adsorption. 48

Figure 10.4.3 Configuration of the core flooding apparatuses used at SCAL 49

Figure 10.4.4 Baseline of pure CO<sub>2</sub> flow through the core (green data) followed by displacement of CO<sub>2</sub> from Berea sandstone core by a 1wt% solution of PFA (batch PD1c-B) in CO<sub>2</sub> (red data) Test conducted at effluent pressure (BP) of 3000 psi and 24 °C. BP controlled by a BPR set at 3000 psi. Although the test ended early due to BPR problems, the accumulation of PFA within the BPR provided direct evidence that a portion of the PFA remained in solution as it passed through the core. 50

Figure 10.4.5 Baseline of pure CO<sub>2</sub> flow through the core (green data) followed by displacement of CO<sub>2</sub> from Berea sandstone core by a 1wt% solution of PFA (batch PD1c-B) in CO<sub>2</sub> (red data), followed by a chaser of pure CO<sub>2</sub> (green data), followed by a chaser of CO<sub>2</sub> at a 10-times higher flow rate (purple data); followed by a chaser of pure CO<sub>2</sub> (green data); followed by reverse flow of CO<sub>2</sub> through the core at 10-times higher flow rate (gold data); followed by flow of pure CO<sub>2</sub> through the core in the original direction and at the original flow rate (blue data). Test conducted at effluent pressure (BP) of 3000 psi and 24 °C. BP controlled by a PD pump set at 3000 psi. 52

Figure 10.4.6. Proposed model of the fate of the PFA that enters the core. The PFA either (a) remains dissolved in CO<sub>2</sub>, (b) deposits reversibly between grains, or (c) adsorbs irreversibly onto the rock surface 53

Figure 10.4.7 Data for first 4 PVI lost (1 PV of CO<sub>2</sub> followed by 3 PVI thickened CO<sub>2</sub>). Subsequent CO<sub>2</sub> flow through the core (green data) followed by a 20 minute rest, followed by displacement of CO<sub>2</sub> from Berea sandstone core by a 1wt% solution of PFA (mix of two batches PD1c-A and PD1-cB) in CO<sub>2</sub> (red and black data). Test conducted at effluent pressure (BP) of 3000 psi and 24 °C. BP controlled by a PD pump set at 3000 psi. Lower pressure drops measured with a pressure transducer, higher pressure drops measured with pressure different of two gages. 54

Figure 10.4.8 Baseline pure CO<sub>2</sub> through the core (green data), followed by displacement of CO<sub>2</sub> from Berea sandstone core by a 1wt% solution of PFA (mix of two batches PD1c-A and PD1-cB) in CO<sub>2</sub> (red and black data), followed by the injection of pure CO<sub>2</sub> (purple). Test conducted at effluent pressure (BP) of 3000 psi and 24 °C. BP controlled by a PD pump set at 3000 psi. Test stopped at 5 PVI when the pressure difference between the inlet CO<sub>2</sub> (4500 psi) and the overburden fluid around the sleeve (5000 psi) reached the 500 psi minimum. 55

Figure 10.4.9 Changes in the wettability of the inlet and outlet faces of the core due to the adsorption of PFA from a PFA-CO<sub>2</sub> solution. 56

Figure 10.4.10 Summary of contact angle changes and permeability reductions cause by PFA-CO<sub>2</sub> solutions on each half of the core 57

## Chapter 10.5

Figure 10.5.1 Recovery of dead SACROC oil from a Berea SS core by CO<sub>2</sub> at 25 °C and 3000 psi. About 79% of the oil is ultimately recovered. 59

Figure 10.5.2 Pressure drop vs PVI CO<sub>2</sub> for the same test; recovery of dead SACROC oil from a Berea SS core by CO<sub>2</sub> at 25 °C and 3000 psi. About 79% of the oil is ultimately recovered. The spike in pressure drop occurs just after CO<sub>2</sub> breakthrough. 60

Figure 10.5.3 Recovery of dead SACROC oil from a Berea SS core by thickened CO<sub>2</sub> at 25 °C and 3000 psi. About 95% of the oil is ultimately recovered. 61

Figure 10.5.4 Pressure drop v. thickened PVI CO<sub>2</sub> for the same test; recovery of dead SACROC oil

from a Berea SS core by CO<sub>2</sub> at 25 oC and 3000 psi. About 95% of the oil is ultimately recovered. 62

## Chapter 10.6

Figure 10.6.1. CO<sub>2</sub>-displacing-brine water production results for the 7 cores 64

Figure 10.6.2. Procedure for tests involving CO<sub>2</sub> (or thickened CO<sub>2</sub>) displacing brine from a brine-saturated core 65

Figure 10.6.3. Equipment configuration for tests involving CO<sub>2</sub> (or thickened CO<sub>2</sub>) displacing brine from a brine-saturated core 66

Figure 10.6.4. Pressure drop and water production vs. PVI CO<sub>2</sub> for CO<sub>2</sub> displacing brine from a 90 mD Berea sandstone core 67

Figure 10.6.5. Pressure drop and water production vs. PVI CO<sub>2</sub> for CO<sub>2</sub> and PFA-CO<sub>2</sub> displacing brine from an 89 mD Berea sandstone core 68

Figure 10.6.6. Pressure drop and water production vs. PVI CO<sub>2</sub> for CO<sub>2</sub> displacing brine from an 8.4 mD Carbon Tan sandstone core 69

Figure 10.6.7. Pressure drop and water production vs. PVI CO<sub>2</sub> for CO<sub>2</sub> and PFA-CO<sub>2</sub> displacing brine from a 20.1 mD Carbon Tan sandstone core 70

Figure 10.6.8. Pressure drop and water production vs. PVI CO<sub>2</sub> for CO<sub>2</sub> displacing brine from a 64 mD Indiana limestone core 71

Figure 10.6.9. Pressure drop and water production vs. PVI CO<sub>2</sub> for CO<sub>2</sub> and PFA-CO<sub>2</sub> displacing brine from a 32 mD Indiana limestone core(70 mD is a nominal value from Kocurek, our data indicated 32 mD) 72

Figure 10.6.10. Pressure drop and water production vs. PVI CO<sub>2</sub> for CO<sub>2</sub> displacing brine from a 3.5 mD Edwards Yellow limestone core 74

Figure 10.6.11. Pressure drop and water production vs. PVI CO<sub>2</sub> for CO<sub>2</sub> and PFA-CO<sub>2</sub> displacing brine from a 3.9 mD Edwards yellow limestone core 75

## Chapter 10.7

Figure 10.7.1. Configuration of dual cores and test strategy for mobility control or conformance control 77

Figure 10.7.2. Mobility control results for the displacement of brine by CO<sub>2</sub> in dual parallel sandstone cores; CO<sub>2</sub> is injected into both cores simultaneously through this experiment 78

Figure 10.7.3. Pressure drop for mobility control test for the displacement of brine by CO<sub>2</sub> in dual parallel sandstone cores; CO<sub>2</sub> is injected into both cores simultaneously through this experiment 79

Figure 10.7.4. Mobility control results for the displacement of brine by thickened CO<sub>2</sub> in dual parallel

sandstone cores; thickened CO <sub>2</sub> is injected into both cores simultaneously through this experiment	80
Figure 10.7.5. Pressure drop for mobility control test for the displacement of brine by thickened CO <sub>2</sub> in dual parallel sandstone cores; thickened CO <sub>2</sub> is injected into both cores simultaneously through this experiment	81
Figure 10.7.6. Mobility control results for the displacement of brine by CO <sub>2</sub> in dual parallel limestone cores; CO <sub>2</sub> is injected into both cores simultaneously through this experiment	82
Figure 10.7.7. Pressure drop for mobility control test for the displacement of brine by CO <sub>2</sub> in dual parallel limestone cores; CO <sub>2</sub> is injected into both cores simultaneously through this experiment	83
Figure 10.7.8. Mobility control results for the displacement of brine by thickened CO <sub>2</sub> in dual parallel limestone cores; CO <sub>2</sub> is injected into both cores simultaneously through this experiment	84
Figure 10.7.9. Pressure drop for mobility control test for the displacement of brine by CO <sub>2</sub> in dual parallel limestone cores; CO <sub>2</sub> is injected into both cores simultaneously through this experiment	85
Figure 10.7.10. Mobility control results for the displacement of brine by thickened CO <sub>2</sub> in dual parallel sandstone cores; the high perm core was isolated and flooded with pure CO <sub>2</sub> , then CO <sub>2</sub> was injected into both cores simultaneously through this experiment	86
Figure 10.7.11. Pressure drop results for the displacement of brine by thickened CO <sub>2</sub> in dual parallel sandstone cores; the high perm core was isolated and flooded with pure CO <sub>2</sub> , then CO <sub>2</sub> was injected into both cores simultaneously through this experiment	87
Figure 10.7.12. Mobility control results for the displacement of brine by thickened CO <sub>2</sub> in dual parallel sandstone cores; the high perm core was isolated and flooded with pure CO <sub>2</sub> , then thickened CO <sub>2</sub> was injected into both cores simultaneously through this experiment	88
Figure 10.7.13. Pressure drop results for the displacement of brine by thickened CO <sub>2</sub> in dual parallel sandstone cores; the high perm core was isolated and flooded with pure CO <sub>2</sub> , then thickened CO <sub>2</sub> was injected into both cores simultaneously through this experiment	89
Figure 10.7.14. Conformance control results for dual parallel brine-saturated sandstone cores; the high perm core was isolated and flooded with thickened CO <sub>2</sub> , then pure CO <sub>2</sub> was injected into both cores simultaneously	91
Figure 10.7.15. Pressure drop results for the dual parallel sandstone core conformance control test. The high perm core was isolated and flooded with thickened CO <sub>2</sub> , then pure CO <sub>2</sub> was injected into both cores simultaneously.	92
Figure 10.7.16. Conformance control results for dual parallel brine-saturated limestone cores; the high perm core was isolated and flooded with pure CO <sub>2</sub> , then both cores were flooded with pure CO <sub>2</sub> , then only the isolated high perm core was flooded with thickened CO <sub>2</sub> (PFA in CO <sub>2</sub> ), and then both parallel cores were flooded with CO <sub>2</sub>	94
Figure 10.7.17. Pressure drop results for dual parallel brine-saturated limestone cores; the high perm core was isolated and flooded with pure CO <sub>2</sub> , then both cores were flooded with CO <sub>2</sub> , then only the isolated high perm core was flooded with thickened CO <sub>2</sub> (PFA in CO <sub>2</sub> ), and then both cores were flooded with CO <sub>2</sub>	95

## Chapter 10.8

Figure 10.8.1 Cement defects that can lead to wellbore integrity failures (after After Carey et al. 2010)	99
Figure 10.8.2 Unique role for new sealant for cracks	100
Figure 10.8.3. The PFA polymer structure, appearance, and properties	102
Figure 10.8.4. Experimental apparatus used to conduct crack-sealing proof-of-concept experiments	103
Figure 10.8.5. Flow rate vs time data for the injection of the CO <sub>2</sub> +PFA solution into the 81 nanoDarcy crack at a constant pressure drop of 1500 psi (outlet P maintained at 1500 psia)	104
Figure 10.8.6. Appearance of the (81 nanoDarcy cracked cement after the test before (left) and after being pried apart	105
Figure 10.8.7. Flow rate vs time data for the injection of the CO <sub>2</sub> +PFA solution into the 89 microDarcy crack at a constant flow rate of 0.25 ml/min (outlet P maintained at 1500 psia)	106
Figure 10.8.8. Appearance of the (89 microDarcy) cracked cement after the test before (left) and after being pried apart	106
Figure 10.8.9. Conceptual diagram for application of the CO <sub>2</sub> +PFA solution to seal cracks or reduce permeability of porous media for conformance control	107

## List of tables

### Chapter 2

Table 2.1 Breakdown of (a) set up time, (b) flood duration, (c) material cost, (d) labor costs per test for single core tests	16
---	----

### Chapter 10

Table 10.1.1 Effect of amount of toluene (co-solvent) needed for dissolution of 1wt% PDMS; effect of toluene concentration on the cloud point pressure (pressure required to attain a single phase)	33
Table 10.2.1 The composition of CO <sub>2</sub> -rich fluids used to simulate the CO <sub>2</sub> -rich solvent that develops during EOR	45
Table 10.3.1 Properties of the cores used at SCAL for the CO <sub>2</sub> -dispalcing-CO <sub>2</sub> , CO <sub>2</sub> -displacing-oil, and CO <sub>2</sub> -displacing brine core tests	46
Table 10.4.1 Changes if the permeability and contact angle of half cores obtained after CO <sub>2</sub> -thickened CO <sub>2</sub> -CO <sub>2</sub> displacement experiments were conducted and the 1.5" x 12" core was vented and then cut in half	57
Table 10.7.1 properties of the dual sandstone cores used in dual parallel core conformance control studies	77

## **List of acronyms and abbreviations**

AIBN	azobisisobutyronitrile
ARPA-E	Advanced Research Projects Agency-Energy
BP	back pressure
BPR	back pressure regulator
C	concentration of PFA in CO <sub>2</sub> , wt%
CO <sub>2</sub>	carbon dioxide
CO <sub>2</sub> -PFA	carbon dioxide-PFA solution
CSTM	continuous stirred tank mixer
EOR	enhanced oil recovery
EPA	Environmental Protection Agency
g	gram
HFE	hydrofluoroether
IOR	improved oil recovery
LS	limestone
mD	millidarcy
ml	milliliter
MMP	minimum miscibility pressure
MS	Master of Science
MW	molecular weight
NETL	National Energy Technology Laboratory
P	pressure
PDMS	polydimethyl siloxane
PD	positive dispalcment
PD1x-x	designation of the batch of PFA, x is a number and/or letter

PFA	polyfluoroacrylate, a type of CO <sub>2</sub> -soluble polymer
PFA'	designation of a particular batch of PFA
PFOA	perfluorooctanoic acid
PFHXA	perfluorohexanoic acid
PhD	doctor of philosophy
Pitt	University of Pittsburgh
PM	project manager
PMP	project management plan
psi	pounds force per square inch
PV	pore volumes
PVI	pore volumes injected
SACROC	Scurry Area Canyon Reef Operators Committee
SCAL	Special Core Analysis Laboratories, Inc.
SPE	Society of Petroleum Engineers
SS	sandstone
T	temperature
TX	Texas
V <sub>CO<sub>2</sub>,ml</sub>	volume of pure CO <sub>2</sub> introduced to the CO <sub>2</sub> -PFA mixing vessel, ml
wt%	weight percent, typically of PFA in CO <sub>2</sub>
ΔP	pressure drop

## **1. EXECUTIVE SUMMARY**

The objective of this project was to promote the application of a CO<sub>2</sub> thickener for CO<sub>2</sub> EOR in the lab using solubility tests, viscosity tests, and core floods. It was hoped that these test results would encourage our industrial contacts (Kinder Morgan, Denbury Resources, Conoco Phillips, Tabula Rasa) to test the thickener in a single injection well mobility control pilot test. Ultimately, it was demonstrated that the CO<sub>2</sub>-soluble polymeric thickeners that were originally intended for mobility control are much better suited for use as CO<sub>2</sub>-soluble conformance control agents for blocking the flow of CO<sub>2</sub> and water into thief zones.

During Phase 1 - the initial phase of this project - various CO<sub>2</sub> EOR operators were contacted by email, phone, and during in-person meetings. Written commitments for field samples (cleaned cores, oil, brine) and details of reservoir conditions were received from these four companies. We had established relationships, especially with Kinder Morgan and Denbury Resources, which would have facilitated field trials if the thickener was successfully developed.

Dr. Enick asked for a one-year no-cost extension on Phase 1 of this project that allowed the University of Pittsburgh (Pitt) to continue developing the best thickener to the fullest extent under ARPA-e funding prior to conducting the Phase 2 core testing associated with this NETL award. The design, synthesis and purification of CO<sub>2</sub> thickeners and initial assessments of their CO<sub>2</sub> solubility and ability to thicken CO<sub>2</sub> were conducted until April 30, 2016 under separate ARPA-e funding.

Phase 2 of this NETL award began on Jan. 1, 2016 and extended to Sept. 30 2017. The ARPA-E-sponsored thickeners were designed to be small associating molecules that aggregate in solution to induce large increases in viscosity at low concentration. Pitt generated several effective small molecule CO<sub>2</sub> thickeners with ARPA-e funding. Unfortunately, none of these small molecule thickeners could dissolve in CO<sub>2</sub> without the addition of unacceptably large amounts of hexane or toluene as a co-solvent (e.g. 20wt% hexane, 80wt% CO<sub>2</sub>). Therefore none of the ARPA-E-funded *small molecule* CO<sub>2</sub> thickeners were viable candidates for Phase 2 of this NETL award.

Therefore during Phase 2 of this NETL award, extensive core testing was conducted using the most promising *polymeric* CO<sub>2</sub> thickener. (This polymer was used as a “control”, or standard against which the small molecules in the ARPA-E study were compared.) One PhD graduate student verified CO<sub>2</sub> solubility with a phase behavior cell and the thickening potential of all polymer samples with a falling ball viscometer and a falling cylinder viscometer at Pitt. He also planned thickener concentrations and compositions at Pitt for the core tests that were conducted at Special Core Analysis Laboratories, Inc., (SCAL) in Midland, TX. A MS graduate student interpreted the core flooding results. During the first seven months of Phase 2, a postdoctoral chemistry student generated several fluoroacrylate homopolymers (PFA) via bulk polymerization

(mixing monomer and initiator, heating, and then separating the polymer from small amounts of un-reacted monomer). In order to produce an environmentally benign polymer, the monomer used to make the new polymers used in this study was a fluoroacrylate that contains only six fluorinated carbons.

Two different viscometers were used to determine the increase in CO<sub>2</sub> viscosity that could be achieved via the dissolution of PFA. Praxair, which has an interest in thickening CO<sub>2</sub> for pilot EOR projects and for waterless hydraulic fracturing, agreed to measure the viscosity of CO<sub>2</sub>-PFA solutions at no cost to the project. Falling cylinder viscometry was conducted at Pitt in our windowed high pressure phase behavior cell. Both apparatuses indicated that at very low shear rates the CO<sub>2</sub> viscosity increased by a factor of roughly 3.5 when 1wt% PFA was dissolved in the CO<sub>2</sub>.

The ability for PFA to reduce CO<sub>2</sub> mobility in a core was then tested at SCAL. During the beginning of these tests, the PFA polymer was then shown to impart reasonable improvements in mobility control during the SCAL core tests; as the CO<sub>2</sub>-PFA solution displaced CO<sub>2</sub> from the core at a constant volumetric flow rate, the pressure drop increased as expected. However, as the test progressed, there was clear and surprising evidence of dramatic reductions in core permeability due to PFA adsorption, especially for sandstones. For example, as the CO<sub>2</sub>-PFA solution displaced pure CO<sub>2</sub> from sandstone and limestone cores, the pressure drop increased by factors of multiple hundreds to over a thousand. It was subsequently demonstrated that the PFA injected into the core either (a) adsorbed strongly and irreversibly onto the rock surfaces, (b) deposited/precipitated within the rock, thereby blocking pores in a manner that could be dislodged by large changes in flow rate or flow direction, or (c) remained in solution and passed completely through the core. The loss of PFA to the porous media and the unacceptably large increases in pressure drop both indicated that PFA was inappropriate for CO<sub>2</sub> EOR mobility control, where thickener adsorption must be minimized and mobility reductions of only 10-100-fold are typically required.

However, we realized that because the CO<sub>2</sub>-PFA solution could greatly reduce the permeability of porous media, it could serve as a near wellbore conformance control agent for blocking “thief zones”, where adsorption is acceptable and dramatic increases in pressure drop are desirable. These effects were more dramatic for sandstone than for limestone. Therefore, these PFA fluoroacrylate polymers can serve as a CO<sub>2</sub>-soluble conformance control agent for CO<sub>2</sub>-EOR, especially in sandstone formations. This injection of a single phase solution of CO<sub>2</sub>-PFA for permeability reduction is (to the best of our knowledge) the first report of a CO<sub>2</sub>-soluble conformance control additive. We also demonstrated that the optimal strategy for using CO<sub>2</sub>-PFA solutions for conformance control is analogous to the application of water-based polymeric gels; the CO<sub>2</sub>-PFA solution should first be injected only in an isolated thief zone to induce

dramatic reductions in permeability only in that thief zone, and then CO<sub>2</sub> should be injected into all of the zones.

Finally, it was noted that given the propensity of PFA to adsorb onto sandstone, the adsorption of PFA from CO<sub>2</sub>-PFA solutions onto cement surfaces may be capable of sealing cracks in casing cement that other remediation fluids (wet cement, solids-free resin, viscous aqueous emulsions) may have trouble accessing. Therefore, at the end of the project we reported on two proof-of-concept experiments for sealing cracked cement samples; the cracked samples had permeability of 81 nanoDarcies and 89 microDarcies. The results indicated that these small cracks could be completely sealed as CO<sub>2</sub>-PFA solutions flowed through them due to the adsorption of amorphous, sticky, elastic, water-repellant, oil-repellant PFA polymer.

The researchers involved in the project intend to present the results of this study at the SPE IOR conference in Tulsa, OK in April 2018, as an SPE paper that encapsulates all of the research from this project (Enick, R., Beckman, E., Cummings, S., Lee, J., Zaberi, H., Vasilache, M., Dailey, C., Fluoroacrylate Polymers as CO<sub>2</sub>-soluble Conformance Control Agents, SPE IOR Conference, Tulsa, OK April 2018, non-peer-reviewed conference proceeding SPE-190176-MS). The researchers will submit this paper for publication after the conference.

## **2. ACCOMPLISHMENTS**

### **Major goals:**

The major goal of this project was to establish a relationship with several CO<sub>2</sub> EOR operators that will enable them to provide researchers with core and fluid samples from the field and operating conditions, which would then allow for the rapid and effective assessment of a CO<sub>2</sub> thickener in lab-scale tests. This, in turn, would provide enough information to give the operators confidence to conduct a pilot test of the thickener in the field. Therefore, we intended to foster these relationships and to employ field data and fluid and rock samples from patterns in which CO<sub>2</sub> mobility control with a CO<sub>2</sub> thickener would be attractive to these operators. The companies include Denbury, Kinder Morgan, Tabula Rasa and ConocoPhillips. Letters of commitments for field samples and operating conditions were obtained from these four companies. Dr. Enick also had the opportunity to help in the design of, and observe the operation of a CO<sub>2</sub>-additive (unrelated to thickening) injection apparatus and mixing system with Denbury Resources. This system is well suited for the introduction of a CO<sub>2</sub>-soluble compound (such as a thickener or conformance control agent) into the CO<sub>2</sub> injection pipe.

As the project proceeded, however, it became evident that because the high molecular weight polyfluoroacrylate (PFA) polymer behaved quite differently than we expected. Therefore, the researchers abandoned the idea of quickly migrating to the use of field cores for mobility control testing and decided to use clean, standard, commercially available outcrop cores in order to better understand conformance control aspects of the polymer. The only reservoir fluid used in this study was dead SACROC crude oil provided by Kinder Morgan.

In the end, Pitt successfully developed the first known CO<sub>2</sub>-soluble conformance control agent, a high molecular weight polyfluoroacrylate (PFA), and also established the best strategy for its application. In a manner that is analogous to the application of water-based gels, the CO<sub>2</sub>-PFA polymer solution should be injected solely into the isolated thief zone. Thereafter, CO<sub>2</sub> can be injected into all of the parallel zones (including the treated thief zone), and a substantial degree of diversion of CO<sub>2</sub> flow from the thief zone should occur.

Pitt has also demonstrated in a proof-of-concept study on an unrelated topic that the (CO<sub>2</sub> + PFA) solutions may have potential for improving wellbore integrity via sealing small cracks in cement with PFA due to the tendency for this elastic, sticky, water-repellant, oil-repellant polymer to adsorb onto cement surfaces.

## **Accomplishments under these goals**

### **Task 1 – Project Management, Planning, and Reporting**

The Project Management Plan (PMP) was provided to NETL.

### **Task 2 – Letters of commitment, Field Site Data and Samples**

Pitt received four letters of commitment for cores, brine, oil and typical field conditions from four CO<sub>2</sub> EOR operators; Denbury, Kinder Morgan, Tabula Rasa and ConocoPhillips. Because we quickly realized that the PFA was not behaving as a mobility control agent, we decided to only use commercially available “standard” outcrop cores (rather than field cores) in order to better understand the behavior of the PFA.

Therefore, researchers conducted all of the Phase 2 core tests with 1.5” x 12” low clay sandstone and carbonate standard cores from Kocurek Industries that supply various types of carbonate and sandstone cores (<http://www.kocurekindustries.com/carbonates-cores>).

### **Task 3 – Approaches for Phase 2 Laboratory Testing of Thickened CO<sub>2</sub>**

We submitted our lab testing plan, to David D’Souza of Denbury Resources, Lanny Schoeling of Kinder Morgan, and Mihai Vasilache of SCAL. Their suggestions for improving the plan were incorporated into the document

During Phase 2 we explored the use of the polyfluoroacrylate homopolymer (PFA) as a conformance control agent.

The tests involved CO<sub>2</sub> or thickened CO<sub>2</sub> displacing

- (a) CO<sub>2</sub> from CO<sub>2</sub>-saturated cores,
- (b) brine from brine-saturated cores, or
- (c) crude oil from crude oil-saturated cores.

All core tests were conducted at room temperature and an outlet pore pressure of about 3000 psi. Pressure drop across the core was measured. 12” long, 1.5” diameter outcrop sandstone or carbonate cores from Kocurek were used. Several tests were done with two cores in parallel; a high per core (representing the thief zone) and a low perm core. No field cores were used.

### **Task 3 – Details of SCAL core testing**

The SCAL “menu” of core experiment costs was:

Sample cutting: \$60/sample (drill, trim and polish the core faces)

Extraction: \$60 to \$350 based on procedure

Porosity and permeability at ambient and reservoir confining pressure: \$ 115/sample

Wettability restoration for about 4 weeks: \$ 805/sample.

Laboratory time: \$ 200/hr.

Sample screening using a liquid permeability test: \$ 390/sample

### Single cores

\$1150: control: high pressure CO<sub>2</sub> at a constant flow rate/velocity (no other fluids in core)

\$1450: repeat control test but with thickener dissolved in CO<sub>2</sub>

\$1450: initially saturate the core with brine; flow in CO<sub>2</sub> at a constant flow rate

\$1725: initially saturate the core with brine; flow in thickened CO<sub>2</sub> at a constant flow rate

\$7825: EOR core flood: waterflood, oil-flood, waterflood, CO<sub>2</sub> flood (Water alternating gas (WAG) or continuous)

\$8050: EOR core flood thickened CO<sub>2</sub>: waterflood, oil-flood, waterflood, thickened CO<sub>2</sub> flood (WAG or continuous)

**Dual parallel cores** (individual brine and water production rates from each core can be monitored, but not individual gas production rates)

\$ 4350: initially saturate the core with brine; flow in CO<sub>2</sub> at a constant flow rate

\$ 2175: initially saturate the core with brine; flow in thickened CO<sub>2</sub> at a constant flow rate

\$23475: EOR core flood: waterflood, oil-flood, waterflood, CO<sub>2</sub> flood (WAG or continuous)

\$24150: EOR core flood thickened CO<sub>2</sub>: waterflood, oil-flood, waterflood, thickened CO<sub>2</sub> flood (WAG or continuous)

**Table 2.1 Breakdown of (a) set up time, (b) flood duration, (c) material cost, (d) labor costs per test for single core tests**

Test	Setup and tear-down time (days)	Flood duration (days)	Material cost	Labor cost	Total cost/test
A. Control: CO <sub>2</sub> in core	0.25	0.25	300	850	1150
B. Thickened CO <sub>2</sub> in core	0.33	0.33	300	1150	1450
C. CO <sub>2</sub> into brine saturated core	0.33	0.33	300	1150	1450
D. Thickened CO <sub>2</sub> into brine saturated core	0.25	0.83	300	1450	1725
E. EOR core flood with CO <sub>2</sub>	2	2	800	7000	7825
F. EOR core flood with thickened CO <sub>2</sub>	2	2	1150	6900	8050

Note: Dual core tests cost 3 times as much as their analogous single core tests

The SCAL subcontract was \$160,000.

## Task 4 – Technical Status of APRA-E Research

**Small Molecules** - Our team concluded the ARPA-e portion of this project. Results were detailed in our earlier quarterlies and are summarized in the following chapter.

Simply put, none of the small associating molecule CO<sub>2</sub> thickeners could dissolve in CO<sub>2</sub> without the addition of very large amounts of co-solvent. Therefore, we did not use the ARPA-e small molecules in Phase 2. We used the only known high molecular polymer that can dissolve in CO<sub>2</sub> at typical EOR conditions without a co-solvent, polyfluoroacrylate (PFA).

### **3. PRODUCTS**

To date our “products” are tech transfer papers and presentations.

We have also perfected a synthesis of the PFA polymer, which is reported in the last quarterly.

We will probably be submitting a patent disclosure on the ability of CO<sub>2</sub>-PFA solutions to seal cracks in cement. We will keep NETL apprised of our progress even though this disclosure will not be submitted until after the project ends.

#### **4. PARTICIPANTS & OTHER COLLABORATING ORGANIZATIONS**

Dr. Eric Beckman and Dr. Enick were supported by this NETL project.

Graduate students (funded by NETL, this award) included:

Stephen Cummings (foreign student from Great Britain, post doc at Pitt, now a permanent resident. Steve now works for Covestro in Pittsburgh.

Jason Lee (PhD student at Pitt; Jason graduated in Dec 2016), no longer supported as of 1-1-17. Jason has started a small company.

There was a “no cost” MS student who was not supported by this project, Husain Zaberi, who assisted in the interpretation of the core flooding results. He graduated in Dec. 2016 with a MS after defending his thesis.

Informal collaborations were made with engineers at Denbury, Kinder Morgan, ConocoPhillips, and Tabula Rasa.

Collaborations with SCAL (core flooding) were effective. We interacted directly and frequently with Mihae Vasilache.

## Phase 2

Name:	Robert Enick
Project Role:	PI
Nearest person month worked:	~3
Contribution to Project:	Leading the project, contacting companies..
Funding Support:	NETL (this award)
Collaborated with individual in foreign country:	No
Country(ies) of foreign collaborator:	No
Travelled to foreign country:	No
If traveled to foreign country(ies), duration of stay:	3 days
Name:	Eric Beckman
Project Role:	PI
Nearest person month worked:	1
Contribution to Project:	Thickener development and strategies for introducing thickeners into CO <sub>2</sub> for lab- and field-tests.
Funding Support:	NETL (this award)
Collaborated with individual in foreign country:	No
Country(ies) of foreign collaborator:	No
Travelled to foreign country:	No
If traveled to foreign country(ies), duration of stay:	N/A
Name:	Jason Lee
Project Role:	PhD
Nearest person month worked:	12
Contribution to Project:	Thickener synthesis and testing
Funding Support:	NETL (this award; <u>graduated in Dec 2016</u> )
Collaborated with individual in foreign country:	No
Country(ies) of foreign collaborator:	No
Travelled to foreign country:	No
If traveled to foreign country(ies), duration of stay:	N/A
Name:	Steve Cummings ( <u>green card holder employed by Covestro</u> )
Project Role:	Post-doc
Nearest person month worked:	7
Contribution to Project:	Thickener synthesis and testing
Funding Support:	NETL (this award; but no longer supported)
Collaborated with individual in foreign country:	No
Country(ies) of foreign collaborator:	No
Travelled to foreign country:	No
If traveled to foreign country(ies), duration of stay:	N/A

## **5. IMPACT**

We believe that this work, along with the PI's recent NETL-sponsored review of mobility control, has helped to re-invigorate industry interest in CO<sub>2</sub> mobility and conformance control. The intended impact of this work was related to the improved rate of oil recovery and increased amount of recoverable oil should a thickener for improved mobility control be designed. However, it has been demonstrated that the PFA polymer may be better suited for conformance control. In fact, PFA appears to be the first CO<sub>2</sub>-soluble conformance control agent ever identified.

This project and the associated ARPA-e project did *not* result in the design of an affordable small molecule CO<sub>2</sub> thickener. However, two environmentally benign C<sub>6</sub>F<sub>13</sub>-based fluoroacrylate-based CO<sub>2</sub>-soluble high molecular weight polymers were identified; a homopolymer fluoroacrylate (PFA) and a fluoroacrylate-styrene co-polymer (polyFAST). Unlike the previously studied polyFAST, which was based on an environmentally persistent and bio-accumulative C<sub>8</sub>F<sub>17</sub> functionality, the two C<sub>6</sub>F<sub>13</sub>-based polymers used in this study would be acceptable for oilfield use.

In an unexpected turn of events, the PFA adsorption onto rock surfaces resulted in dramatic reductions in permeability. Therefore this project (which was originally aimed at developing CO<sub>2</sub>-soluble mobility control additives) may provide a starting point for the use of PFA as a CO<sub>2</sub>-soluble conformance control agents. This conformance control application would require much smaller amounts of the expensive PFA polymer than in-depth mobility control. Therefore, this PFA polymer may have far more impact as a conformance control agent than it would as a mobility control agent.

A few proof-of-concept experiments conducted during this study have indicated that it may be possible to improve wellbore integrity by sealing small cracks in casing cement with high pressure solutions of PFA dissolved in CO<sub>2</sub>.

This project combines basic research, chemistry, chemical engineering, and petroleum engineering, and is an excellent example of how a team consisting of chemists, chemical engineers and petroleum engineers can address energy-related problems.

## **6. CHANGES/PROBLEMS**

This project was initiated on September 25, 2012. The agreement, as originally awarded, had two one-year budget periods. When this project was awarded, Dr. Enick (PI) had also been awarded a complementary project from ARPA-e to research the design, synthesis, purification and initial assessments of CO<sub>2</sub> solubility and (for compounds that dissolve in CO<sub>2</sub>) viscosity enhancement. As research under the ARPA-e project was nearing completion at the end of 2015, a formal request was made to change the start date of BP 2 from April 1, 2016 to January 1, 2016. In addition, Pitt requested that the project end date be extended to September 30, 2017, providing BP 2 with a duration of 21 months. Part of this modification was to also reduce both the government share and the recipient share for BP 2 and the total project. The BP 2 government share was reduced from \$1,050,000 to \$597,997 and the recipient share was reduced from \$165,360 to \$149,499. The overall government share was reduced from \$1,200,000 to \$747,997 and the overall recipient share was reduced from \$300,000 to \$284,139.

This modification is complete.

As of July 2017 the new NETL PM for this project is Bruce Brown, 412-386-5534

[Bruce.Brown@netl.doe.gov](mailto:Bruce.Brown@netl.doe.gov)

## **7. SPECIAL REPORTING REQUIREMENTS**

## **8. BUDGETARY INFORMATION**

Phase 1 has been completed.

Phase 2 started under the new reduced budget and was completed.

Our revised Phase 2 budget and SOPO were provided to Gary Covatch (NETL Project manager) in November 2015.

## **9. TRAINING AND PROFESSIONAL DEVELOPMENT**

### **Dissemination of results**

We made five companies aware of our three-pronged (Types 1, 2 and 3) approach for development of a CO<sub>2</sub> thickener and the PFA polymeric thickener.

During the last quarter we re-submitted the following paper to the journal *Polymer*.

### **Fluoroacrylate-Aromatic Acrylate Copolymers for the Viscosity Enhancement of CO<sub>2</sub>**

Sevgi Kilic, Robert M. Enick, Eric J. Beckman

Department of Chemical and Petroleum Engineering

University of Pittsburgh, Pittsburgh, Pennsylvania 15261

The effect of the structure of aromatic acrylate-fluoroacrylate copolymers on the viscosity of CO<sub>2</sub> at elevated pressures was investigated. In general, these copolymers were all found to be miscible with CO<sub>2</sub> at 295 K (pressures above 10 MPa) and induce an increase in the viscosity to some degree, depending upon the type and content of the aromatic acrylate unit in the copolymer. The ability to significantly increase the viscosity of high pressure CO<sub>2</sub> could lead to improved flow characteristics in porous media that would result in greater oil recovery during CO<sub>2</sub> miscible displacement in sandstone or limestone oil formations. It appears that stacking of aromatic rings is the key factor in viscosity enhancement. Miscibility pressures of the copolymers were found not to be strongly affected by the type and/or content of the aromatic acrylate unit, which can be attributed to the dominance of the highly CO<sub>2</sub>-philic fluoroacrylate unit in the copolymer on miscibility. The results showed that viscosity of the solution increases with the increasing content of the aromatic acrylate unit in the copolymer, but a point is reached beyond which additional comonomer causes the relative viscosity to drop. Existence of such an optimum composition suggests that, beyond an optimum, the aromatic rings associate through intramolecular rather than intermolecular interactions, resulting in a decrease in viscosity enhancement. It is surmised that decreasing affinity of CO<sub>2</sub> for the copolymer with increasing content of aromatic acrylate unit in the copolymer (i.e. decreasing hydrodynamic volume) is the reason for this effect.

Keywords: CO<sub>2</sub>, viscosity enhancement, fluoroacrylate copolymers,  $\pi$ - $\pi$  association

During the last quarter of this project the team submitted an abstract for the SPE IOR conference in Tulsa, OK in 2018. This abstract was accepted for a poster presentation, and the SPE paper for the conference will contain all of the core-related results from this project. We will then publish this paper in a peer-reviewed journal. (The ability of the CO<sub>2</sub>-PFA solutions to seal a crack will be saved for a separate publication.)

The details of the SPE IOP conference abstract are provided below.

**Title: Fluoroacrylate Polymers as CO<sub>2</sub>-soluble Conformance Control Agents**

Session: Conformance control for gas injection: chemical method

Enick, Robert	rme@pitt.edu
Cummings, Stephen	stephen.cummings@covestro.com
Zaberi, Husain	<a href="mailto:husain.zaberi@gmail.com">husain.zaberi@gmail.com</a>
Beckman, Eric	beckman@pitt.edu
Dailey, Chris	SCAL, Inc. chrisdailey@scalinc.com
Vasilache, Mihai	SCAL, Inc. mv@scalinc.com

Keywords: Conformance control, CO<sub>2</sub>-soluble, polymer, polyfluoroacrylate, wettability

Most chemical methods for conformance control have been based on the injection of an aqueous solution into a high permeability thief zone. In this study, we propose the addition of a conformance control agent directly to high pressure CO<sub>2</sub>, thereby promoting the flow of the conformance control agent to the regions within thief zones where CO<sub>2</sub> is most likely to flow.

We synthesized a novel CO<sub>2</sub>-soluble polyfluoroacrylate (PFA); an amorphous, sticky, transparent, homopolymer that dissolves readily in CO<sub>2</sub> in well-mixed vessels at pressures commensurate with CO<sub>2</sub> EOR. PFA is based on a monomer that contains six (rather than eight) fluorinated carbons, thereby eliminating the environmental concerns associated with possible degradation products. Because PFA has high molecular weight, the addition of ~1wt% PFA to CO<sub>2</sub> slightly thickened CO<sub>2</sub>, but the CO<sub>2</sub>-PFA solution was still significantly less viscous than water or oil. We then conducted numerous core floods to determine if the adsorption of PFA onto the rock surfaces could provide conformance control.

We have found that when a CO<sub>2</sub>-PFA solution is injected into porous media, a portion of the dissolved PFA strongly adsorbs onto the mineral surfaces, regardless of what fluid was originally present in the pores. Because PFA is highly hydrophobic and oil-phobic, the thin PFA film deposited within the rock changes the wettability and dramatically reduces the permeability to subsequently injected fluids, especially for sandstones. Although PFA is CO<sub>2</sub>-soluble, this change in wettability coupled with the relatively poor mixing within the pores reduces the permeability of the rock to CO<sub>2</sub> by several orders of magnitude. A series of dual parallel core

floods were conducted to demonstrate the efficacy of PFA for conformance control. Excellent conformance control results were obtained when a CO<sub>2</sub>-PFA solution was injected solely into an isolated high permeability (80 mD) Berea sandstone core (the thief zone) that was previously flooded with brine and CO<sub>2</sub>. After this treatment, the Berea core was then placed in parallel with a 20 mD Carbon Tan sandstone core. All of the subsequently injected CO<sub>2</sub> was diverted to the Carbon Tan core. Similar results were obtained with dual parallel limestone cores.

To the best of our knowledge, PFA is the first known example of a CO<sub>2</sub>-soluble conformance control agent. This provides operators with another tool to improve volumetric sweep efficiency during CO<sub>2</sub> EOR. Interestingly, PFA also adsorbs strongly onto cement, and we have conducted several proof-of-concept tests that indicate CO<sub>2</sub>-PFA solutions can promote wellbore integrity by sealing extremely small cracks in casing cement as the adsorbed PFA completely blocks these gas-permeable pathways.

We have also generated papers and presentations related to our ARPA-e and NETL-sponsored projects.

## 2 Peer-reviewed papers related to this NETL project

Enick, R., Zaberi, H., Cummings, S., Beckman, R., Dailey, C., Vasilache, M., Fluoroacrylate Polymers as CO<sub>2</sub>-soluble Conformance Control Agents, being prepared for SPE Journal or Journal of Petroleum Science and Engineering (based on the SPE paper associated with the Tulsa 2018 conference)

Kilic, S.; Enick, R.; Beckman, E.; Fluoroacrylate-Aromatic Acrylate Copolymers for the Viscosity Enhancement of CO<sub>2</sub>, re-submitted to Polymer

## 9 papers directly related to CO<sub>2</sub> thickeners and NGL thickeners written during this project, based on a mix of ARPA-e, NETL and RUA projects

Aman Dhuwe, James Sullivan, Jason Lee, Stephen Cummings, Alex Klara, Eric Beckman, Robert Enick, Robert Perry, *Close-clearance high pressure falling ball viscometer assessment of ultra-high molecular weight polymeric thickeners for ethane, propane and butane*, Journal of Petroleum Science and Engineering, IF 1.1, 145 (2016) 266-278

Aman Dhuwe, Jason Lee, Stephen Cummings, Eric Beckman, Robert Enick, *Small Molecule Thickeners for Ethane, Propane and Butane*, JSCF, IF 2.4, Vol 114, August 2016, Pages 9-17.

R.M. Enick, P. Koronaios, C. Stevenson, S. Warman, D. Luebke, *Thermally Stable Silicone Solvents for the Selective Absorption of CO<sub>2</sub> from Warm Gas Streams that also Contain H<sub>2</sub> and H<sub>2</sub>O*, Energy and Fuels 2016, 5901-5910 IF 2.8

Baled, H., Tapriyal, D., Gamwo, I., Bamgabade, B., McHugh, M., Enick, R., *Viscosity Measurements of Two Prospective Deepwater Viscosity Standard Reference Fluids at High Temperature and High Pressure*, in press 2016, Journal of Chemical & Engineering Data Special Issue in Honor of Kenneth R. Hall, 2016, IF 2.04, , 2016, 61 (8), pp 2712–2719, DOI: 10.1021/acs.jced.6b00128

Michael J. O'Brien, Robert J. Perry, Mark Doherty, Jason Lee, Aman Dhuwe, Eric Beckman, Robert Enick, *Anthraquinone Siloxanes as Thickening Agents for Supercritical CO<sub>2</sub>*, Energy & Fuels, April 2016, 30, 5990-5998, IF 2.8

Lee, J., Stephen Cummings, Beckman, E., Enick, R., Michael J. O'Brien, Robert J. Perry, Mark Doherty *The Solubility of Low Molecular Weight Poly(Dimethyl siloxane) in Dense CO<sub>2</sub> and its Use as a CO<sub>2</sub>-philic Segment*, Journal of Supercritical Fluids, 2017, 17-25 IF 2.4

Mark D. Doherty, Jason J. Lee, Aman Dhuwe, Stephen Cummings, Michael J. O'Brien, Robert J. Perry, Eric J. Beckman, Robert M. Enick, *Small molecule cyclic amide and urea based thickeners for organic and sc-CO<sub>2</sub>/organic solutions*, Energy and Fuels, 2016, IF 2.8, 30, 5601-5610, IF 2.8

Xu Zhou, Mona M. Obadia, Surendar R. Venna, Elliot A. Roth, Anatoli Serghei, David R. Luebke, Christina Myers, Robert Enick, Eric Drockenmuller, Hunaid B. Nulwala, *Highly Cross-linked Polyether-based 1,2,3-triazolium Ion Conducting Membranes with Enhanced Gas Separation Properties*, European Polymer Journal, 84 (2016) 65-76 IF 3.2

Aaron J. Rowane, Rajendar R. Mallepally, Babatunde A. Bamgbade, Matthew S. Newkirk, Hseen O. Baled, Ward A. Burgess, Isaac K. Gamwo, Deepak Tapriyal, Robert M. Enick, Mark A. M<sup>c</sup>Hugh, *High-Temperature, High-Pressure Viscosities and Densities of Toluene*, Journal of Chemical Thermodynamics, 115 (2017) 34–46, IF 2.7

1 presentation that will be 100% based on this NETL project

Enick, R., Zaberi, H., Cummings, S., Beckman, R., Dailey, C, Vasilache, M., Fluoroacrylate Polymers as CO<sub>2</sub>-soluble Conformance Control Agents, April 14-18, 2018, Tulsa OK (100% from this NETL project, a summary of this entire project)

8 presentations since the start of Phase 1 based on a mix of ARPA-e, NETL and RUA projects

R.M. Enick, P. Koronaios, D.R. Luebke, H. Nulwala, S. Warman, C. Stevenson, Hydrophobic Polymeric Solvents for the Selective Absorption of CO<sub>2</sub> from Warm Gas Streams that also Contain H<sub>2</sub> and H<sub>2</sub>O, Presented at the A.C.S Meeting, New Orleans April 7-11, 2013. Presented by Lei Hong

R.M. Enick, P. Koronaios, D.R. Luebke, H. Nulwala, S. Warman, C. Stevenson, Hydrophobic Polymeric Solvents for the Selective Absorption of CO<sub>2</sub> from Warm Gas Streams that also

Contain H<sub>2</sub> and H<sub>2</sub>O, Presented at the Carbon Capture and Sequestration Meeting, Pittsburgh May 13-16, 2013

Enick, R., Koronaios, P., Nulwala, H., Hydrophobic polymeric solvents for pre-combustion CO<sub>2</sub> capture from hot post-WGS streams 2013 NETL CO<sub>2</sub> CAPTURE TECHNOLOGY MEETING, Pittsburgh PA, July 8-11, 2013

Enick, et al. "Hydrophobic Polymeric Solvents for the Selective Absorption of CO<sub>2</sub> From Warm Gas Streams That Also Contain H<sub>2</sub> and H<sub>2</sub>O", presented at the National AIChE Conference and Exhibit, San Francisco CA, Nov 3-8, 2013

R. Enick, H. Baled, P. Koronaios, R. Miles, I. Gamwo, D. Tapriyal, W. Burgess, M. McHugh, B. Bamgbade, Y. Wu, R. Perry, M. Doherty, M. O'Brien, Viscosity Study of Hydrocarbon Liquids at Extreme Conditions, 19<sup>th</sup> Symposium on Thermophysical Properties, sponsored by NIST and the Joint ASME-AIChE Committee on Thermophysical Properties in Boulder Colorado.

Enick, et al. "Experimental Measurements and Modeling of Viscosity for Liquid Hydrocarbons At Pressures Up to 243 MPa and Temperatures Up to 534 K" presented at the National AIChE Conference and Exhibit, San Francisco CA, Nov 3-8, 2013

Robert M. Enick, Hseen O. Baled, Peter Koronaios, Randy L. Miles, Ma Luo, Ward Burgess, Yee Soong, Isaac K. Gamwo, Deepak Tapriyal, Mark A. McHugh, Yue Wu, Babatunde A. Bamgbade, Viscosity of Hydrocarbons at Extreme Temperatures and Pressures, ACS National Meeting, San Francisco, CA, August 2014

Koronaios, P., Enick, R., "Viscosity of hydrocarbons at high temperatures and pressures"; Division: ENFL: Division of Energy and Fuels; Session: Challenges and Opportunities in Petroleum Oil Production, Refining and Utilization; 248th ACS National Meeting, San Francisco, California, August 10-14, 2014

#### 10 presentations of 100% ARPA-e content

Enick, et al. "The CO<sub>2</sub>-Solubility and Viscosity Enhancing Potential of CO<sub>2</sub>-Philes Functionalized with Aromatic Groups" presented at the National AIChE Conference and Exhibit, San Francisco CA, Nov 3-8, 2013

J. Lee, S. Cummings, A. Dhuwe, R.M. Enick, E.J. Beckman, University of Pittsburgh Department of Chemical and Petroleum Engineering, R. Perry, M. Doherty, M. O'Brien, General Electric Global Research; Development of Small Molecule CO<sub>2</sub> Thickeners for EOR and Fracturing; paper SPE 179587 presented at the SPE IOR Symposium, Tulsa, OK April 12-16, 2014.

Robert M. Enick, Jason J. Lee, Stephen D. Cummings, Eric J. Beckman, Robert J. Perry, Michael O'Brien, Mark Doherty, CO<sub>2</sub> Thickeners for Improved Oil Recovery or Hydraulic Fracturing, ACS National Meeting, San Francisco, CA, August 2014

Lee, J., Enick, R.; "Small associative thickeners for supercritical CO<sub>2</sub>" Sci-Mix for the technical program of the 248th ACS National Meeting that will be held in San Francisco, California, August 10-14, 2014. Paper ID: 27361; Division: ENFL: Division of Energy and Fuels; Session: Sci-Mix; Poster

Perry, R., OBrien, M., Doherty, M. Enick, R. et al. Silicones for CO<sub>2</sub> Capture and EOR, 248th ACS National Meeting, San Francisco, California, August 10-14, 2014

Lee, J., Enick, R., Perry, R. et al., Development of Associative Small Molecule CO<sub>2</sub> Thickeners, presentation at the 2014 AIChE Annual Meeting in Atlanta, GA.

Aman Dhuwe, Robert Enick, Jason J. Lee, Eric J. Beckman, Robert J. Perry, Mark Doherty, Michael O'Brien and Stephen Cummings; 422260 Thickeners for NGLs to Improve Performance of Gas Miscible EOR and Dry Fracking, Presented at the 2015 AIChE Annual Meeting, Nov 8-13, 2015

Jason J. Lee, Aman Dhuwe, Stephen Cummings, Mark Doherty, Michael O'Brien, Eric J. Beckman, Robert J. Perry and Robert Enick, Low Molecular Weight CO<sub>2</sub> Thickener Design for EOR, Presented at the 2015 AIChE Annual Meeting, Nov 8-13, 2015

R. Enick, Novel Surfactants for Mobility and Conformance Control CO<sub>2</sub> Foams, OMICS International Conference and Expo on Oil & Gas, Nov. 16-18, 2015, Dubai, UAE

R. Enick, J. Lee, A. Dhuwe, E. Beckman, S. Cummings, R. Perry, M. O'Brien, M. Doherty, Polymeric and small molecule thickeners for CO<sub>2</sub>, ethane, propane and butane for improved mobility control, SPE IOR Conference and Exhibition, Tulsa, OK, April 2016

## 6 Invited presentations

CO<sub>2</sub> Thickeners for EOR and Fracturing, PraxAir, Buffalo, NY, April 23, 2013

CO<sub>2</sub> Additives for Improved EOR and Fracturing Performance, LBNL, Sept 19 2014, Hydrogeology Department in the Earth Sciences Division (ESD) at Lawrence Berkeley National Laboratory (LBNL) Distinguished Scientist Seminar Series (DSSS).

CO<sub>2</sub> Thickeners for Improved CO<sub>2</sub> EOR, BASF Wintershall, Kassel, Germany, Dec 2014

Foams and Thickeners for Improved Mobility Control, ITF EOR in Carbonates Workshop, Hilton Kuwait, Jan 27, 2015

Thickeners for CO<sub>2</sub> EOR and Hydraulic Fracturing, 2015 IGERT Energy for the 21<sup>st</sup> Century Seminar, Rochester University, May 1 2015

CO<sub>2</sub> Miscible and Immiscible Displacement in the US, The Problems, the Promise and the Lessons Learned for Others, OMICS International Conference and Expo on Oil & Gas, Nov. 16-18, 2015, Dubai, UAE

## **10. PROJECT RESULTS**

## **10.1 ARPA-E funded efforts to design a small molecule CO<sub>2</sub>-thickener**

This section of the report summarizes all of the ARPA-E-funded efforts that were conducted in parallel with this NETL project. “Type 1” thickener refers to small molecules with CO<sub>2</sub>-philic cores and aromatic associating groups at each end of the molecule. “Type 2” thickener refers to molecules with CO<sub>2</sub>-philic cores and CO<sub>2</sub>-reactive amine groups at each end of the molecule. Our team synthesized many Type 1 and Type 2 small associative molecules under separate ARPA-E funding. About half of the ARPA-E funding supports our collaborators at GE Global Research in Niskayuna NY.

Type 1 molecules included triphenoxymethanes, simple organogelators, silicone oligomers with aromatic end groups, and polyether (specifically polypropylene glycol, PPG) oligomers with aromatic end groups. We also assessed the “universal gelator” molecule bis-(R,β-dihydroxy ester); this is an oxygenated hydrocarbon molecule with two hydroxyls and an isopropyl group on each end that is capable of thickening an incredibly diverse set of solvents (2H,3H-perfluoropentane (HPFP) and 1H,1H-heptafluorobutanol (HFB), water, toluene, cyclohexane, a 10:1 hexane-chloroform-hexane mixture, dichloromethane, and water. These solvents were gelled with less than 1wt% of the universal gelator, with the exception of the dichloromethane, which required about 5wt%. The universal gelator was not CO<sub>2</sub> soluble, however, even when co-solvent was added.

The most promising Type 1 compound is shown below in Figure 10.1.1, it is a benzene trisurea; specifically benzene tris[{tris(trimethylsiloxy)silyl}propyl urea], designated as 2300-10 in the figures that follow. We were not able to develop a new Type 1 compound similar to this compound that could thicken CO<sub>2</sub> without the need for a co-solvent. This compound was by far the most effective thickener of CO<sub>2</sub>-rich solutions.

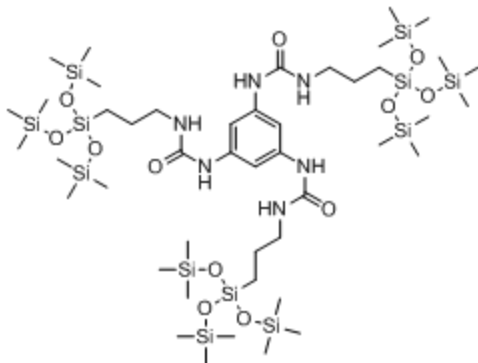


**Figure 10.1.1 Type 1 compound benzene tris[{tris(trimethylsiloxy)silyl}propyl urea], designated as 2300-10. This small molecule was the most effective ARPA-e-funded small molecule thickener for CO<sub>2</sub>. Unfortunately this molecule required substantial amounts of organic co-solvents for dissolution in CO<sub>2</sub>.**

Type 2 molecules included silicone oil oligomers with terminal primary and/or secondary amines, including PPG oligomers with terminal primary and/or secondary amines, and silicone oil oligomers terminated with amide groups leading to aromatic groups. We concluded the testing of CO<sub>2</sub> solubility and viscosity enhancement of these compounds. We found that the anthraquinone group is particularly effective at intermolecular associations. For example, the molecular structure of a thickener designated as 2008-90 is shown in Figure 10.1.2. The silicone portions -(Si-CH<sub>3</sub>CH<sub>3</sub>O)<sub>n</sub>- (shown as -(Si-MeMeO)<sub>n</sub>-) promote solubility in CO<sub>2</sub>, while the aromatic group anthraquinone composed of three benzene rings and two =O groups provide intermolecular associations.

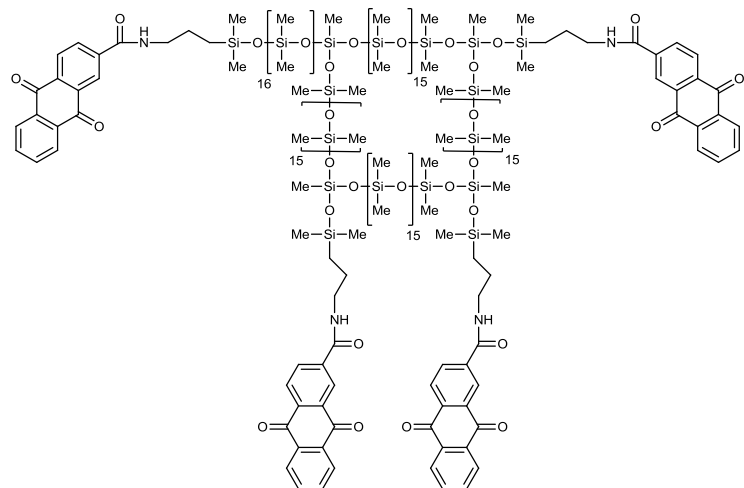


**Figure 10.1.2** Type 2 compound, a silicone-amide-anthraquinone compound, designated as 2008-90. This small molecule was the most effective Type 2 ARPA-e-funded small molecule thickener for CO<sub>2</sub>. Unfortunately this molecule required substantial amounts of organic co-solvents for dissolution in CO<sub>2</sub>.

This compound forms transparent rigid gels if liquids like hexane, as shown below in 10wt% concentration, as shown in Figure 10.1.3. It was hoped that similar gels could be formed in pure CO<sub>2</sub>. Alternately, if the thickener is insoluble in CO<sub>2</sub>, this result indicated that hexane is a good co-solvent to be added to the CO<sub>2</sub> to help the compound dissolve in a CO<sub>2</sub>-rich fluid.



**Figure 10.1.3 Transparent rigid gel formed by adding 10wt% 2008-90 to hexane, gently heating, and cooling**

Unfortunately this compound (2008-90) was not soluble in CO<sub>2</sub>. However the compound (2008-90) was capable of thickening mixtures of CO<sub>2</sub> and hexane. We were not able to develop a new Type 2 compound similar to this compound that could thicken CO<sub>2</sub> without the need for a co-solvent.

Although the ARPA-e project was focused on small molecules, we also tested ultra-high molecular weight (~1,000,000) silicone oil polydimethyl siloxane (PDMS), the most CO<sub>2</sub>-soluble non-fluorous polymer, as a control for comparison with small molecules. We have previously shown that 5wt% of more toluene in CO<sub>2</sub> is needed to dissolve ~1wt% PDMS in the CO<sub>2</sub>-toluene solution (see Table 10.1.1 below).

Composition	Cloud point (in psig)		
	23 °C	40 °C	60 °C
Silanol (1wt.%) + Toluene (10 wt%); balance CO <sub>2</sub>	2825	3070	4045
Silanol (1wt.%) + Toluene (7.5 wt%); balance CO <sub>2</sub>	4868	3750	4200
Silanol (1wt.%) + Toluene (5 wt%); balance CO <sub>2</sub>	Insoluble (to 9500)	5104	4900

**Table 10.1.1 Effect of amount of toluene (co-solvent) needed for dissolution of 1wt% PDMS; effect of toluene concentration on the cloud point pressure (pressure required to attain a single phase)**

The CO<sub>2</sub>-thickening results for these Type 1 and Type 2 small molecule compounds are summarized below in Figure 10.1.4, where relative viscosity is the ratio of the viscosity of the solution to the viscosity of pure CO<sub>2</sub> at the same temperature (T) and pressure (P). This data was acquired with a falling ball viscometer, and the average shear rate for each datum is about 9000s<sup>-1</sup>(relative viscosity). (Because all of the solutions are shear-thinning, much greater relative viscosity values should be realized when these solutions are tested in flow-through-Berea-sandstone tests characterize by shear rates of roughly 1-10 s<sup>-1</sup> at low superficial velocities.) Every thickener shown in the following figure required a co-solvent to dissolve in CO<sub>2</sub>.

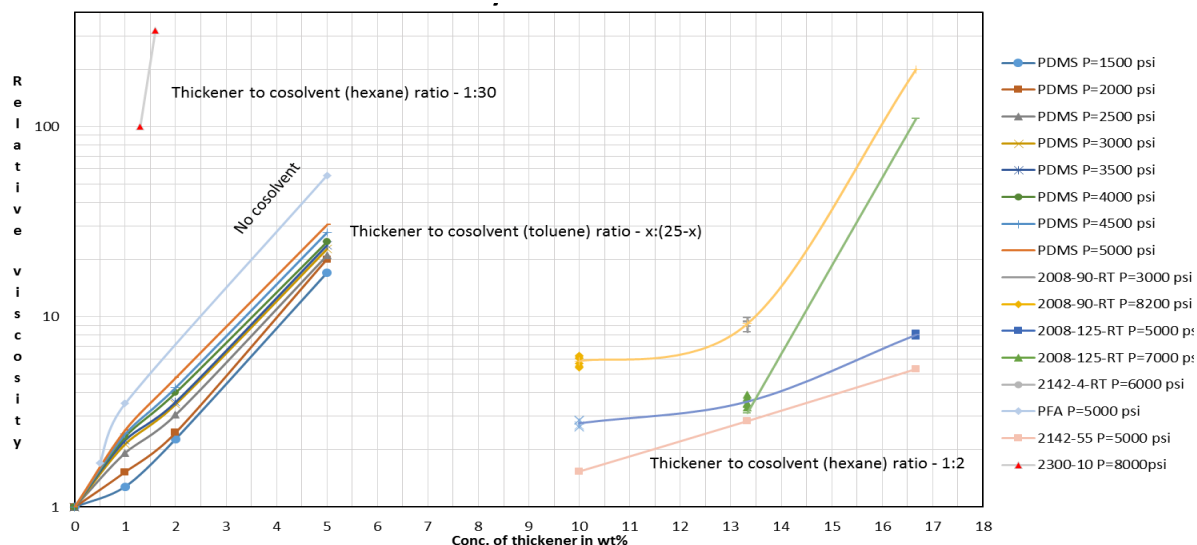


**Figure 10.1.4 Relative viscosity of solutions of (CO<sub>2</sub> + co-solvent + thickener) at ~22-25 °C, average shear rate = 9000 s<sup>-1</sup>(relative viscosity). The best Type 1 thickener 2300-10 corresponds to the red triangle data; the best Type 2 thickener 2008-90 corresponds to the yellow diamonds. (The PDMS curves correspond to high molecular weight silicone oil data which was used for comparison with the small molecule data.)**

The Type 2 branched low molecular weight PDMS end functionalized with anthraquinone amides such as 2008-90, are represented by the family of curves on the right hand side of this figure. About 10+ wt% of this thickener is required to attain a substantial viscosity enhancement. Further, excess co-solvent was used in these mixtures. To assure dissolution in CO<sub>2</sub>, we added twice as much hexane as the branched low molecular weight PDMS end functionalized with anthraquinone amides thickener. This amount of co-solvent may be decreased slightly while maintaining solubility.

The Type 1 benzene tris(urea) with three bulky CO<sub>2</sub>-philic groups attached to the urea (2300-10), shown at the upper left hand portion of Figure 10.1.4, provided the most remarkable viscosity enhancement at dilute concentration; 100-fold increase at 1.3wt% and 300-fold at 1.6wt%. Unfortunately, this compound 2300-10 required ~30 times as much hexane as thickener to dissolve in CO<sub>2</sub>, and very high pressures of ~8000 psi were required to attain a single phase. Therefore we attempted to improve the CO<sub>2</sub>-philic nature of this compound, but were unsuccessful.

High molecular PDMS polymer results are represented by the family of curves at the bottom left hand corner of Figure 10.1.4. PDMS also requires a co-solvent (toluene appears to be the best liquid solvent) to attain dissolution at pressures commensurate with EOR conditions. In these results, the combined concentration of PDMS and toluene was maintained at 25wt% in 75wt% CO<sub>2</sub>.

Figure 10.1.4 demonstrates that the best small molecule thickener for CO<sub>2</sub>-hexane solutions was benzene tris[ {tris(trimethylsiloxy)silyl}propyl urea] 2300-10, followed by high molecular weight PDMS, followed by the Type 2 compound 2008-90.

Two publications contain all of the ARPA-e-funded results for small molecule thickeners (O'Brien et al. 2016, Doherty, et al. 2016).

This concludes the summary of the ARPA-e funded work. Because we were unable to design a small molecule capable of thickening CO<sub>2</sub> without the addition of substantial amounts of an organic liquid co-solvent such as hexane or toluene, we did not use any of these small molecules in the NETL project. Neither did we use the polymer PDMS because it also required the use of large amounts of co-solvent.

## **10.2 High molecular weight polyfluoroacrylate (PFA) as a CO<sub>2</sub>-soluble thickener that does not require a co-solvent**

The polymer that is to be dissolved in the CO<sub>2</sub> is a polyfluoroacrylate (PFA; (CHCH<sub>2</sub>OCOC<sub>2</sub>H<sub>4</sub>C<sub>6</sub>F<sub>13</sub>)<sub>n</sub>) based on the homopolymerization of the CHCH<sub>2</sub>OCOC<sub>2</sub>H<sub>4</sub>C<sub>6</sub>F<sub>13</sub> tridecafluoroctyl acrylate liquid monomer (Mw 418). This polymer can be synthesized in an organic liquid solvent, in high pressure liquid CO<sub>2</sub> (DeSimone et al. 1992), or by bulk polymerization of the monomer. PFA has long been recognized as extraordinarily CO<sub>2</sub> soluble (DeSimone et al. 1992; Mawson et al. 1995; Blasig et al. 2002; Luna-Barcenas et al. 1998; Huang et al. 2000). PFA is the only polymer that can dissolve in compressed liquid CO<sub>2</sub> or supercritical CO<sub>2</sub> at pressures that are commensurate with oilfield applications; CO<sub>2</sub> is such a feeble solvent that it can only dissolve a few other high molecular weight polymers such as polyvinyl acetate or polydimethyl siloxane, but only at pressures of 10000 - 40000 psi [Shen et al. 2003]. PFA is completely insoluble in CO<sub>2</sub> vapor or supercritical fluids several hundred psi below the cloud point pressure; therefore if the CO<sub>2</sub> – PFA solution experiences low pressures the PFA will precipitate. (In addition to the previously described adsorption mechanism, “PFA precipitation” due to large pressure reduction would also occur with the proposed CO<sub>2</sub>-PFA solutions if they experience large pressure drops. The only other solvents known to be capable of dissolving PFA are fluorinated fluids that are high density, low viscosity, low boiling point liquids at ambient pressure (3M Novec HFE-7100 hydrofluoroether (F<sub>9</sub>C<sub>4</sub>OCH<sub>3</sub>; 1.5 g/ml; 0.6 cp at 23°C; b.p.61°C), and Vertrel XF decafluoropentane (C<sub>5</sub>F<sub>10</sub>H<sub>2</sub>; 1.6 g/ml; 0.67 cp at 25°C; b.p. 55°C)).

Because polyfluoroacrylates are susceptible to hydrolysis, the degradation of PFA based on 8 fluorinated carbons in the monomer would lead to the formation of perfluorooctanoic acid (PFOA). If a fluoroacrylate based on a 6 fluorinated carbon chain monomer is used, a more benign perfluorohexanoic acid (PFHXA) product would form if any hydrolysis occurs (Washington and Jenkins, 1995; Washington et al. 2005). Polymers such as PFA made using the -C<sub>6</sub>F<sub>13</sub> fluorinated side chain chemistry enjoy global regulatory approval in a wide variety of applications. They are safe and effective replacements for the older C<sub>8</sub>F<sub>17</sub>-based water repellent articles, especially because data in non-human primates indicate that their degradation products such PFHXA have substantially shorter half-lives in these animals than PFOA associated with the C<sub>8</sub>F<sub>17</sub>-based polymers. Therefore in 2013 the EPA affirmed that compounds containing -C<sub>6</sub>F<sub>13</sub> groups would not be targeted by EPA’s 2009 Long-Chain Perfluorocarbon Action Plan Proposal (Poston and Connell 2013).

Our team members (Huang et al. 2000; Xu et al. 2003; Enick, et al. 2005; Shen et al. 2003), along with others (DeSimone, 1992, McClain et al. 1996; Luna-Barcenas et al. 1998; Dawson et al. 1995), have demonstrated that polyfluoroacrylates and fluoroacrylate-containing co-polymers are the most CO<sub>2</sub>-soluble high molecule weight homopolymers that have ever been identified;

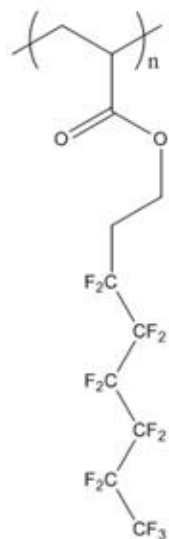
with molecular weight so high that viscosity enhancement is possible. They are capable of dissolving in CO<sub>2</sub> at typical EOR conditions to concentrations of roughly 1 wt% without the need for the addition of a co-solvent such as toluene or hexane. It should be noted that the more environmentally benign version of this polymer, which contains only 6 fluorinated carbons, was used in all tests, rather than the version with 8 fluorinated carbons.

The detailed synthesis of the CO<sub>2</sub>-soluble, high molecular weight, C<sub>6</sub>F<sub>13</sub>-based polyfluoroacrylate (PFA) polymer used in all phase behavior and core tests described in this report follows.

1. A glass column is filled at the narrow end with a small amount of cotton wool, and then with inhibitor remover up to three quarters of the length of the column (Sigma Aldrich #306312, Inhibitor Remover to remove monomethyl ether hydroquinone). The column is held vertically upright with a clamp and stand – with the cotton wool at the bottom. The following step was done with dry nitrogen being passed over the top and exit of the glass column, by using a Schleck manifold to direct nitrogen through two lines. It can also be done inside a glove box or glove bag. Fluoroacrylate monomer 2-(perfluorohexyl)ethyl acrylate was passed through the vertical inhibitor remover column, to remove the inhibitor and prepare the monomer for reaction. The monomer was added in portions to the top of the vertical column from the bottle and the monomer was collected in a glass flask beneath the column. Once enough monomer has been collected, estimated by using density and having a graduated receiving flask, the flask is sealed.
2. This step must be performed inside a nitrogen (or inert gas) filled glove box or glove bag. 30.0 g of monomer (CH<sub>2</sub>=CH[COOC<sub>2</sub>H<sub>4</sub>C<sub>6</sub>F<sub>13</sub>]) fluoroacrylate (MW 418; 0.0239 mol) and 0.0002 g re-crystallized AIBN initiator (Sigma Aldrich #755745), (0.002wt% of mass of monomer) were weighed out and added to a pressure vial (Ace Glassware #8648-96). Once the addition of the monomer and initiator were completed a small magnetic stir bar was added.
3. The vial was subsequently sealed under nitrogen inside the glove box/glove bag, by screwing on the lid.
4. The reaction vial was then removed from the glove bag/glove box, and placed into an oil bath. The oil bath used was a tall, large volume Pyrex beaker (750 ml). The pressure vial was held in place using clamps almost completely submerged in a silicone oil bath resting on a hotplate with rotating magnet. The vial was heated to 75 °C for 12 hours while the stir bar was rotating at a speed of 600+ rpm.
5. After the 12 hour time had elapsed, the reaction was allowed to cool to ambient temperature.
6. The pressure vial was opened and the polymer product and un-reacted monomer, was observed to form a sticky, clear mixture, which is a very tough, almost gum like gel. 50 ml of HFE-7100 was added to the vial with the polymer still inside. More HFE-7100 can be added, but the vial must not be more than 80% full. The polymer is left to soften in the solvent for 30 minutes, before a steel spatula is used to loosen and break up the polymer in the vial. The vial is then re-sealed (important), placed back in the oil bath, and heated to 85 °C for 15-20 minutes.

After this, the vial is removed again, and left in a rack to cool for 5 to 10 minutes (very important: if you open the vial immediately with HFE-7100 at 85 °C, under pressure, it will boil right out the vial and all over the place, which is obviously dangerous though HFE-7100 is not flammable).

7. After cooling the vial is cracked open slowly, until pressure is relieved, and the HFE-7100 with some dissolved polymer can be decanted into a clean glass beaker. During steps 6 & 7, some of the homopolymer is removed from the main homopolymer gel slug and dissolved into the HFE-7100 solvent, but it is a slow process due to the relative weakness of HFE-7100 as a solvent for the high MW homopolymer. To dissolve more polymer into the solvent (in order to use less in total/save solvent) you can open the vial (after allowing it cool, so it is safe to open), and again use a steel spatula to loosen and mix the polymer into the solvent, before returning the resealed vial back to the oil bath for another 20 minutes.
8. Repeat steps 6 & 7 with as much solvent as is required, for this specific synthesis about 500 ml of HFE-7100 is needed and typically 8-10 hours of time to heat, dissolve and cool. It can be collected and recycled with a distillation set-up if required (separate process). Heating the polymer inside the sealed pressure vial is required in order to not use inordinate quantities of solvent and time trying to dissolve the homopolymer cold. This is because by partially melting the polymer it is able to dissolve much faster.
9. Once dissolution of the product was achieved, the HFE-7100/polymer solution was added to 600 ml of methanol to precipitate the polymer product whilst leaving unreacted monomer dissolved in the bulk solvent phase. The solid, sticky polymer was collected from the bottom of the beaker using a spatula, and transferred to a wide Pyrex beaker.
10. This Pyrex beaker was placed on the hotplate for drying at 65 °C, and covered with a large glass Petri dish, the beaker spout allowing methanol vapour to escape. (A vacuum oven could also be used, however the polymer will bubble up and expand and possibly escape its container). The polymer is left to dry in the beaker at 65 °C for 3 – 4 hours, as necessary. The polymer will be dry when its consistency has changed from a gooey solid to a very elastic, but tough waxy solid. When the homopolymer is still warm it is best to roll the polymer into a ball and slowly remove it from the glass beaker rather than trying to rip it off the glass or scrape it off with a spatula. It will initially be very firmly stuck to the glass so patience is required. Eventually the polymer will form a tacky ball which can be easily pulled out of the beaker (or wide mouthed glassware), and placed into a wide mouthed screw top container.
11. Once cool, the polymer will be considerably more plastic in consistency and behavior, and will be a clear extremely sticky, elastic polymer as shown in the Figure 10.2.1.



**Polyfluoroacrylate (PFA) – a  
CO<sub>2</sub>-soluble (1500+ psi)  
high molecular weight,  
completely amorphous,  
elastic,  
extremely sticky polymer  
that is water-repellant,  
and oil-repellant;  
Tg 6°C**

Figure 10.2.1 Chemical structure, appearance and description of high molecular weight PFA

## Solubility of PFA in CO<sub>2</sub>

As shown in Figure 10.2.2 for 3 separate batches of PFA, at a temperature of 24 °C, PFA dissolves completely in CO<sub>2</sub> at pressures above 1450 psia at concentrations of PFA up to 2 wt%. If one desired to dissolve 4-8 wt% PFA in CO<sub>2</sub> at 24 °C, then 2500 psi is required for one of the batches, while only 1450 psi was required for the other two batches. It is likely that the higher pressure data in one batch is attributable to an impurity in the polymer sample for the batch with the higher pressure values.

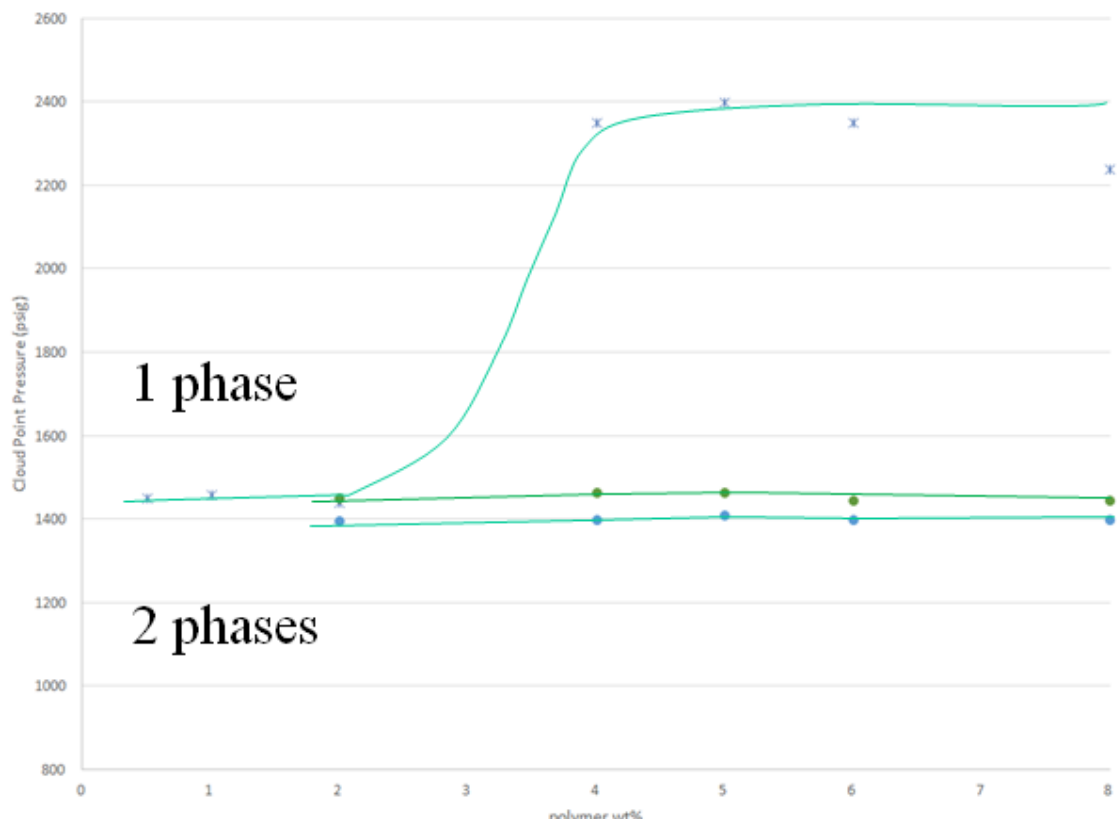
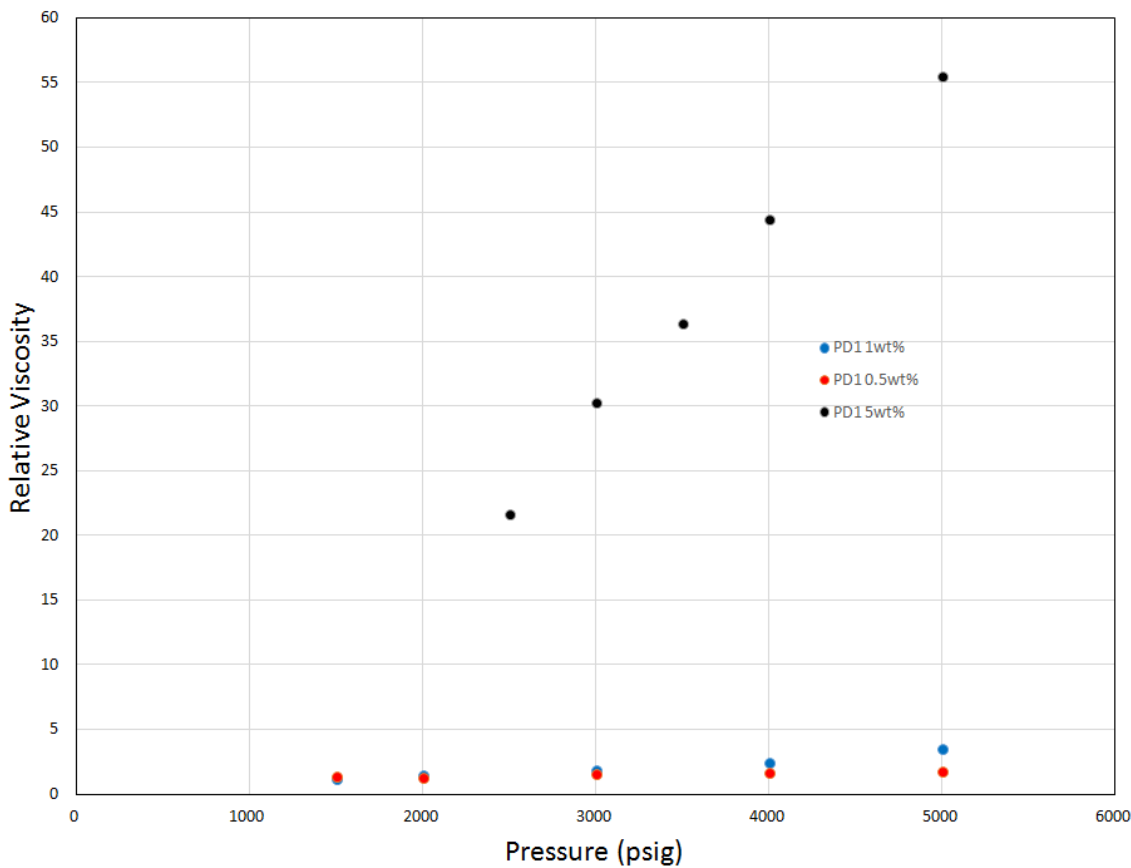


Figure 10.2.2 pressure required at 24 °C to dissolve PFA in CO<sub>2</sub> as a function of PFA concentration for three batches of PFA. (The higher pressure data for one batch is likely due to an impurity in the sample.)

## Viscosity of CO<sub>2</sub>-PFA solutions

High molecular weight PFA remains the only thickener candidate observed to date that requires no co-solvent for dissolution in CO<sub>2</sub>. In this report, we will provide solution viscosity data in terms of “relative viscosity”, which is the dimensionless ratio of the viscosity of the CO<sub>2</sub>-PFA solution to the viscosity of CO<sub>2</sub> at the same temperature and pressure. For example, if the falling object falls 10 times slower in the CO<sub>2</sub>-PFA solution than it does in pure CO<sub>2</sub>, then the solution is approximately 10 times more viscous than pure CO<sub>2</sub> and the relative viscosity is 10. This approximation assumes that the density of the CO<sub>2</sub>-PFA solution is approximately the same as the density of pure CO<sub>2</sub>.

In the Figure 10.2.3 the relative viscosity for a 5wt%, 1.0 and 0.5wt% solutions of PFA in CO<sub>2</sub> at 25 °C and pressures up to 5000 psi are shown. Note that falling ball viscometer data is provided for pressures greater than the pressure required to attain a single-phase solution of PFA in CO<sub>2</sub>. The increase in relative viscosity with increasing pressure is attributed to the ability of denser CO<sub>2</sub> to more fully expand the dissolved polymer coils, thereby increasing the viscosity of the solution. In all cases the polymer is PFA, the other nomenclature (PD1) refers to the batch number of the sample. This plot provides insight into the approximate concentration of PFA required to attain a desired increase. For example, if one desires to attain a 30-fold increase in viscosity at 25 °C and 3000 psi, then 5wt% PFA is required. However, if a 4-fold increase is desired at 5000 psi, then 1wt% PFA in CO<sub>2</sub> is required.



**Figure 10.2.3 Relative Viscosity of  $\text{CO}_2$  + PFA solutions at 0.5%, 1.0 and 5.0wt% concentrations of PFA in  $\text{CO}_2$  at  $25^\circ\text{C}$  and 5000 psi. No co-solvent was required.**

More falling ball viscometry results for two other batches of PFA (designated as PFA and PFA') are presented below for concentrations of 1 and 5wt% PFA in  $\text{CO}_2$ . Falling ball viscometry is easier to conduct (because it is easier to mix the PFA and  $\text{CO}_2$  with a ball in the sample volume than it is to mix the PFA and  $\text{CO}_2$  when a cylinder is in the sample volume). One of the disadvantages of falling ball technique, however, is that the falling ball is subject to a wide range of shear rates over its surface as it falls. The range of surface-area-averaged shear rates for these experiments is provided in the Figure 10.2.4.

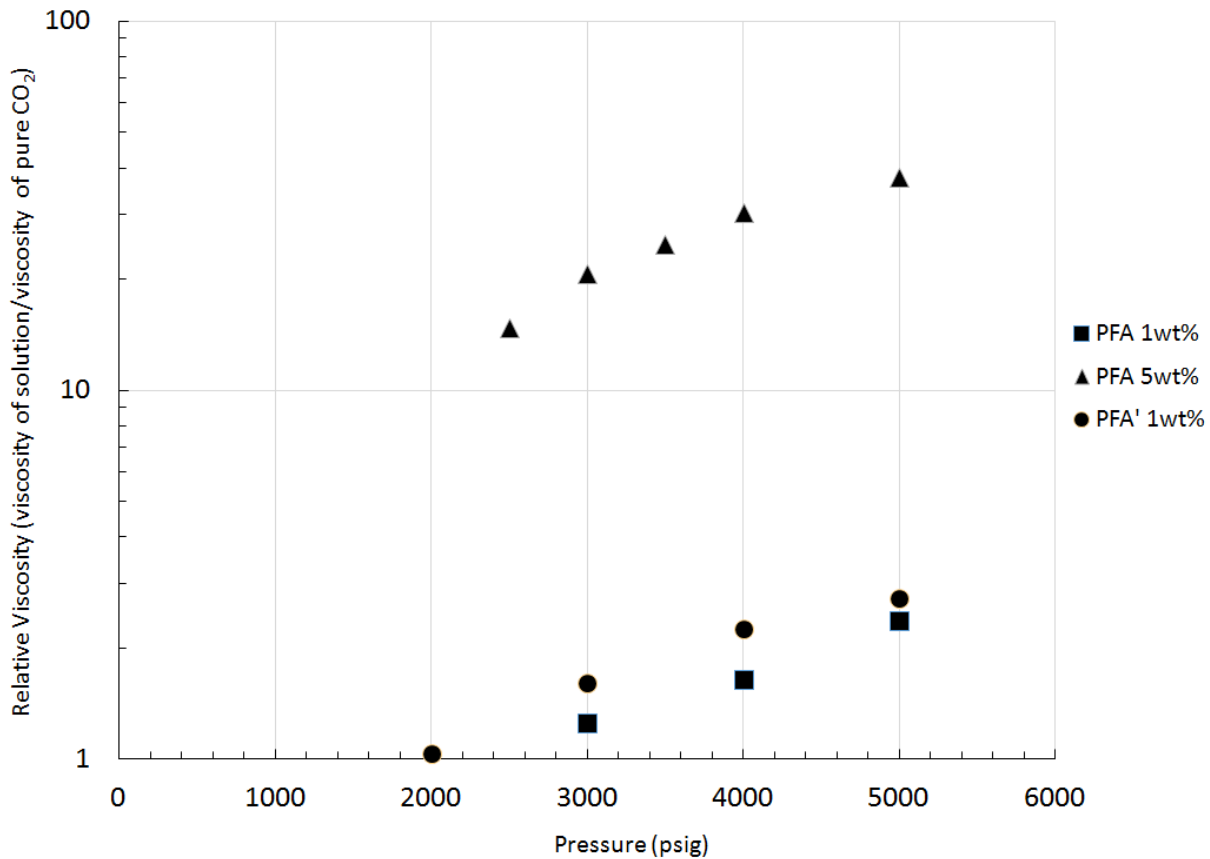
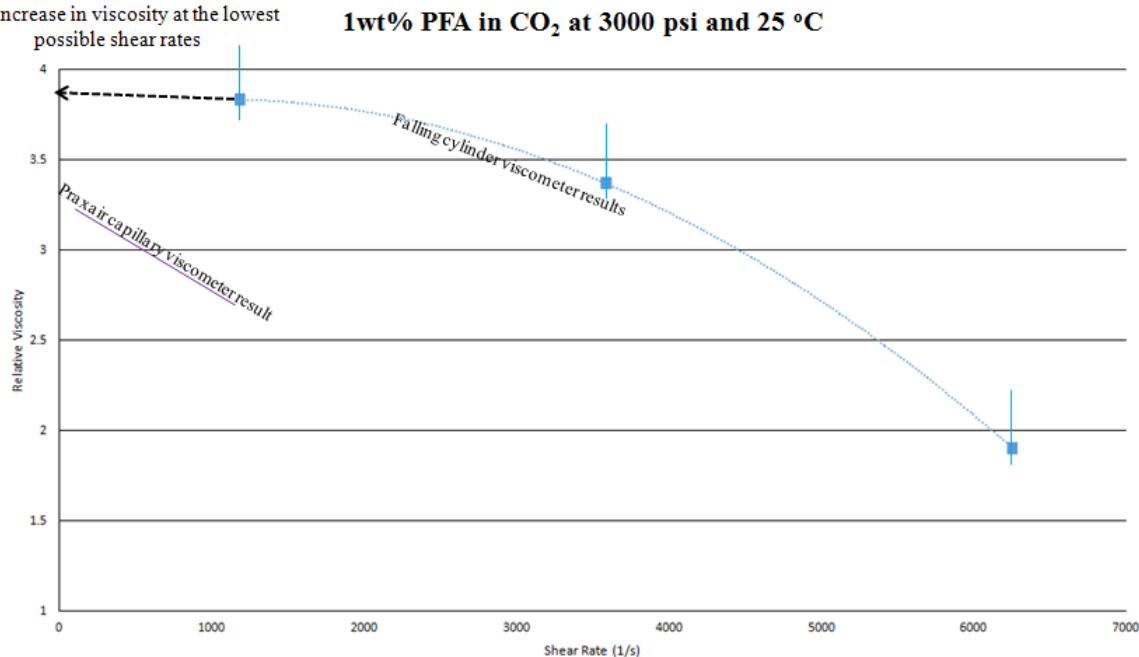


Figure 10.2.4 The ability of PFA to increase the viscosity of  $\text{CO}_2$  at 24  $^{\circ}\text{C}$ . Falling ball viscometry results. The average shear rate on the falling ball is in the  $1000 - 10000 \text{ s}^{-1}$  range.

In order to attain viscosity data at well defined shear rates, falling cylinder viscometry was conducted. In this case, there is a single shear rate associated with the cylinder falling coaxially within a cylindrical sample volume. As shown in Figure 10.2.5, in all cases, close clearance aluminum cylinders were used, meaning that a small gap existed between the outer surface of the falling aluminum cylinder and the inner wall of the cylindrical Pyrex sample volume. A series of polished aluminum cylinders of varying diameter was used in the following tests to allow for the determination of the effect of shear rate on viscosity of  $\text{CO}_2$ -PFA solutions. Note that this data in Figure 10.2.5 was obtained at shear rates that are much higher than those associated with core flooding. However, the falling cylinder data extrapolates to a maximum relative viscosity of roughly 3.8 at low shear rates associated with EOR ( $\sim 1-100 \text{ s}^{-1}$ ) for a 1wt% solution of PFA in  $\text{CO}_2$  at 25  $^{\circ}\text{C}$  and 3000 psi.

An extrapolation of this data indicates that one would expect more than a 3.8-fold increase in viscosity at the lowest possible shear rates



**Figure 10.2.5 Falling cylinder viscometry results for single-phase solutions of 1wt% PFA in CO<sub>2</sub> at 25 °C and 3000 psi, PFA batch PD1C. Each data point corresponds to a different aluminum cylinder.**

This result clearly shows that the 1wt% solution of the commercial fluoroacrylate homopolymer will increase the viscosity of CO<sub>2</sub> by a factor of about 3.8 at 25 °C and 3000 psia.

Our colleagues at Praxair also tested PFA in their capillary viscometer, which is shown on the left portion of Figure 10.2.5. At a concentration of 1 wt% PFA in CO<sub>2</sub> at 25 °C and 3000 psi; the maximum relative viscosity at low shear rates was 3.3. This agreement in the maximum possible degree of thickening using 1 wt% PFA in CO<sub>2</sub> at 25 °C and 3000 psi (3.8-fold via falling cylinder viscometry and 3.3-fold increase via capillary viscometry) is very good. As a rule of thumb they confirm that the maximum degree of thickening one could expect is roughly 4-fold.

As a result, the core floods in which only CO<sub>2</sub> or thickened CO<sub>2</sub> was in the core were expected to exhibit no more than a ~4-fold increase in pressure drop as the pure CO<sub>2</sub> in a core is displaced by thickened CO<sub>2</sub> at a constant volumetric flow rate if there was no effect of the polymer on the core itself. Increases in pressure drop greater than a factor of 4 would be attributable to changes in the rock properties caused by adsorption/deposition/precipitation of the PFA in the core.

### **Effect of extracted hydrocarbons on PFA solubility in CO<sub>2</sub>**

There is a very unusual aspect of PFA that is counter-intuitive. Many scientists and engineers have used ambient pressure organic solvents to “model” high pressure liquid CO<sub>2</sub> for screening tests or to approximate the solvent strength of CO<sub>2</sub>. For example, CO<sub>2</sub> has been considered as “similar” to pentane, hexane, and isooctane. Therefore, one may be tempted to conclude that if a polymer is soluble in liquid or supercritical CO<sub>2</sub>, then it will be soluble in light alkanes such as pentane, hexane and isooctane. This issue is especially important for CO<sub>2</sub> EOR because as the CO<sub>2</sub> and crude oil mix in the porous media, light alkanes will be extracted into the CO<sub>2</sub>-rich phase, facilitating the development of a first-contact miscible CO<sub>2</sub>-rich fluid that is an exceptional solvent for crude oil. Therefore, if one wants to use a polymeric thickener for CO<sub>2</sub> mobility control it would be beneficial if the light alkanes that enter the CO<sub>2</sub>-phase would cause the polymer to remain in solution. It would be detrimental for mobility control if these light alkanes act as an anti-solvent that causes the polymer to come out of solution.

Unfortunately, PFA is insoluble in all of the hydrocarbons found in crude oil. PFA dissolves in very few solvents, namely dense CO<sub>2</sub> and several fluorinated solvent such as HFE-7100, a hydrofluoroether. Therefore, the PFA is expected to become less soluble in the CO<sub>2</sub>-rich fluid as one progresses away from the injection well because it is insoluble in brine and insoluble in crude oil, and the extracted hydrocarbons that enter the CO<sub>2</sub>-rich phase act as an anti-solvent for PFA.

This was experimentally verified during our phase behavior study when the dissolution of PFA in CO<sub>2</sub>-alkanes mixtures, which are described in the Table 10.2.1, was investigated. For example, it was determined that the PFA polymer at a concentration of 0.5 wt% was insoluble in a CO<sub>2</sub>-rich fluid containing 30wt% of “extractable” C<sub>6</sub>-C<sub>20</sub> hydrocarbons.

When only 15wt% of these C<sub>6</sub>-C<sub>20</sub> hydrocarbons was present, the cloud point pressure was for dissolving 0.5 wt% PFA in the fluid was 3000 psi, about 1550 psi higher than the cloud point pressure for 1wt% PFA in pure CO<sub>2</sub>.

These results clearly demonstrate that the extraction of light alkanes into CO<sub>2</sub> will significantly reduce the solubility of PFA in CO<sub>2</sub>.

The anti-PFA-solvent effect of light alkanes provides yet another disincentive for the injection of (CO<sub>2</sub>-PFA) solutions for mobility control in oil-rich zones because it is likely that the PFA will precipitate as the light alkanes are extracted into the CO<sub>2</sub>-rich phase during the EOR process.

	Alkane makeup	Wt.%	Wt.%
<b>C6</b>	40.0%	12.0%	6.0%
<b>C10</b>	26.7%	8.0%	4.0%
<b>C14</b>	13.3%	4.0%	2.0%
<b>C16</b>	6.7%	2.0%	1.0%
<b>C18</b>	6.7%	2.0%	1.0%
<b>C20</b>	6.7%	2.0%	1.0%
<b>Alkanes</b>		<u>30.0%</u>	<u>15.0%</u>
<b>PD-C1-C</b>		1.0%	0.5%
<b>CO2</b>		<u>69.0%</u>	<u>84.5%</u>
		<u>100.0%</u>	<u>100.0%</u>

**Table 10.2.1 The composition of CO<sub>2</sub>-rich fluids used to simulate the CO<sub>2</sub>-rich solvent that develops during EOR**

At this point in the project it became apparent that PFA was the only CO<sub>2</sub>-thickener that could be used for mobility control testing in cores. However, the observation that extracted light hydrocarbons would act as an anti-solvent for PFA was a troubling sign that could impede this CO<sub>2</sub> EOR mobility control application.

At the same time we realized that if the CO<sub>2</sub>-PFA solution was injected into an oil-depleted thief zone, then there would be no hydrocarbons to cause the PFA to precipitate. If the PFA was found to strongly adsorb on the rock surfaces and reduce permeability via changing wettability, then PFA could serve as a conformance control agent.

If, however, PFA would not adsorb on the rock surfaces and decrease the permeability of the rock, then PFA would not be appropriate for conformance control.

The remainder of this report will document that PFA is indeed well-suited for conformance control applications, but PFA is not recommended for mobility control.

## **10.3 Cores for the flow-through-porous-media studies**

After discussions were held with our industry contacts at Kinder Morgan and Denbury resources and the NREL PM, it was decided that clean, dry, “standard” outcrop cores should be used in this study rather than field cores. There was a consensus that the field cores from our industry advisors would only be used if the PFA proved to be an effective mobility control agent for CO<sub>2</sub> EOR. Initial testing at SCAL was also conducted with high permeability Berea sandstone.

The following 1.5” diameter, 12” long cores, Table 10.3.1, were purchased from Kocurek for use at SCAL. Nominal permeability values were provided by Kocurek. The “K<sub>brine</sub> measured at SCAL” column represents values of permeability determined at SCAL for a single example of each core type (our project only used one core in a single test; no cores were re-used).

Name of core	Type of core	UCS* psi	K <sub>brine/gas</sub> , mD – estimated Nominal values from Kocurek	K <sub>brine</sub> measured at SCAL mD	Φ %	Formation
Berea A-101	Sandstone	6,500	(60-100)/ (200-315)	94	20	Kipton
Carbon Tan A-116	Sandstone	7,600	11/42	7	15	Utah
Kirby A-105	Sandstone	7,000	9/30	44.6	21	Edwards Plateau
Indiana LS 8- 10mD B-101b	Limestone	5,000	9/17	0.4	18	Bedford
Indiana LS 70mD B-101c	Limestone	5,000	70/200	114	19	Bedford
Edwards Yellow B-104	Carbonate - Limestone	2,500	40/75	4.2	22	Edwards Plateau
Guelph Dolomite B-111	Carbonate - Dolomite	10,000	10/35	5.9	17	Niagara

\*UCS = unconfined strength - SCAL must not have a pressure difference between the overburden pressure and the pore pressure (which is lowest at the core outlet) that is greater than this value

**Table 10.3.1 Properties of the cores used at SCAL for the CO<sub>2</sub>-displacing-CO<sub>2</sub>, CO<sub>2</sub>-displacing-oil, and CO<sub>2</sub>-displacing brine core tests**

Note that throughout the report, the nominal values of permeability reported by Kocurek are in text boxes at the top of figures, while data indicative of actual permeability measured by SCAL may be found in the text or figure title for some of the experiments.

Preliminary tests conducted at NREL used 2” diameter by 6” length Berea sandstone with permeability of 125mD or 285 mD.

## 10.4 Cores floods: Thickened CO<sub>2</sub> displacing CO<sub>2</sub>

### **Effect of PFA-CO<sub>2</sub> solutions flowing through porous media**

As demonstrated in Section 10.2, it was anticipated that as long as the entire pore space of the core remained above the single-phase pressure of ~1450 psi for CO<sub>2</sub>-PFA solutions, the viscosity of the CO<sub>2</sub>-PFA solution would be about 4-times greater than the viscosity of pure CO<sub>2</sub>. Therefore, if the volumetric flow rate of the CO<sub>2</sub> was held constant and if the back pressure (BP) of the apparatus (i.e. the effluent pressure of the core) was maintained at a constant value with a back pressure regulator (BPR) or a computer controlled positive displacement (PD) pump, then the pressure drop for the core should increase by a factor of ~4 as the CO<sub>2</sub>-PFA solution displaced the CO<sub>2</sub> originally in the core.

Indeed, as shown in Figure 10.4.1, initial core floods at NETL did show a 3-4 fold increase in pressure drop as thickened CO<sub>2</sub> displaced pure CO<sub>2</sub> from the core, however a very significant pressure drop ( $\Delta P$ ) increase followed as injection continued as shown in Figure 10.4.2. This increase could not be attributed to viscosity or precipitation; therefore it had to be due to polymer adsorption and wettability changes, and/or the blocking of pore throats by layers of adsorbed polymer, and/or the retention of small amounts of CO<sub>2</sub>-insoluble impurities in the PFA sample.

**1wt% high MW PFA (250000) increased the viscosity of CO<sub>2</sub> by 2.5 at 1wt% and 10'/day in a 125 mD Berea sandstone core**

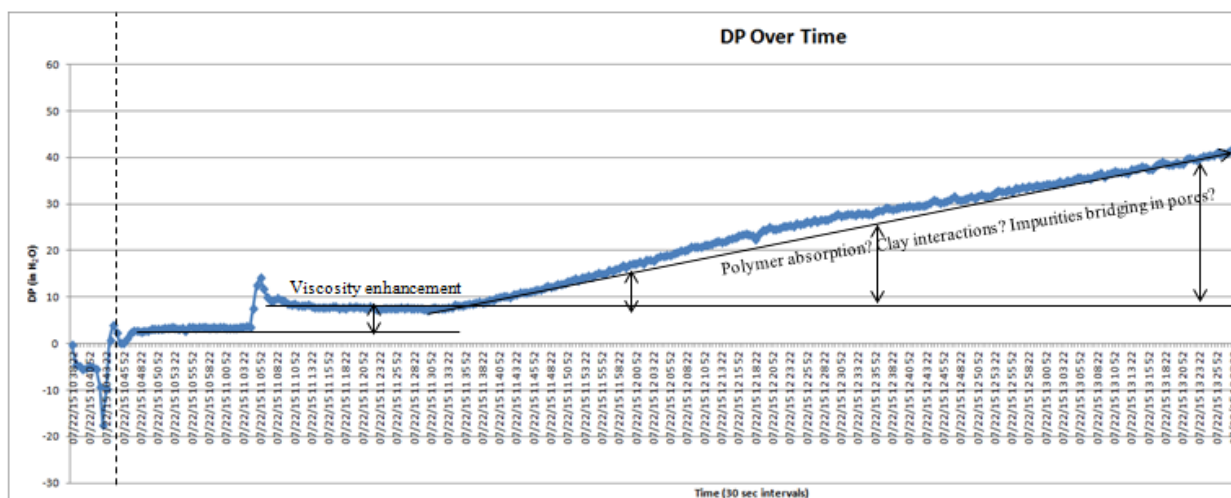
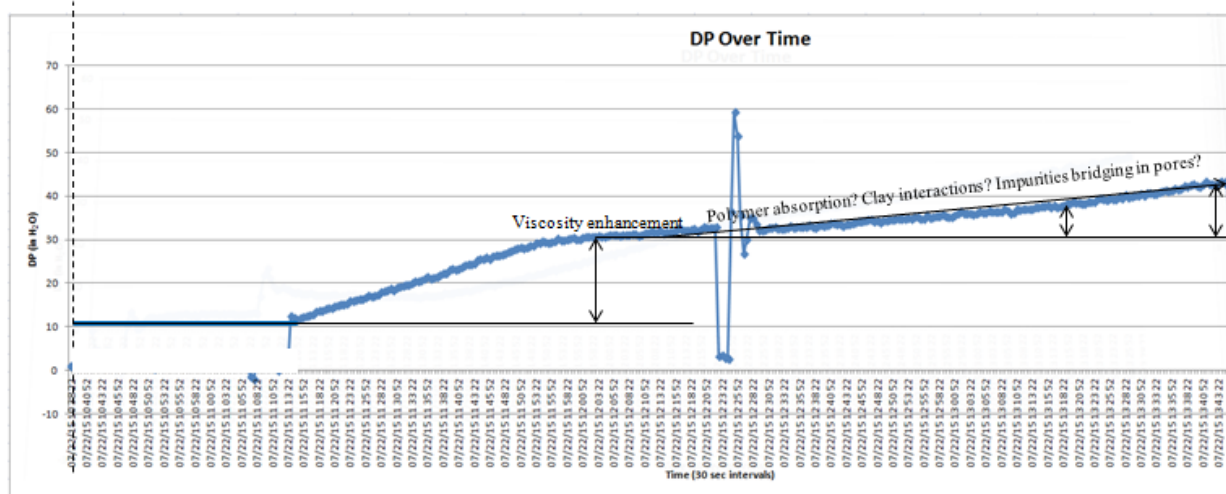


**Figure 10.4.1** Pressure drop as a function of time for the displacement of pure CO<sub>2</sub> from a 125 mD Berea core by a solution of 1wt% PFA in CO<sub>2</sub> at the same T and P. The initial increase in viscosity was commensurate with that expected from thickening, however the subsequent increase in pressure drop was attributed to PFA adsorption.

**1wt% high MW PFA (250000) increased the viscosity of CO<sub>2</sub> by 4 at 1wt% and 10'/day in a 285 mD Berea sandstone core**



It appears that the increase in viscosity is attributable to viscous CO<sub>2</sub> and some type of rock-polymer interaction or slowly accumulating CO<sub>2</sub>-insoluble entrained particles bridging across pores

**Figure 10.4.2 Pressure drop as a function of time for the displacement of pure CO<sub>2</sub> from a 285 mD Berea core by a solution of 1wt% PFA in CO<sub>2</sub> at the same T and P. The initial increase in viscosity was commensurate with that expected from thickening, however the subsequent increase in pressure drop was attributed to PFA adsorption.**

In order to determine if this long-term continual increase in pressure drop was attributed to very small solid impurities in the PFA, the synthesis was changed to that provided in Section 10.2. The original synthesis of PFA was done using an emulsion polymerization step that involved CO<sub>2</sub>-insoluble surfactants that were “washed” out of the final product, however there was a chance that some of the surfactant remained in the PFA. Therefore we developed a surfactant-free bulk polymerization method (detailed in Section 10.2) that yielded transparent, amorphous PFA samples. Further, SCAL installed very fine, high pressure fabric filters prior to the core inlet. These methods assured the team that there were no particles present in the PFA that were responsible for this long term. There was no reason to suspect that the change in permeability was due to clay swelling due to interactions with CO<sub>2</sub> or PFA.

Therefore any pressure increases observed in subsequent tests would be attributed to PFA adsorption and changes in wettability and permeability, and possibly the blockage of small pore throats due to the adsorbed PFA. In all cases, the PD1x-x notation is a representation of the batch of PFA used for the test.

Subsequent displacements were conducted by SCAL using a system represented by Figure 10.4.3. In all tests, the concentration of PFA in  $\text{CO}_2$  within the mixture was controlled to 1 wt% PFA. During the displacement, pure  $\text{CO}_2$  was introduced to the mixer as the  $\text{CO}_2$ -PFA solution was withdrawn from this 600 ml continuous stirred tank mixer (CSTM). Therefore the 1 wt% PFA in  $\text{CO}_2$  solution was diluted during the experiment. A material balance on this transient system was used to demonstrate that the concentration of PFA in  $\text{CO}_2$  ( $C$ ) could be calculated using the following equation;

$$C = 1 \text{ wt\% exp} (- V_{\text{CO}_2, \text{ml}} / 600 \text{ ml}) \quad \text{eq 1}$$

For example, the pore volume of the core was 70 ml. After the injection of 1 PV of pure  $\text{CO}_2$ ,

$$C = 1 \text{ wt\% exp} (-70 / 600) = 0.89 \text{ wt\%} \quad \text{eq 2}$$

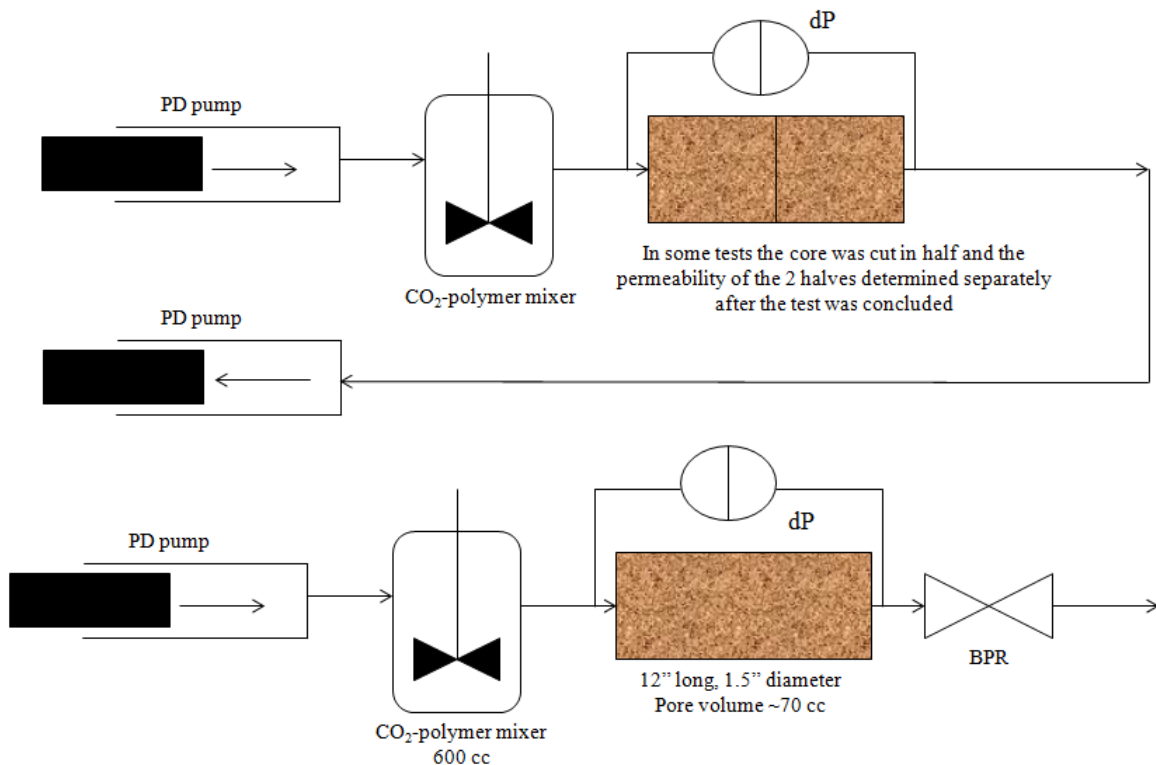
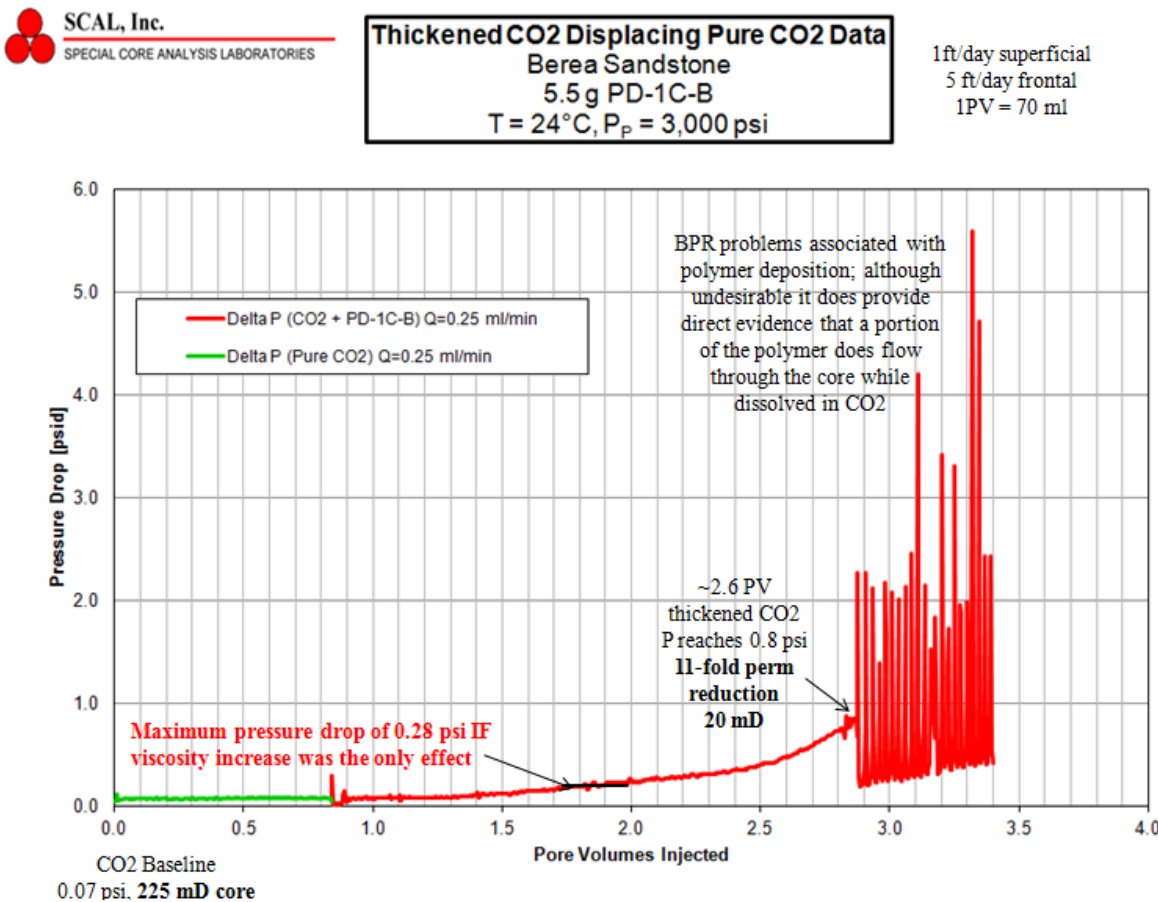


Figure 10.4.3 Configuration of the core flooding apparatuses used at SCAL

The core was initially filled with CO<sub>2</sub>. Figure 10.4.4 shows pure CO<sub>2</sub> was displaced into the cell (green data), followed by thickened CO<sub>2</sub> (the CO<sub>2</sub>-PFA solution, red data), which was to be followed by a “chaser” of pure CO<sub>2</sub>. This test exhibited dramatic increases in pressure drop; far beyond those induced by the increased viscosity. In this first test, there were difficulties associated with the BPR. Therefore, as shown in the following figure, the test was ended prematurely. Nonetheless, this experiment yielded two important results. First, baseline pressure drop for the core with pure CO<sub>2</sub> flowing through it was 0.07 psi. Therefore, if viscosity enhancement was the only effect of PFA, then the pressure drop should have increased to only about 0.28 psi; a 4-fold increase. But the pressure drop increased to about 0.8 psi before erratic data was reported. This 11-fold increase was much greater than 4, indicating that something other than viscosity enhancement was occurring in the core, and a reduction in core permeability was occurring. Secondly, PFA was found within the BPR. The pressure drop associated with the BPR caused the sticky PFA polymer to “gum up” the BPR. This provided direct evidence that a portion of the PFA remained in solution as it passed through the core.



**Figure 10.4.4** Baseline of pure CO<sub>2</sub> flow through the core (green data) followed by displacement of CO<sub>2</sub> from Berea sandstone core by a 1wt% solution of PFA (batch PD1c-B) in CO<sub>2</sub> (red data) Test conducted at effluent pressure (BP) of 3000 psi and 24 °C. BP controlled by a BPR set at 3000 psi. Although the test ended early due to BPR problems, the accumulation of PFA within the BPR provided direct evidence that a portion of the PFA remained in solution as it passed through the core.

It should be noted that several tests were made to do a PFA material balance to determine the amount of PFA adsorption and the amount that passed through the core. However, when the cores were removed from the core holder, some particles of the core fell off. Therefore we could not accurately attribute changes in the weight of the core to PFA retention. Secondly, PFA is a very sticky polymer and it was not possible to easily remove the PFA from the components of the tubing, core holder and BPR. Lastly, it was difficult to remove PFA from the PD pump that received the core effluent in the subsequent tests.

In the following test, depicted in Figure 10.4.5, the BPR was replaced with PD pump running in reverse that received the core effluent at a constant pressure of 3000 psi. This resulted in a superior ability to control the experiment. The (initial segment, green data line) baseline pressure drop of 0.10 psi for the CO<sub>2</sub> pressure drop would have increased to only 0.4 psi during the injection of the CO<sub>2</sub>-PFA solution (second segment, red data), but the pressure drop actually increased to ~11 psi after 3 pore volume (PV) of thickened CO<sub>2</sub> were injected, a 110-fold increase after 3 pore volumes injected (PVI). In order to separate the effect of viscosity from the effect of adsorption, 3 PV of pure CO<sub>2</sub> (third segment, green data) was then introduced to the core. Rather than the pressure drop returning to ~0.10 psi after the injection of several pore volumes of pure CO<sub>2</sub>, the pressure drop had only dropped to 8 psi. Therefore an 80-fold reduction in permeability had occurred due to the adsorption or retention of PFA by the core. Further, this indicated that even though pure CO<sub>2</sub> was injected into the core at a pressure significantly greater than the cloud point pressure for dilute solutions of PFA in CO<sub>2</sub>, the CO<sub>2</sub> was not removing significant amounts of PFA from the rock. This indicated that the adsorption was strong and/or the mixing in the pores was weak, both of which would have made it difficult to remove the retained PFA. In an attempt to break any PFA bridges that may have formed and to enhance mixing within the pre space, the CO<sub>2</sub> was then injected at a flow rate that was 10-times greater than the original flow rate (fourth segment, purple data). The pressure drop did not increase by a factor of 10, however, but only by a factor of about 2 from 7.5 to 15 psi. This provided indirect evidence that PFA had been removed from the core and/or some of the pore blockages had been removed. In order to verify this, pure CO<sub>2</sub> was then introduced to the core at the original, slower flow rate (fifth segment, green data), which resulted in the pressure drop approaching 3 psi, which was still 30-times greater than the original pressure drop but less than the 80-fold increase at the end of the prior pure CO<sub>2</sub> slug. Therefore, PFA adsorption and/or retention was still Affecting the core. The final attempt to recover permeability was realized by flowing CO<sub>2</sub> through the core in the reverse direction at the elevated flow rate that was 10-times greater than the original flow rate (sixth segment, gold data; this equipment modification is not illustrated in Figure 10.4.3); the core was not de-pressurized during this step. The erratic pressure drop data and the reduction in average pressure drop indicated that this process did remove a portion of the PFA. Finally, pure CO<sub>2</sub> was introduced to the core in the reverse direction at the original low flow rate (seventh segment, blue data), and the pressure drop attained 0.45 psi, which is 4.5 times greater than the original pressure drop in the forward direction.

These results in Figure 10.4.5 indicate that (a) a portion of the PFA remains in solution and passes through the core, (b) a portion of the PFA adsorbs strongly and irreversibly on the rock surfaces, reducing permeability, and (c) a portion of the PFA apparently forms solid bridges across pore throats that can be mechanically removed by dramatic increases in flow rate in or reversals of flow direction and possibly by re-dissolution into  $\text{CO}_2$ .

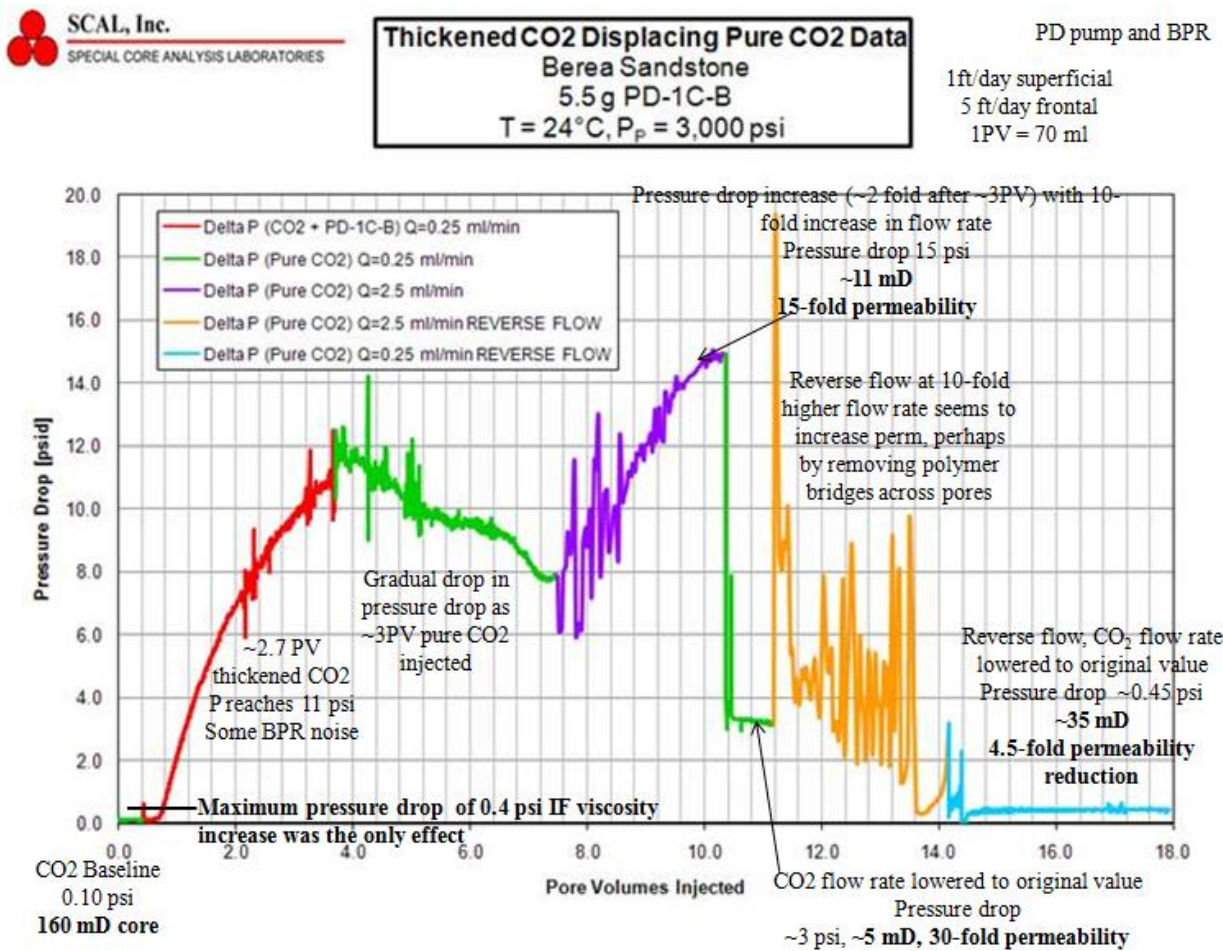
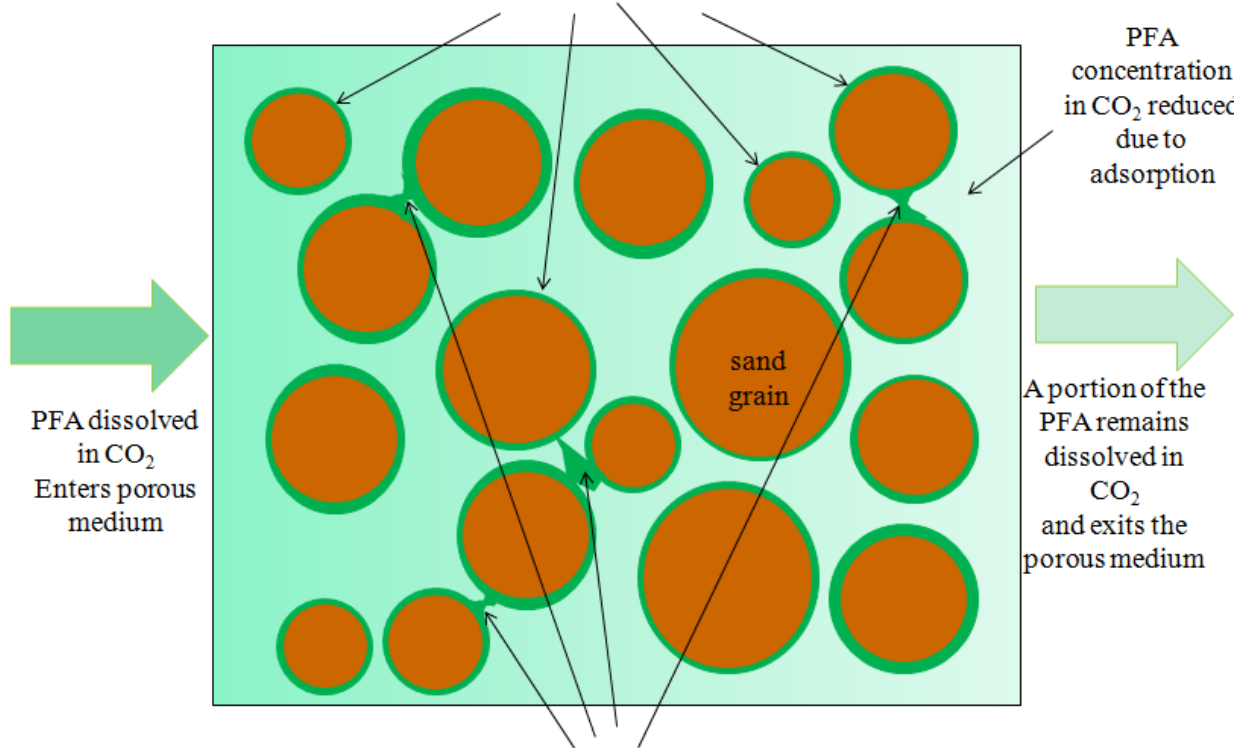


**Figure 10.4.5** Baseline of pure  $\text{CO}_2$  flow through the core (green data) followed by displacement of  $\text{CO}_2$  from Berea sandstone core by a 1wt% solution of PFA (batch PD1c-B) in  $\text{CO}_2$  (red data), followed by a chaser of pure  $\text{CO}_2$  (green data), followed by a chaser of  $\text{CO}_2$  at a 10-times higher flow rate (purple data); followed by a chaser of pure  $\text{CO}_2$  (green data); followed by reverse flow of  $\text{CO}_2$  through the core at 10-times higher flow rate (gold data); followed by flow of pure  $\text{CO}_2$  through the core in the original direction and at the original flow rate (blue data). Test conducted at effluent pressure (BP) of 3000 psi and  $24^\circ\text{C}$ . BP controlled by a PD pump set at 3000 psi.

Figure 10.4.6 provides a conceptual illustration of this model of PFA retention by a core.

A portion of the PFA adsorbs irreversibly onto the rock surfaces, making the porous medium hydrophobic and oil-phobic, and greatly reducing permeability



A portion of the PFA forms bridges across pore throats; these “reversible” PFA deposits can be removed by increases in flow rate, flow direction reversal, and/or re-dissolution in  $\text{CO}_2$

**Figure 10.4.6. Proposed model of the fate of the PFA that enters the core. The PFA either (a) remains dissolved in  $\text{CO}_2$ , (b) deposits reversibly between grains, or (c) adsorbs irreversibly onto the rock surface**

The following experiments on Berea sandstone core also confirm that at least a portion of the retained PFA is mobile or removable or reversible, as shown in Figure 10.4.6. Experimental data used to generate Figure 10.4.7 indicates that the initial pressure drop data for the 1 PVI baseline of pure  $\text{CO}_2$  was lost. However, the baseline initial pressure drop of 0.39 psi for pure  $\text{CO}_2$  was deemed a reasonable estimate based on the supplier’s permeability value. The pressure drop data for the 3 PVI of thickened  $\text{CO}_2$  ( $\text{CO}_2$ -PFA solution) was also lost. The recovered data shows that for the following 3.4 PVI of pure  $\text{CO}_2$ , the pressure drop was relatively flat and reached 20 psi. The team then decided to stop flow for 20 minutes. When flow of thickened  $\text{CO}_2$  was then initiated, the pressure drop fell to only 2 psi. This may have been caused by re-dissolution of PFA into the  $\text{CO}_2$  and/or migration of the PFA deposits within the core. Permeability reduction, as evidenced by a steadily increasing pressure drop, occurred thereafter (red data used a pressure transducer for pressure drop; black data used the pump pressure gage to determine pressure drop).

**Thickened CO<sub>2</sub> Displacing Pure CO<sub>2</sub> Data**  
Berea Sandstone  
3.227 g PD-1C-B, 2.273 g PD-1C-A  
T = 24°C, P<sub>P</sub> = 3,000 psi

4 ft/day superficial  
20 ft/day frontal  
1PV = 70 ml

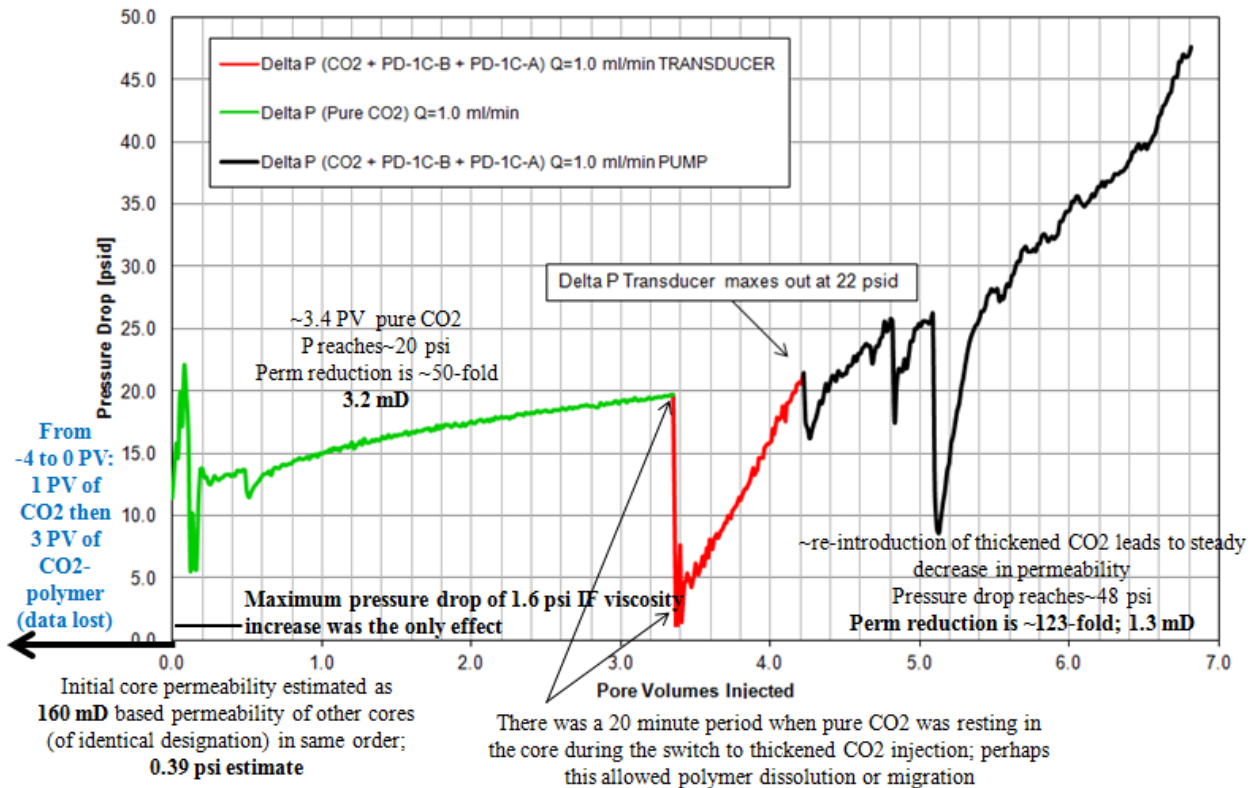


Figure 10.4.7 Data for first 4 PVI lost (1 PV of CO<sub>2</sub> followed by 3 PVI thickened CO<sub>2</sub>). Subsequent CO<sub>2</sub> flow through the core (green data) followed by a 20 minute rest, followed by displacement of CO<sub>2</sub> from Berea sandstone core by a 1wt% solution of PFA (mix of two batches PD1c-A and PD1c-B) in CO<sub>2</sub> (red and black data). Test conducted at effluent pressure (BP) of 3000 psi and 24 °C. BP controlled by a PD pump set at 3000 psi. Lower pressure drops measured with a pressure transducer, higher pressure drops measured with pressure different of two gages.

The results for the following experiment, shown in Figure 10.4.8, exhibited a similar reduction in pressure drop with a 22-minute rest with pure CO<sub>2</sub> in the core. Even after this reduction, however, the core was 120-times less permeable to CO<sub>2</sub> than it was originally. This clearly affirms that a portion of the PFA deposition/retention is reversible, while another portion that led to a 120-fold permeability reduction is essentially irreversible.

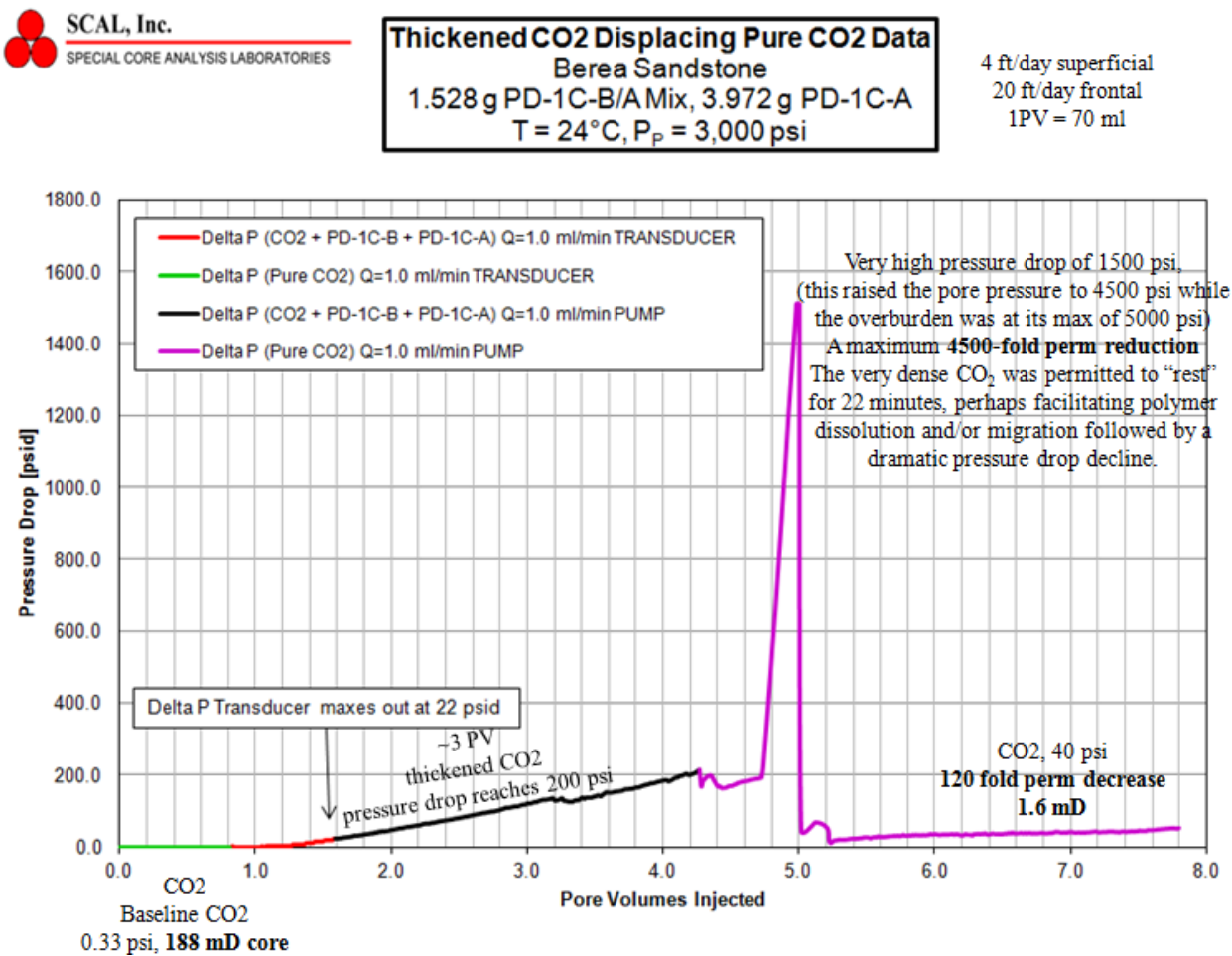


Figure 10.4.8 Baseline pure CO<sub>2</sub> through the core (green data), followed by displacement of CO<sub>2</sub> from Berea sandstone core by a 1wt% solution of PFA (mix of two batches PD1c-A and PD1c-B) in CO<sub>2</sub> (red and black data), followed by the injection of pure CO<sub>2</sub> (purple). Test conducted at effluent pressure (BP) of 3000 psi and 24 °C. BP controlled by a PD pump set at 3000 psi. Test stopped at 5 PVI when the pressure difference between the inlet CO<sub>2</sub> (4500 psi) and the overburden fluid around the sleeve (5000 psi) reached the 500 psi minimum.

## Wettability changes in the porous media induced by PFA adsorption

A simple ambient pressure wettability study was conducted on this Berea Sandstone core after testing, Figure 10.4.9. Initially (top of Figure 10.4.9), drops of mineral oil and brine quickly spread onto the flat ends of the core. The dry core was easily wet by both fluids.

However, after the completion of a test in which  $\text{CO}_2$  flowed through the core, followed by PFA- $\text{CO}_2$  solution, the core was slowly vented. Drops of brine and mineral oil “beaded up” on both ends of the core, with the effect being more distinct for mineral oil on the inlet face, as shown at the bottom of Figure 10.4.9. The results, shown in the following diagram, clearly indicate that a PFA fluoropolymer coating had been applied to the entire surface area of the porous media; rendering the surface of this porous medium both hydrophobic and oil-phobic.

### The initial wettability of a fresh Berea sandstone core



### Wettability after a $\text{CO}_2 + 1\%$ PFA solution flowed through the core; A portion of the PFA adsorbed onto the rock, causing dramatic wettability changes



Figure 10.4.9 Changes in the wettability of the inlet and outlet faces of the core due to the adsorption of PFA from a PFA- $\text{CO}_2$  solution.

Having firmly established that PFA was making the porous media more oil-phobic and hydrophobic while greatly reducing  $\text{CO}_2$  permeability, we turned our attention to “split core” tests in which the 1.5” diameter by 12” long cores were cut in half (forming two 1.5” diameter by 6” length cores) after the completion of the PFA- $\text{CO}_2$  tests. In these tests pure  $\text{CO}_2$  flowed through the core, followed by 5-7 PV of thickened  $\text{CO}_2$  (1 wt% PFA in  $\text{CO}_2$ ), followed by a chaser of at least 2 PV of  $\text{CO}_2$ . A single small half-core was then re-inserted in the core holder and its permeability to  $\text{CO}_2$  was determined. This was repeated for an Indiana Limestone core. Table 10.4.1 summarizes the results for various cores.

Core and Initial permeability of the 1.5” x 12” core to $\text{CO}_2$ at 3000 psi and 24 °C mD	$\text{CO}_2$ Permeability to $\text{CO}_2$ after the PFA- $\text{CO}_2$ flowed through the core	$\text{CO}_2$ permeability of the inlet half-core after the large core was vented and cut in half	$\text{CO}_2$ permeability of the outlet half- core after the large core was vented and cut in half	Range of contact angle for drops of water at various positions on the inlet and outlet faces of the core (no correlation to the core or the face) degrees	Contact angle for drops of oil at various positions on the inlet and outlet faces of the core (no correlation to the core or the face) degrees
Berea SS 188	5.8	11	152	33-65	33-50
Indiana LS 116	0.36	0.28	23.5	33-65	33-50

**Table 10.4.1 Changes in the permeability and contact angle of half cores obtained after  $\text{CO}_2$ -thickened  $\text{CO}_2$ - $\text{CO}_2$  displacement experiments were conducted and the 1.5” x 12” core was vented and then cut in half**

It appears that the additional chaser of  $\text{CO}_2$  reduced the amount of PFA retained by the core, resulting in less dramatic wettability alteration shown in the following figure (relative to the wettability changes shown in Figure 10.4.9.) However, there was no correlation of wettability changes with respect to which core was being tested or what position in each core was evaluated. In both tests, however, the reduction in permeability was more dramatic for the inlet half of the core than the outlet half. The wettability changes are illustrated in Figure 10.4.10.

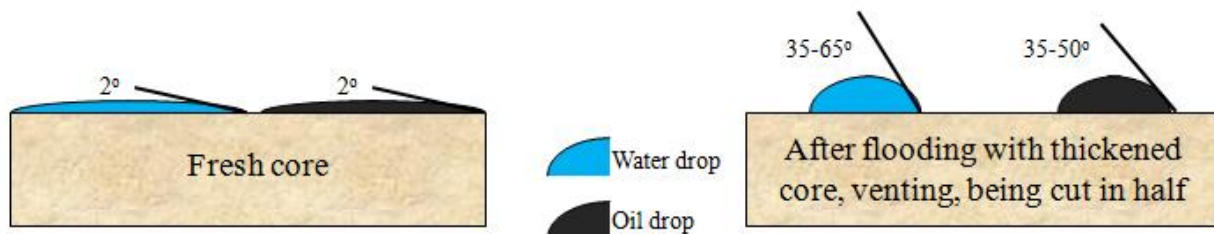


**Figure 10.4.10 Summary of contact angle changes and permeability reductions cause by PFA- $\text{CO}_2$  solutions on each half of the core**

The “lessons learned” from this extensive set of core floods, in which only neat CO<sub>2</sub> and/or thickened CO<sub>2</sub> (CO<sub>2</sub> + 1% PFA solutions) were present in the core are:

1. The increase in pressure drops associated with the injection of CO<sub>2</sub> + fluoroacrylate-based polymers into sandstone or limestone greatly exceeds the 4-fold change associated solely with increased viscosity.
2. A portion of the dissolved polymer remains in solution and flows through the core and thickens the CO<sub>2</sub>.
3. A portion of the polymer strongly adsorbs onto the surface of the rock, significantly reducing its permeability and altering its wettability (increasing hydrophobicity and oil-phobicity).
4. A portion of the polymer is more weakly retained by the rock and can be removed by reversing CO<sub>2</sub> flow direction, greatly increasing the pressure of CO<sub>2</sub> flowing into the core especially with a “rest” period, increasing the velocity of the CO<sub>2</sub> flowing through the core, and/or venting the core.
5. Due to the polymer retention, the pressure drop across the core increases continually with CO<sub>2</sub>-PFA solution injection (even though the concentration of polymer in CO<sub>2</sub> is dropping slightly due to dilution of the original 1% solution in the mixer).
6. There are significant concerns associated with the use of PFA for mobility control because PFA solubility in CO<sub>2</sub> is reduced by the presence of light extracted hydrocarbons, and the permeability reductions caused by these solutions are so incredibly high.
7. Although PFA-CO<sub>2</sub> can be expected to yield improved nobility control and oil recovery from a core (as will be proven in the following section of this report), it is likely that the associated pressure drops will be excessively high for an in-depth mobility control use.
8. PFA may prove to be the first known example of a CO<sub>2</sub>-soluble conformance control agent that can be used to “block” thief zones and thereby divert subsequently injected pure CO<sub>2</sub> into lower-perm oil-rich zones. Given the substantial hydrophobicity imparted to the cores, it is very likely that permeability to water may also be reduced. However, this can only be ascertained by displacements involving brine that demonstrate the permeability of the porous media to brine is reduced (to be detailed sections of this report following the oil displacements).

## 10.5 Core floods: CO<sub>2</sub> or thickened CO<sub>2</sub> displacing crude oil

The next set of core flood tests was designed to illustrate the effect of injecting CO<sub>2</sub>-PFA solutions into cores initially saturated with dead crude oil. The Berea sandstone cores were saturated with filtered dead SACROC crude oil provided by Kinder Morgan.

Figure 10.5.1 illustrates the results when the core was flooded with CO<sub>2</sub> at a pressure of 3000 psi, a value that is well above the minimum miscibility pressure (MMP) of 1614 - 2350 psia at 54.4 °C reported in the literature. Because MMP decreases with decreasing temperature, our conditions of 3000 psi at 23 °C were sufficient to ensure miscible displacement. The CO<sub>2</sub> was injected at a constant rate of 0.25 ml/min and the core effluent pressure was maintained at 3000 psi.

When neat CO<sub>2</sub> was used to displace the oil, approximately 80% of the oil was recovered from the Berea core, as shown by the blue data line in Figure 10.5.1, below. CO<sub>2</sub> breakthrough occurred at approximately 0.12 PVI (the PVI value at which the production of oil becomes less than the injection of CO<sub>2</sub>).

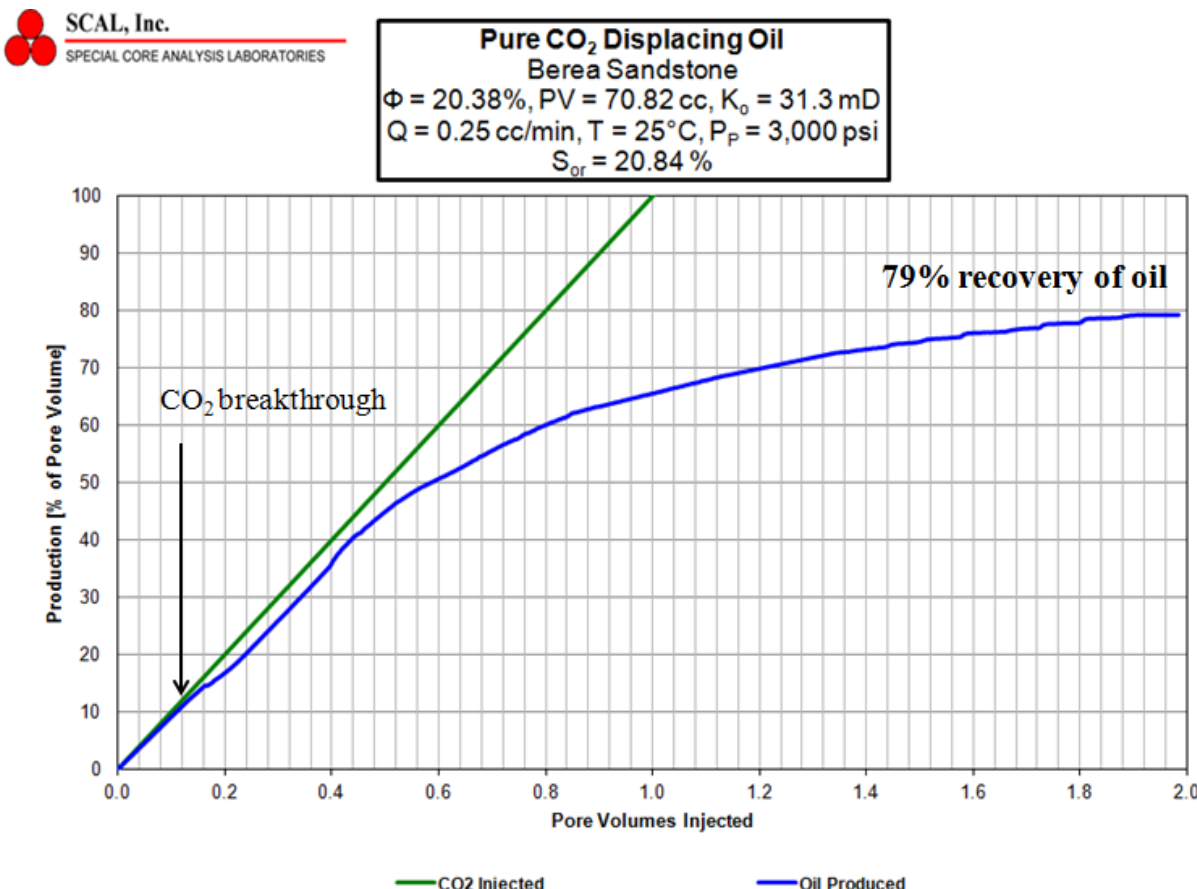
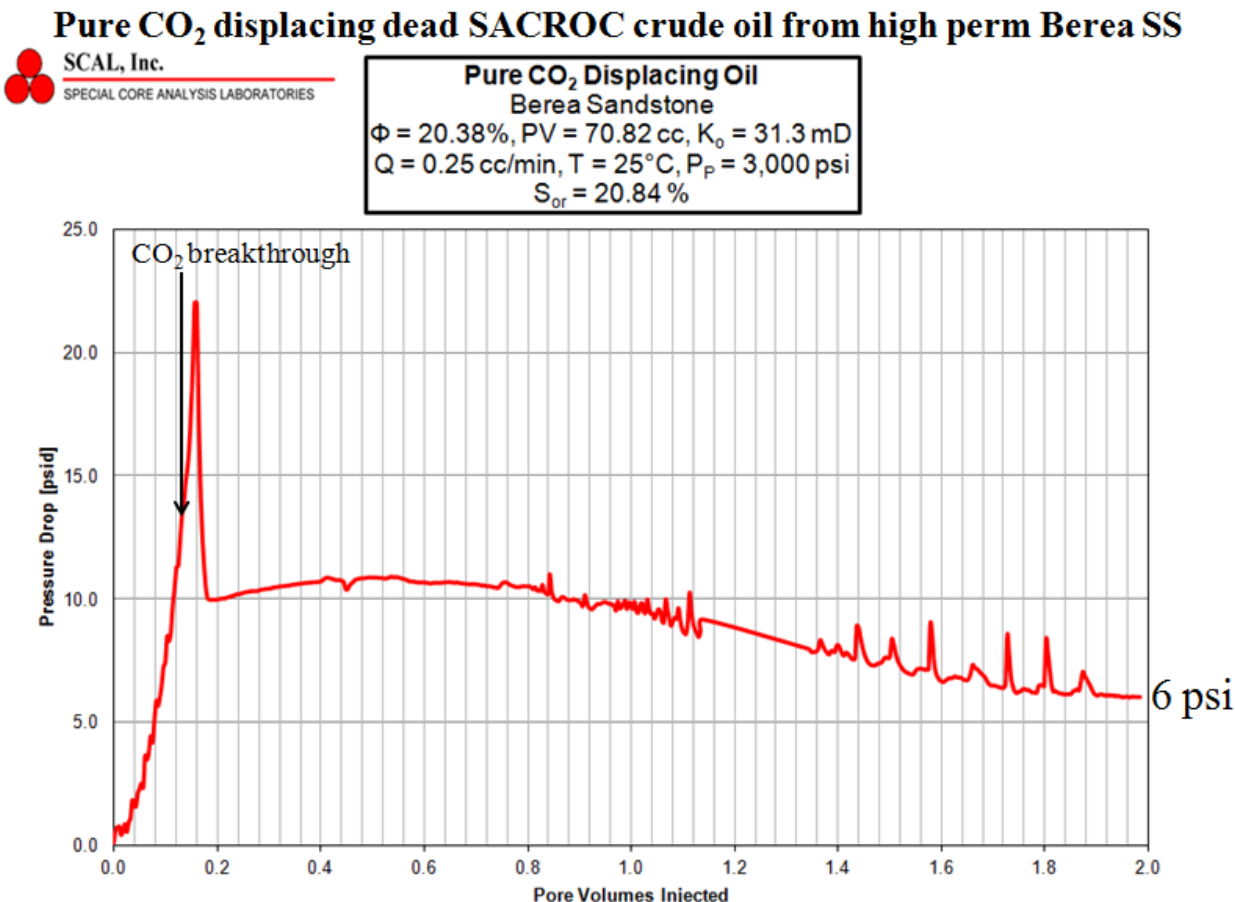


Figure 10.5.1 Recovery of dead SACROC oil from a Berea SS core by CO<sub>2</sub> at 25 °C and 3000 psi. About 79% of the oil is ultimately recovered.

As shown in the Figure 10.5.2 the pressure drop for this test reached a maximum just after  $\text{CO}_2$  breakthrough and decreases quickly at first and then gradually to about 6 psi when oil recovery has leveled off.



**Figure 10.5.2 Pressure drop vs PVI  $\text{CO}_2$  for the same test; recovery of dead SACROC oil from a Berea SS core by  $\text{CO}_2$  at 25 oC and 3000 psi. About 79% of the oil is ultimately recovered. The spike in pressure drop occurs just after  $\text{CO}_2$  breakthrough.**

As shown in Figure 10.5.3, when the test was repeated with a solution of 1 wt% PFA in  $\text{CO}_2$ , a significant increase in oil recovery (from 79% to 95%) occurred (blue data line, Figure 10.5.3), due to increased viscosity and/or changes in rock wettability. Such a substantial increase in oil recovery in a small core is a promising sign for a mobility control agent. However, the price paid for this improvement in sweep efficiency was a very dramatic increase in pressure drop, as illustrated in Figure 10.5.4. At the end of the test the pressure drop across the core was 160 psi as a result of polymer adsorption and/or precipitation. If the viscosity increase was the only effect, the maximum pressure drop should have been only four times greater, or 24 psi. Because more of the core was filled with  $\text{CO}_2$ , the relative permeability of  $\text{CO}_2$  would have been greater, further reducing the pressure drop below 24 psi. The fact that the pressure drop was roughly 160 psi at the end of the test is yet another indication that the  $\text{CO}_2$ -PFA solutions are best suited for near-wellbore conformance control via reducing the permeability of watered out thief zones, rather than in-depth mobility control within oil bearing zone.

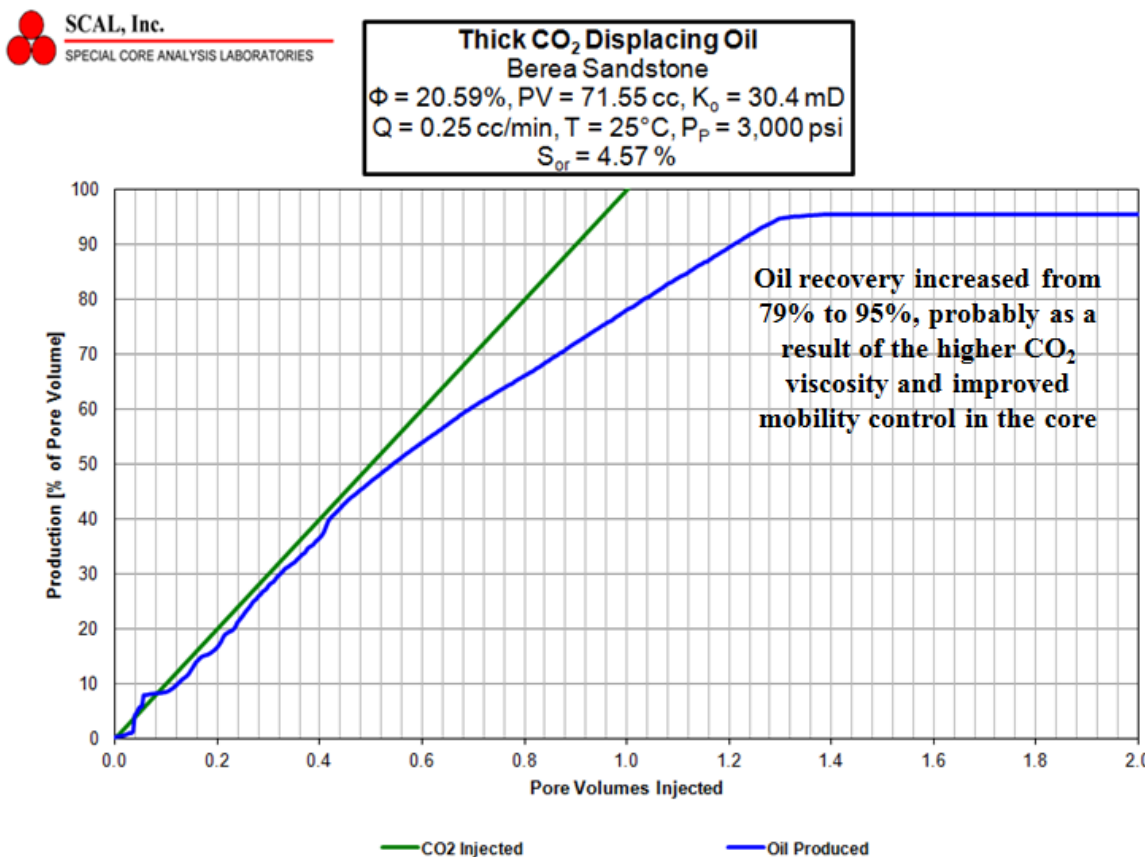


Figure 10.5.3 Recovery of dead SACROC oil from a Berea SS core by thickened  $\text{CO}_2$  at  $25^\circ\text{C}$  and 3000 psi. About 95% of the oil is ultimately recovered.

The lessons learned from these experiments

1.  $\text{CO}_2$  -PFA solutions do provide increased mobility control and greater oil recovery in small cores, but at a “price”.

**Thick CO<sub>2</sub> Displacing Oil**  
Berea Sandstone  
 $\Phi = 20.59\%$ ,  $PV = 71.55$  cc,  $K_0 = 30.4$  mD  
 $Q = 0.25$  cc/min,  $T = 25^\circ\text{C}$ ,  $P_P = 3,000$  psi  
 $S_{or} = 4.57\%$

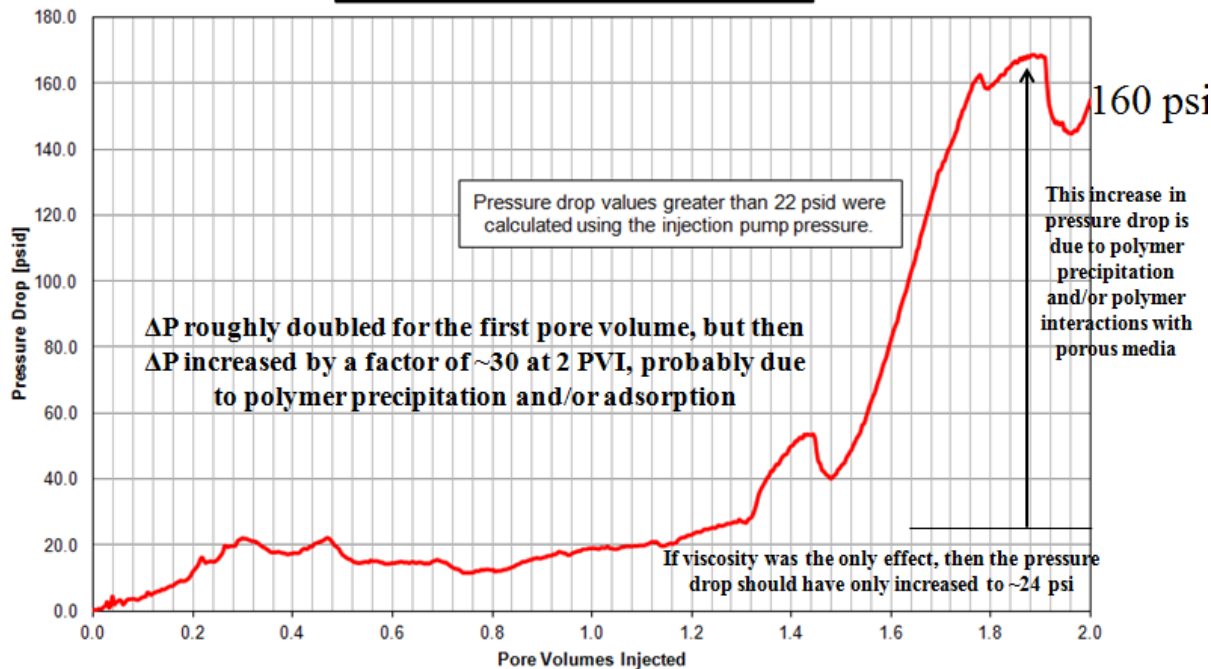


Figure 10.5.4 Pressure drop v. thickened PVI CO<sub>2</sub> for the same test; recovery of dead SACROC oil from a Berea SS core by CO<sub>2</sub> at 25 oC and 3000 psi. About 95% of the oil is ultimately recovered.

2. Light alkanes act as anti-solvents for PFA and the extraction of light alkanes into the CO<sub>2</sub>-rich phase will cause a portion of the PFA to precipitate. It appears that enough PFA remained in solution to give increased viscosity, but enough of the PFA adsorbed or precipitated to induce marked reductions in permeability and increases in pressure drop for a given volumetric flow rate. If the core was longer, or if a pilot test was conducted in a single injection well, it is expected that an increasing amount of the PFA would either precipitate due to the presence of alkanes in the CO<sub>2</sub>-rich phase while the PFA continued to adsorb. This would make mobility control untenable, but it would actually favor near-wellbore conformance control. (This effect cannot be substantiated, however, until the tests conducted with brine – which would be the fluid within a thief zone – are conducted; these results will be presented in the next section of this report.)
3. The pressure drop required to recover oil from the cores increased from 6 psi for neat CO<sub>2</sub> to 160 psi for thickened CO<sub>2</sub>; far greater than the 4-fold increase to 24 psi expected if increased viscosity was the only effect. This is more evidence that dramatic changes in rock properties (reduced permeability) were occurring due to PFA interactions with the porous media.
4. These results indicate that PFA is better suited for conformance control than mobility control.

## **10.6 Core floods: CO<sub>2</sub> or thickened CO<sub>2</sub> displacing brine**

In these proof-of-concept core floods, we wanted to select porous media that exhibited signs of fingering or preferential CO<sub>2</sub> flow through high permeability bedding planes in the core because these types of cores would probably show the benefit of a CO<sub>2</sub> thickener most convincingly.

The superficial velocity/injection rate for the cores, which were 12" long and 1.5" diameter, was then established. For a porosity of 20%, the pore volume is ~70 ml (cc, cm<sup>3</sup>), therefore at an injection rate of 0.25 ml/min the frontal velocity is 5 ft/day injection and the injection of 1 pore volume (PV) will take ~280 minutes. This was a reasonable duration logically for SCAL that corresponded to a reasonable frontal velocity for an EOR study, therefore our team selected a baseline volumetric flowrate of 0.25 cm<sup>3</sup>/min. For longer tests either 0.25 or 1.0 cm<sup>3</sup>/min was selected.

The CO<sub>2</sub> thickener performance should not be affected by the brine composition because PFA is completely insoluble in brine. Therefore Pitt and SCAL team members decided to use a representative synthetic brine composition for these tests that will have enough salinity to prevent any core damage via clay swelling. The brines used contained 2-4 wt% KCl in water.

These core floods were intended to be proof-of-concept displacements that were conducted in order to understand the behavior of thickened CO<sub>2</sub> flowing into a brine-saturated core. Therefore we did not conduct these tests over a wide range of reservoir temperatures. Rather we conducted the displacement at 25°C, even though it is lower than typical reservoir temperatures.

Although no oil was used in this set of test, we decided to operate these CO<sub>2</sub>-displacing-brine core floods with a core effluent pressure that was consistent with the CO<sub>2</sub>-displacing-oil tests using dead SACROC crude oil. As previously explained, MMP values reported for SACROC oil at reservoir T of ~130° F (54.4° C) range from 1614 psia to 1850 psia, with one other report at 2350 psi. Therefore conducting the flood at 3000 psia will certainly yield miscibility at any temperature up to 54.4 °C. Further, this higher pressure allowed us to get better thickening of CO<sub>2</sub> at a given temperature for a fixed PFA concentration, as shown in Figure 10.2.3. Therefore the effluent core pressure was maintained at 3000 psi. The results are shown in Figure 10.6.1.

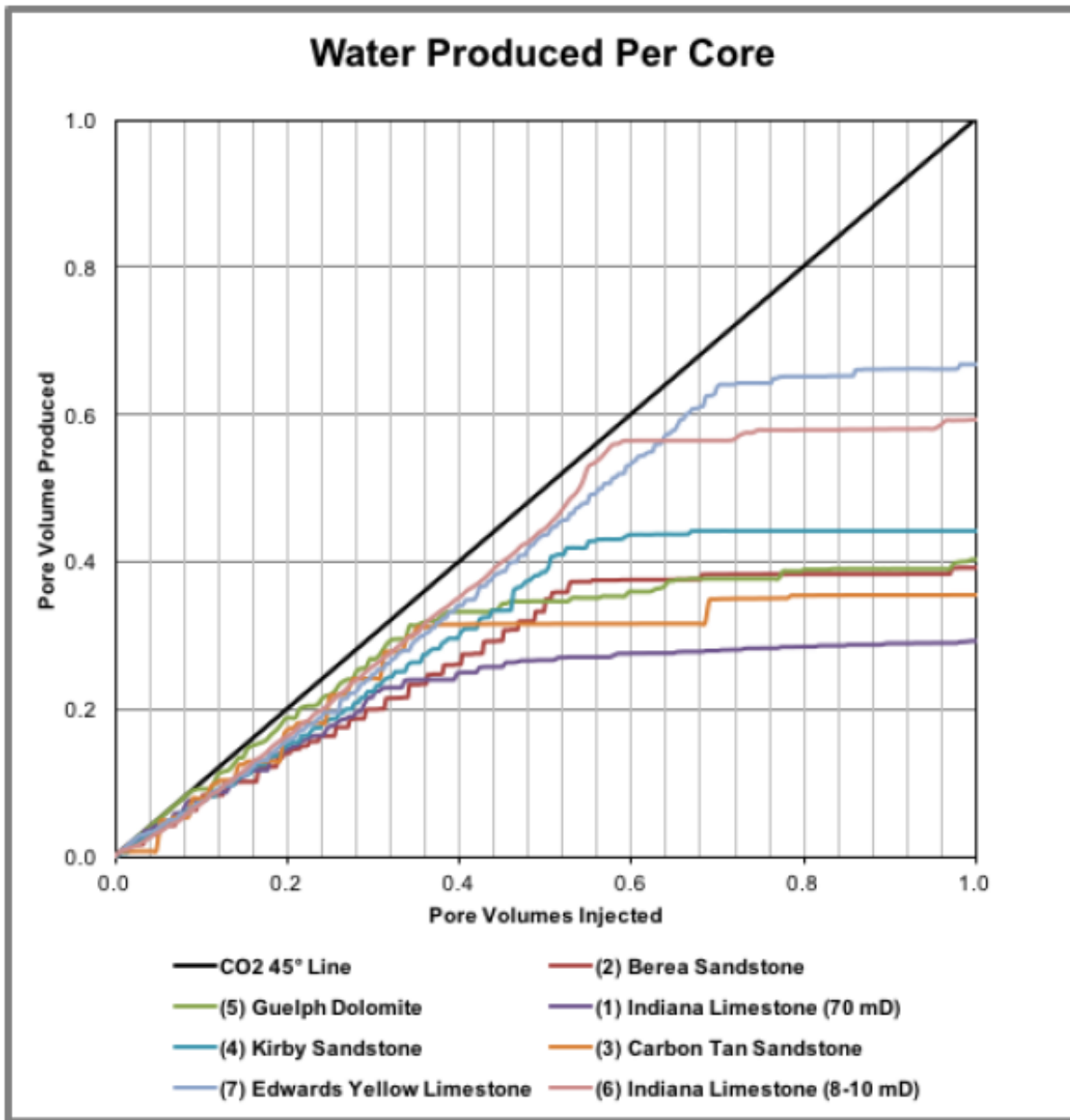


**Figure 10.6.1. CO<sub>2</sub>-displacing-brine water production results for the 7 cores**

Note that deviation of the water production from the 45° CO<sub>2</sub> reference line in the figure above is indicative of CO<sub>2</sub> breakthrough and subsequent production. Also, note that the asymptotic value of pore volume water produced corresponds to the saturation of CO<sub>2</sub> in the core. For example, the PV brine production for the 70 mD Indiana limestone core (purple line in figure 10.6.1, above) CO<sub>2</sub> breakthrough occurred after only 0.08 PVI CO<sub>2</sub> and after 1 PV of CO<sub>2</sub> injection leveled off at ~0.30. Therefore, the average CO<sub>2</sub> saturation remaining in the core at that time is ~0.30, and the average water saturation remaining in the core is about 0.70 or 70%.

Remember that in these proof-of-concept core floods, we wanted to select porous media that exhibited signs of fingering or preferential  $\text{CO}_2$  flow through high permeability bedding planes in the core because these types of cores will probably show the benefit of a  $\text{CO}_2$  thickener most convincingly. Therefore, we selected the **Indiana Limestone**, **Berea Sandstone**, and **Carbon Tan sandstone** for further testing. (Nominal values of permeability are provided for these cores in Table 10.3.1 and are listed at the top of the figures in the results. When actual permeability values for the specific cores used in each experiment were determined by SCAL, these permeability values were reported in the text, figure title or text boxes within the figure.)

In this set of  $\text{CO}_2$ -displacing-brine tests we began to more purposefully investigate the ability for the PFA- $\text{CO}_2$  solutions to reduce the permeability of the sandstone or limestone. Figure 10.6.2 illustrates the procedures used in these tests.



#### Control test

1. Saturate core with brine; flow brine through core
2. Inject  $\text{CO}_2$  through the core; measure water production; continue until steady state  $\text{S}_w,\text{ir}$  achieved
3. Inject water through the core until  $\text{S}_g,\text{res}$ ; measure  $\Delta P$ .

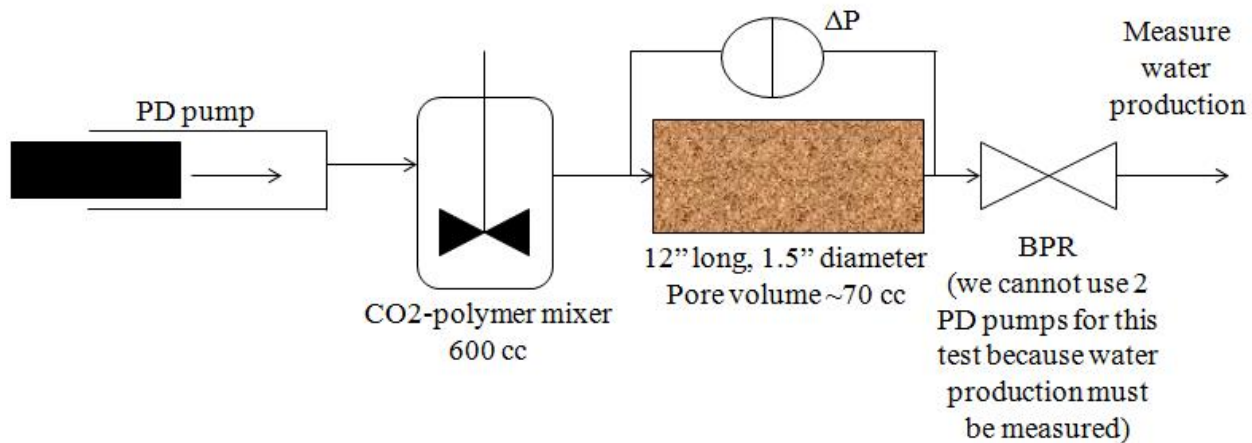
#### Effect-of-polymer test

1. Saturate core with brine; flow brine through core
2. Inject  $\text{CO}_2$  through the core; measure water production; continue until steady state  $\text{S}_w,\text{ir}$  achieved
3. Inject ( $\text{CO}_2$  + polymer) solution into the core
4. Inject  $\text{CO}_2$  through the core until steady state  $\text{S}_g,\text{res}$  attained
5. Inject water through the core

**Figure 10.6.2. Procedure for tests involving  $\text{CO}_2$  (or thickened  $\text{CO}_2$ ) displacing brine from a brine-saturated core**

Figure 10.6.3 illustrates the equipment layout used for these displacements. The back pressure was controlled with a BPR, rather than receiving the effluent fluids into a PD pump running in reverse, because the produced water and  $\text{CO}_2$  had to be separated and the volume of water production determined. In general, more care had to be taken when performing these experiments the BPR was used because the significant pressure reduction that occurs as the PFA- $\text{CO}_2$  solution flows through the BPR causes the PFA that remained in solution in the core effluent to precipitate in the BPR or just downstream of the BPR. These sticky PFA deposits can

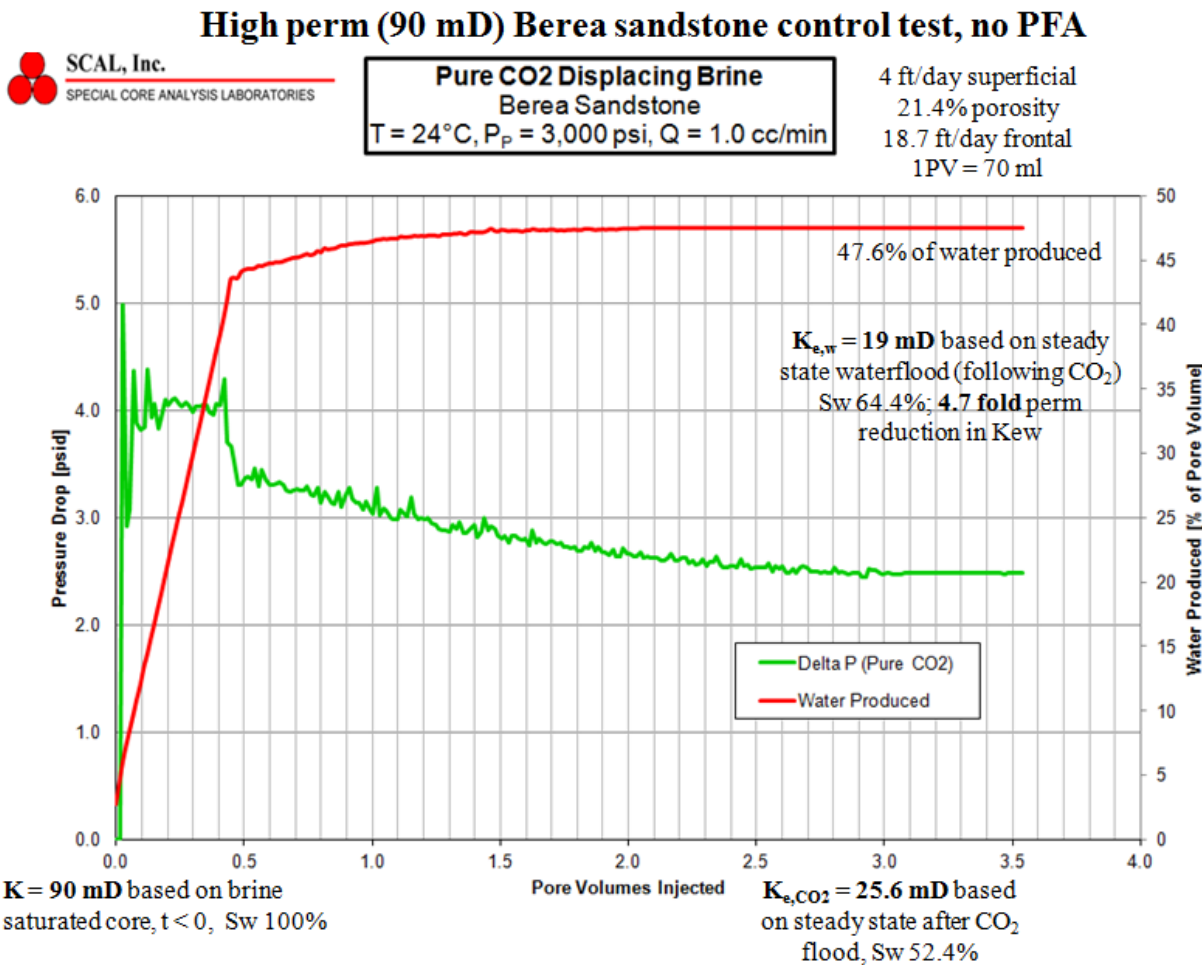
cause noise in the pressure pressure data. The BPR was carefully cleaned after each experiment.



**Figure 10.6.3. Equipment configuration for tests involving CO<sub>2</sub> (or thickened CO<sub>2</sub>) displacing brine from a brine-saturated core**

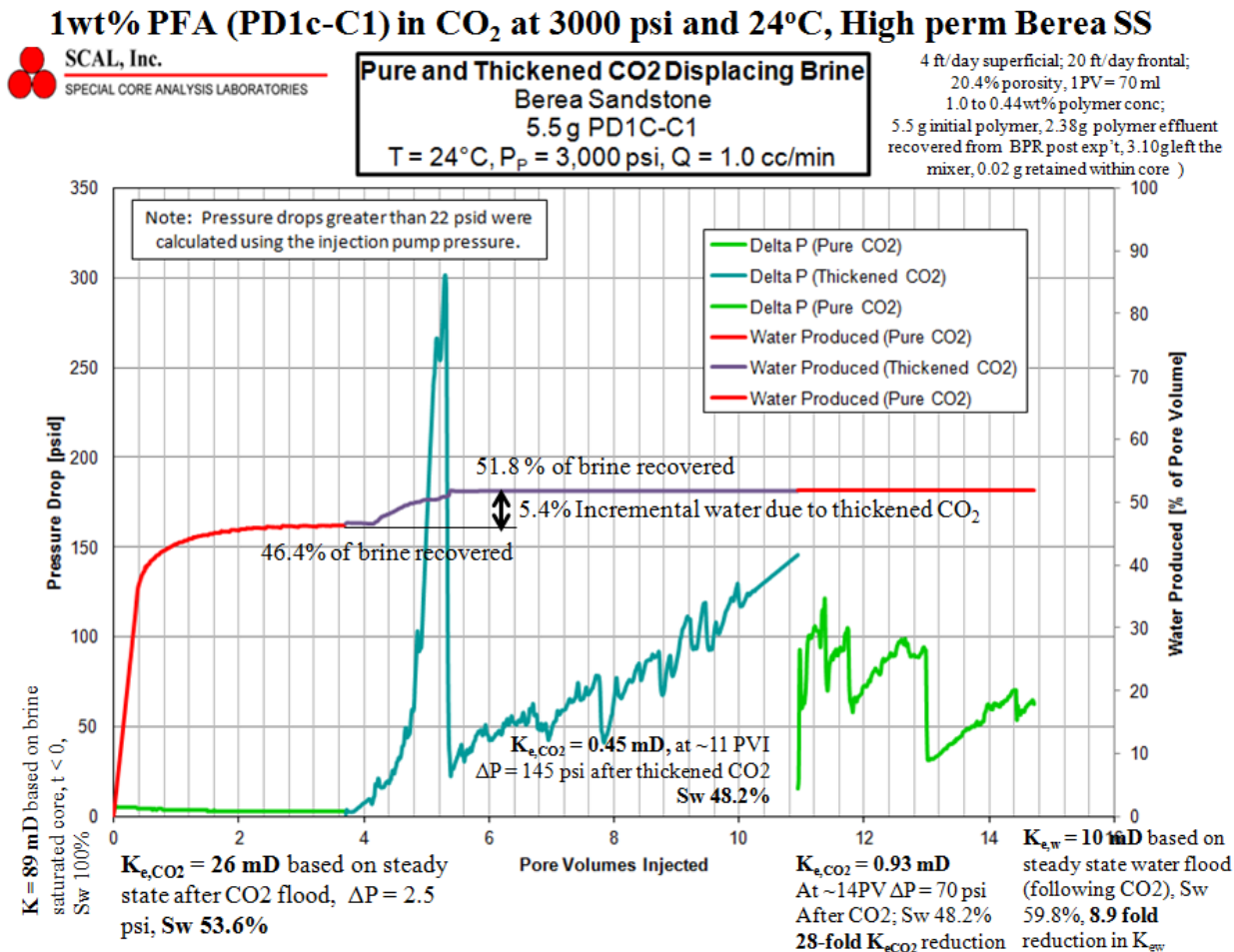
In this Berea sandstone (90 mD) test, meant to be qualitatively representative of a **high perm sandstone** test, CO<sub>2</sub> injection was followed by the injection of (PFA-CO<sub>2</sub> solution), followed by a chaser of pure CO<sub>2</sub>. This was followed by waterflooding the core. The intent was to determine if thickened CO<sub>2</sub> improved water displacement (mobility control) and/or resulted in significant reductions of CO<sub>2</sub> permeability (conformance control).

Figure 10.6.4 illustrates the results of the control test that involved no PFA; only CO<sub>2</sub> was used in this experiment. 47.6% of the water initially in the core was recovered (red data line), and the pressure drop leveled off at 2.5 psi (green data line).



**Figure 10.6.4. Pressure drop and water production vs. PVI CO<sub>2</sub> for CO<sub>2</sub> displacing brine from a 90 mD Berea sandstone core**

This experiment was repeated with a comparable high permeability Berea sandstone (89 mD). However, the injection of pure CO<sub>2</sub> (green data line) was followed by injection of thickened CO<sub>2</sub> (aqua data line) to determine if incremental water displacement occurred and if dramatic changes in the pressure drop occurred. The results are shown in Figure 10.6.5.



**Figure 10.6.5. Pressure drop and water production vs. PVI CO<sub>2</sub> for CO<sub>2</sub> and PFA-CO<sub>2</sub> displacing brine from an 89 mD Berea sandstone core**

Referring to Figure 10.6.5, the injection of thickened CO<sub>2</sub> resulted in the recovery of an additional 5.4% PV water, as the water recovery rose from 46.4% to 51.8% due to the injection of thickened CO<sub>2</sub>. This is indicative of improved mobility control. However, it also caused dramatic increases in pressure drop (the aqua data) as the pressure drop rose from only 2.5 psi after the pure CO<sub>2</sub> flood to a spike of 300 psi followed by a steady increase to 145 psi during the injection of 7 PV thickened CO<sub>2</sub>. When slightly more than 3 PV pure CO<sub>2</sub> was re-introduced to the core (green data) the pressure drop varied but was about 60 psi; indicative of a significant reduction in the permeability of the core. Therefore, although improved mobility control occurred, a very substantial reduction (28-fold) in the effective permeability of the core to CO<sub>2</sub> resulted, which indicated that the PFA may be more appropriate for conformance control.

In this Carbon Tan sandstone (8.4 mD) test, meant to qualitatively reflect a displacement in a **low permeability sandstone**, the control test involved only the injection of pure CO<sub>2</sub> into the core for the displacement of the brine (Figure 10.6.6). CO<sub>2</sub> injection (green data line) was followed a waterflood (the final waterflood data is not shown in the plot). Figure 10.6.6 illustrates the results of the control test that involved no PFA; only CO<sub>2</sub> was used in this experiment. 40.3% of the water initially in the core was recovered, and the pressure drop leveled off at 20 psi.

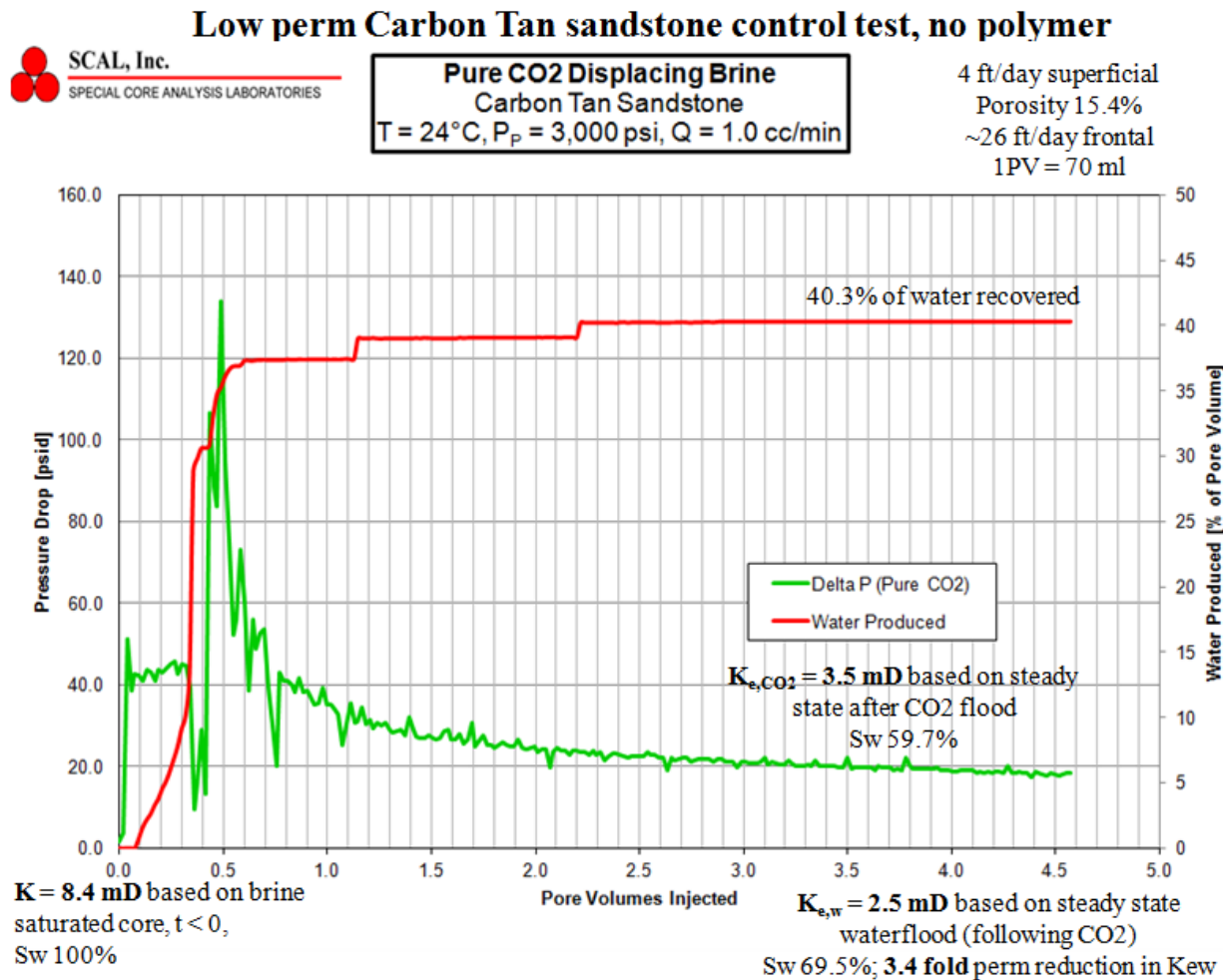


**Figure 10.6.6. Pressure drop and water production vs. PVI CO<sub>2</sub> for CO<sub>2</sub> displacing brine from an 8.4 mD Carbon Tan sandstone core**

This experiment was repeated with a comparable low permeability Carbon Tan sandstone (20.1 mD). However, the injection of pure CO<sub>2</sub> (green data line) was followed by injection of thickened CO<sub>2</sub> (aqua data line) to determine if incremental water displacement occurred and if dramatic changes in the pressure drop occurred. The results are shown in Figure 10.6.7.

### 1wt% PFA in CO<sub>2</sub> at 3000 psi and 24°C, Low perm Carbon Tan SS

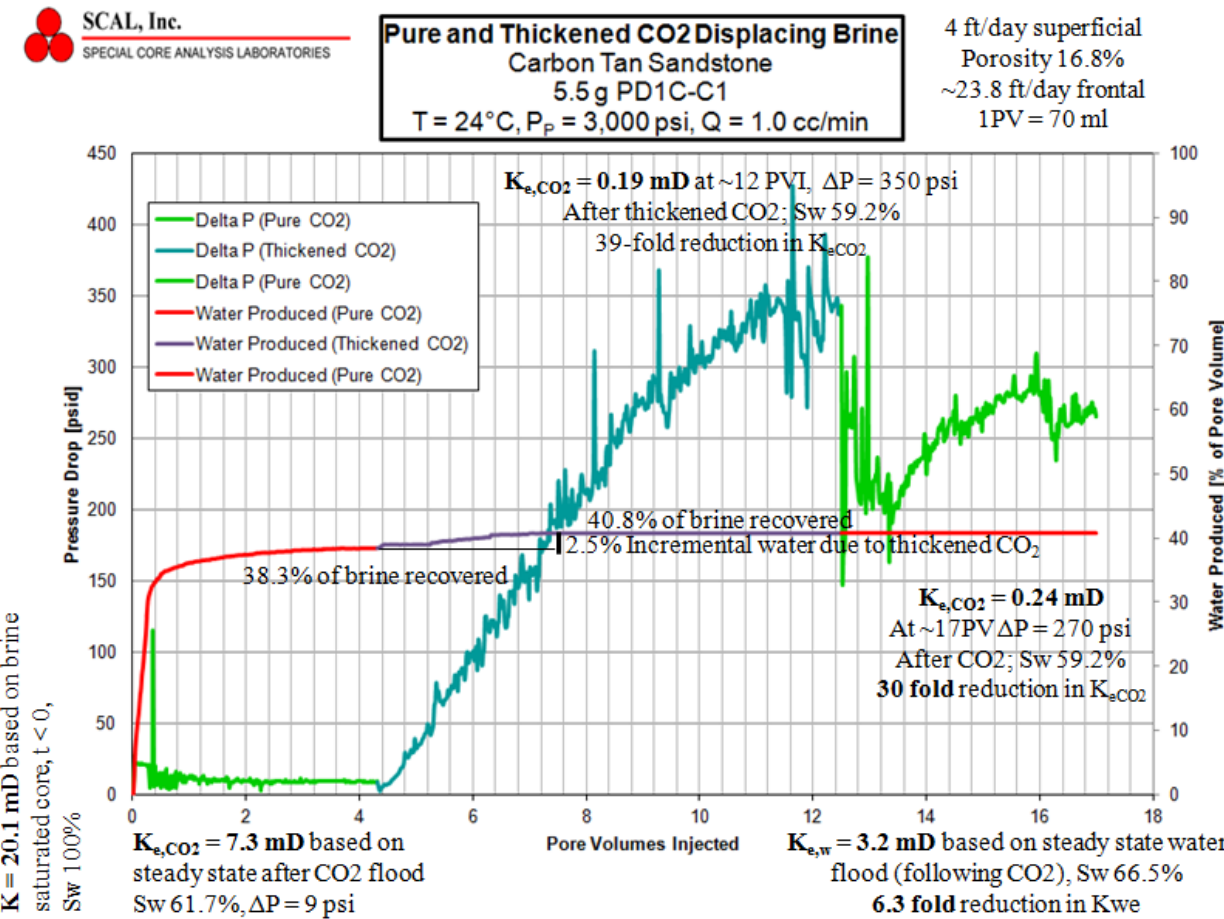


Figure 10.6.7. Pressure drop and water production vs. PVI CO<sub>2</sub> for CO<sub>2</sub> and PFA-CO<sub>2</sub> displacing brine from a 20.1 mD Carbon Tan sandstone core

Referring to Figure 10.6.7, the injection of thickened CO<sub>2</sub> resulted in the recovery of an additional 2.5% PV water, as the brine recovery rose from 38.3% to 40.8% due to the injection of thickened CO<sub>2</sub>. This is indicative of improved mobility control, although more modest than observed in the higher permeability Berea core (Figure 10.6.5). However, it also caused dramatic increases in pressure drop (the aqua data) as the pressure drop rose from only 9 psi after the pure CO<sub>2</sub> flood to 350 psi during the injection of 8 PV thickened CO<sub>2</sub>. When slightly more than 4 PV pure CO<sub>2</sub> was re-introduced to the core (green data) the pressure drop varied but was about 270 psi; indicative of a significant reduction in the permeability of the core. Therefore, although improved mobility control occurred, a very substantial reduction (30-fold) in the

effective permeability of the core to  $\text{CO}_2$  resulted, which again indicated that the PFA may be more appropriate for conformance control.

In this Indiana limestone (64 mD) experiment illustrated in Figure 10.6.8, meant to represent a **high perm limestone** test, the control test involved only the injection of pure  $\text{CO}_2$  (green data line) into the core for the displacement of the brine.  $\text{CO}_2$  injection was followed a waterflood (the final waterflood data is not shown in the plot). Figure 10.6.8 illustrates the results of the control test that involved no PFA; only  $\text{CO}_2$  was used in this experiment. 50% of the water initially in the core was recovered, and the pressure drop leveled off at 4.7 psi.

### High perm Indiana Limestone control test, no polymer

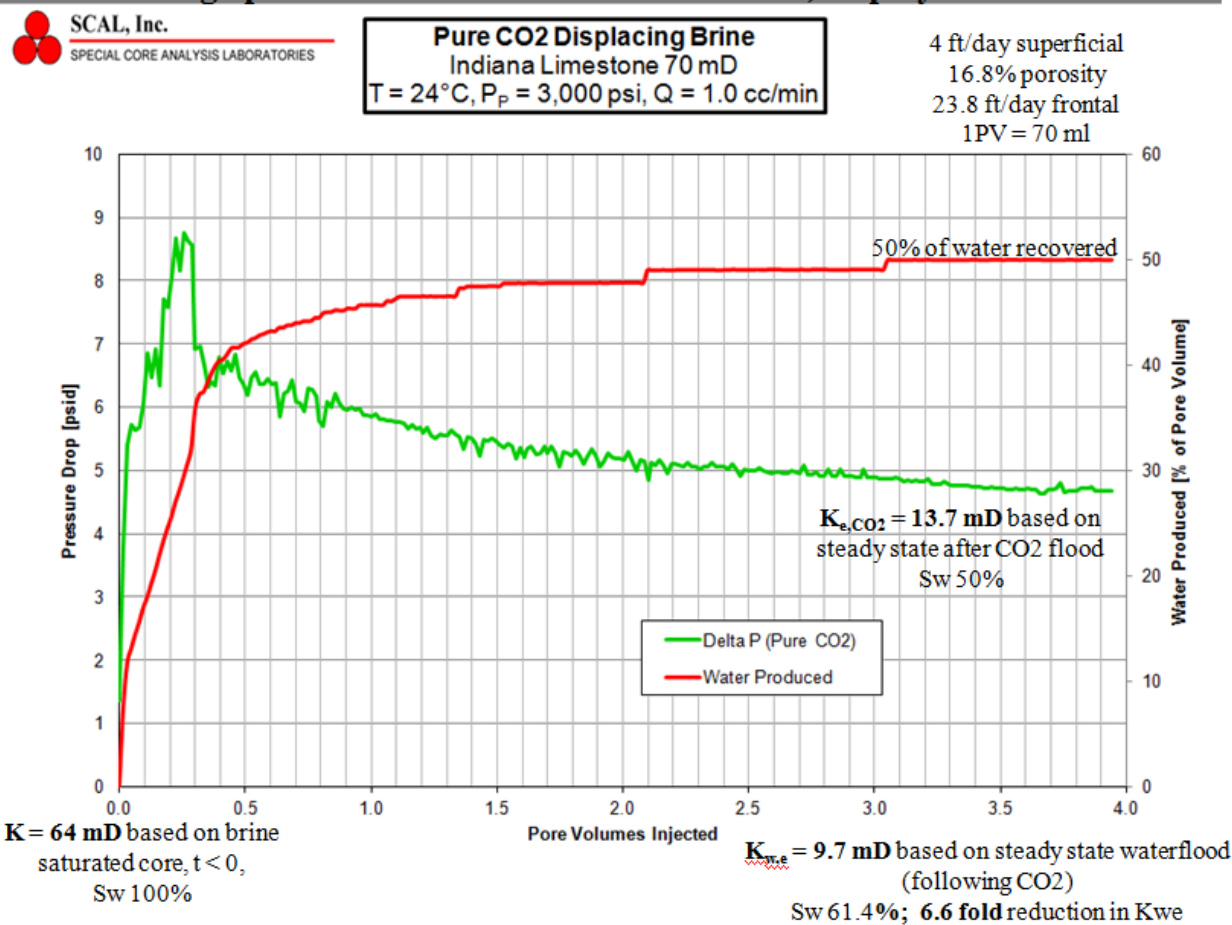
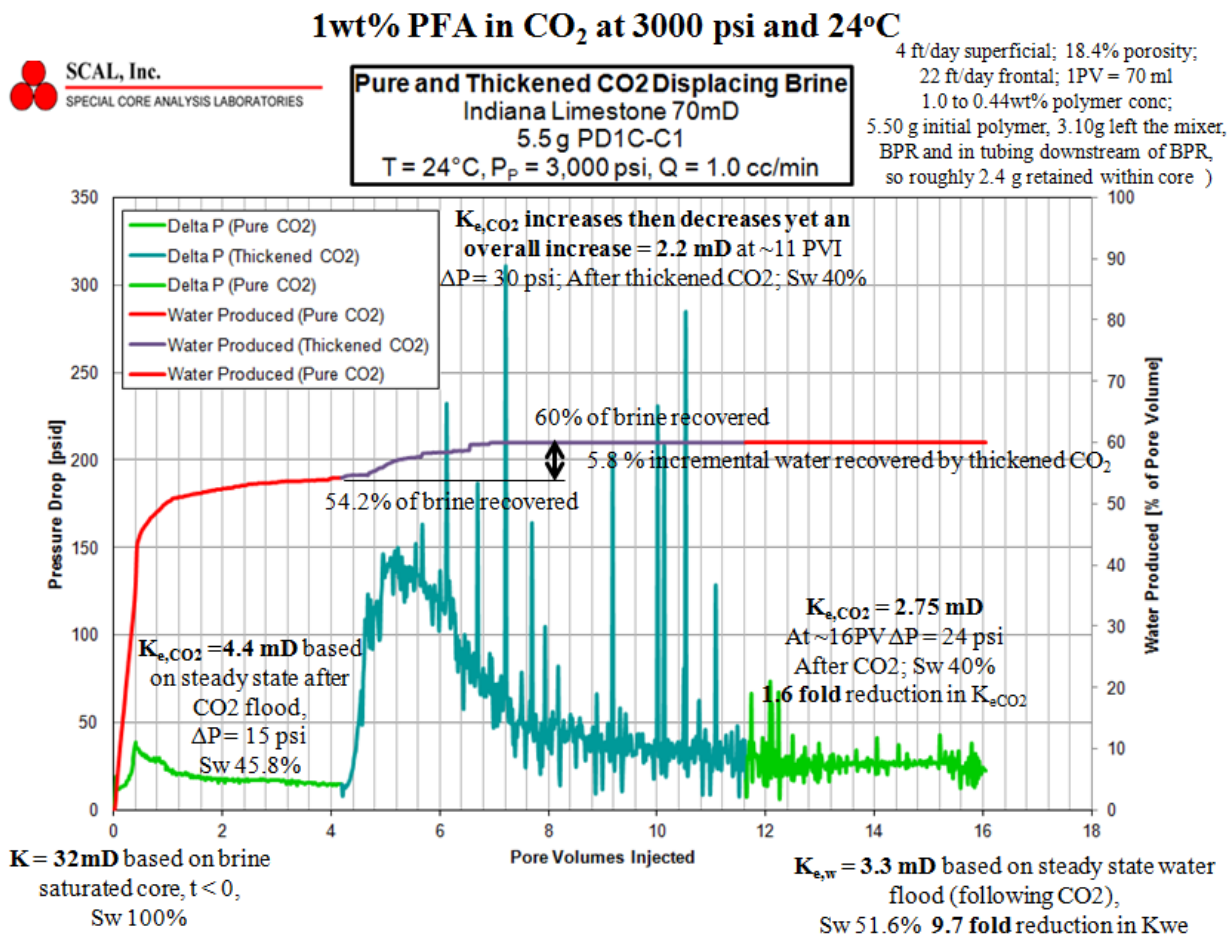


Figure 10.6.8. Pressure drop and water production vs. PVI  $\text{CO}_2$  for  $\text{CO}_2$  displacing brine from a 64 mD Indiana limestone core

This experiment was repeated with an Indiana limestone (70 mD nominal permeability, but the permeability as measured by SCAL was 32 mD). However, the injection of pure CO<sub>2</sub> (green data) was followed by injection of thickened CO<sub>2</sub> (aqua data line) to determine if incremental water displacement occurred and if dramatic changes in the pressure drop occurred. The results are shown in Figure 10.6.9.



**Figure 10.6.9. Pressure drop and water production vs. PVI CO<sub>2</sub> for CO<sub>2</sub> and PFA-CO<sub>2</sub> displacing brine from a 32 mD Indiana limestone core (70 mD is a nominal value from Kocurek, our data indicated 32 mD)**

Referring to Figure 10.6.9, the injection of thickened CO<sub>2</sub> resulted in the recovery of an additional 5.8% PV water, as the brine recovery rose from 54.2% to 60% due to the injection of thickened CO<sub>2</sub>. This is indicative of improved mobility control. However, it also caused increases in pressure drop (the aqua data) as the pressure drop rose from 15 psi after the pure CO<sub>2</sub> flood to 30 psi during the injection of 7 PV thickened CO<sub>2</sub>. This increase in pressure drop for the high permeability limestone core was much more modest increase than that observed during the high permeability Berea tests (Figure 10.6.5). When slightly more than 4 PV pure CO<sub>2</sub> was re-introduced to the core (green data) the pressure drop varied but remained at about 30 psi; indicative of a reduction in the permeability of the core. Therefore, although improved mobility control occurred, a modest reduction (1.6-fold) in the effective permeability of the core to CO<sub>2</sub>

resulted. Although this would favor some degree of conformance control, this effect was much less significant than it was in the sandstone experiments.

An attempt was made to do a PFA material balance on this test. 5.5 g PFA was initially put in the mixer. After the test a total of 3.1 g was found in the mixer, in the BPR and downstream of the BPR. Additional PFA may have been retained within the high pressure core holder and tubing and BPR. A material balance would indicate that approximately 2.4 g of PFA was retained by the core.

Using the expression,  $C = 1 \text{ wt\%} \exp(-V_{CO_2,ml}/600 \text{ ml})$  for 7 PV of  $CO_2$  injected ( $V_{CO_2,ml} = 500 \text{ ml}$ ), one can estimate that 44% (2.42 g) would have remained in the mixer and 56% (3.08 g) of the PFA would have passed out of the mixer and into the core. Therefore 2.4/3.08 = 77% (2.37g) of the PFA that entered the core would have been retained by the core and 23% (0.71 g) of the PFA that entered the core would have passed through the core.

In this Edwards Yellow limestone (3.5 mD) experiment, meant to represent a **low perm limestone** test, the control test involved only the injection of pure CO<sub>2</sub> into the core for the displacement of the brine. CO<sub>2</sub> injection was followed a waterflood (the final waterflood data is not shown in the plot). Figure 10.6.10 illustrates the results of the control test that involved no PFA; only CO<sub>2</sub> was used in this experiment. 50% of the water initially in the core was recovered, and the pressure drop leveled off at 4.7 psi.

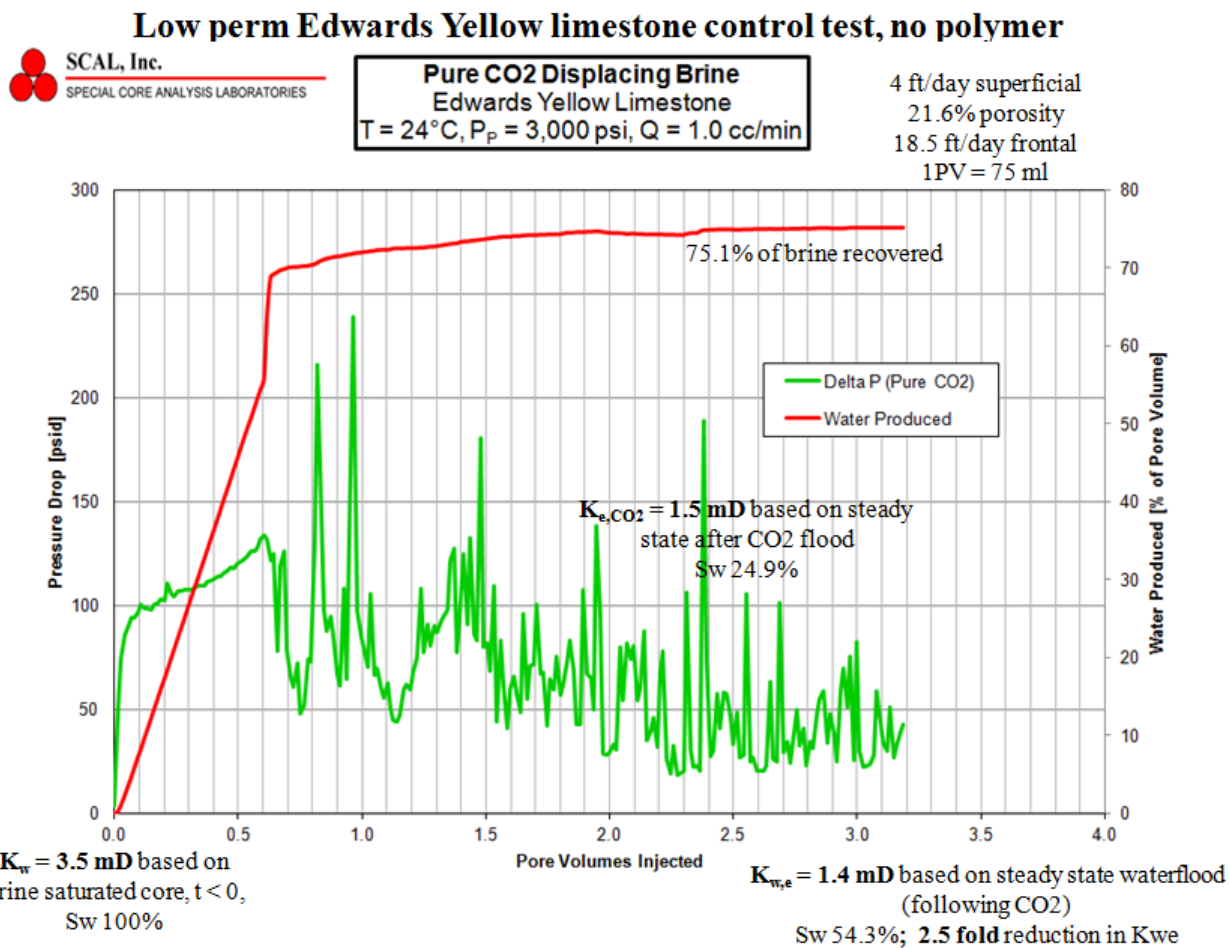


**Figure 10.6.10. Pressure drop and water production vs. PVI CO<sub>2</sub> for CO<sub>2</sub> displacing brine from a 3.5 mD Edwards Yellow limestone core**

This experiment was repeated with a comparable low permeability Edwards Yellow limestone (3.9 mD). However, the injection of pure CO<sub>2</sub> (green data line in Figure 10.6.11) was followed by injection of thickened CO<sub>2</sub> (aqua data line) to determine if incremental water displacement occurred and if dramatic changes in the pressure drop occurred. The results are shown in Figure 10.6.11.

### 1wt% PFA in CO<sub>2</sub> at 3000 psi and 24°C, Low perm Edwards Yellow Limestone

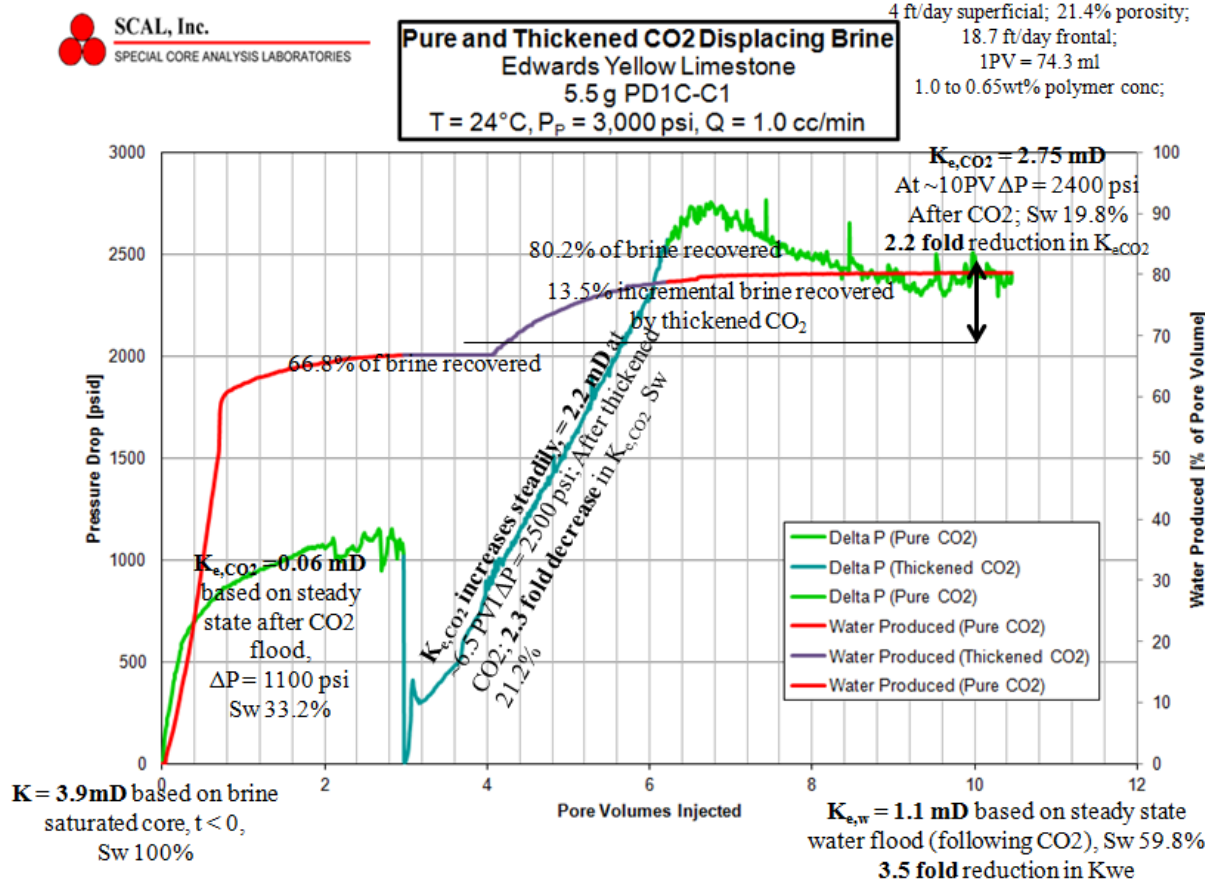


**Figure 10.6.11. Pressure drop and water production vs. PVI CO<sub>2</sub> for CO<sub>2</sub> and PFA-CO<sub>2</sub> displacing brine from a 3.9 mD Edwards yellow limestone core**

Referring to Figure 10.6.11, the injection of thickened CO<sub>2</sub> resulted in the recovery of an additional 13.5% PV water, as the brine recovery rose from 66.8% to 80.2% due to the injection of thickened CO<sub>2</sub>. This is indicative of substantially improved mobility control. However, it also caused increases in pressure drop (the aqua data) as the pressure drop rose from 1100 psi after the pure CO<sub>2</sub> flood to 2400 psi during the injection of 7 PV thickened CO<sub>2</sub>. This increase in pressure drop for the low permeability limestone core was very modest, in fact the relative increase of a factor of 2.2 is what would be expected in viscosity was the only effect. When slightly more than 4 PV pure CO<sub>2</sub> was re-introduced to the core (green data) the pressure drop leveled off at about 2400 psi; indicative of a very reduction in the permeability of the core. Therefore, although improved mobility control occurred, a modest reduction (2.2-fold) in the

effective permeability of the core to CO<sub>2</sub> resulted due to retention of the PFA. Although this would favor some degree of conformance control, this effect was markedly less significant than it was in the sandstone experiments.

Lessons learned from the tests involving the displacement of brine from single sandstone or limestone cores by CO<sub>2</sub> followed by thickened CO<sub>2</sub> followed by CO<sub>2</sub> are as follows.

These results indicate that

1. When cores are initially brine saturated, additional brine is recovered from the cores,
2. However, very significant increases in pressure drop due to CO<sub>2</sub> permeability reduction occurs in sandstone (~ 30-fold).
3. However, the CO<sub>2</sub> permeability decreases observed in limestone cores are quite modest (~ 2-fold).
4. We did not have the resources to use either experiments or molecular modeling to determine the mechanisms that could explain why the effect was so much more significant in sandstone compared to limestone.
5. These results indicate that PFA may be best suited for conformance control applications in sandstone formations, rather than limestone formations.
6. Our best attempt to close a material balance indicated that 77% of the PFA that entered the core during the injection of 7 PV of thickened CO<sub>2</sub> was retained by the core.

## **10.7 Dual parallel core floods; Thickened CO<sub>2</sub> displacing brine for mobility control or conformance control**

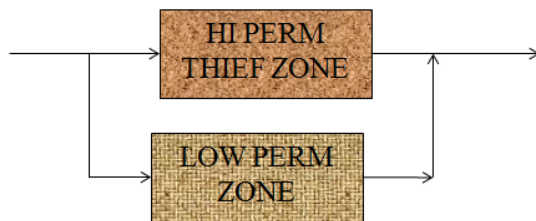
In the following dual parallel core flood experiments, two cores of varying permeability (two sandstone cores, or two limestone cores) were used. Both cores were initially brine-saturated. The objective of these tests was to determine if the PFA-CO<sub>2</sub> solution could reduce the permeability of the high perm core enough to divert a substantial amount of the flow of subsequently injected CO<sub>2</sub> into the lower perm core, which would mimic the sealing of a thief zone to divert CO<sub>2</sub> flow and improve conformance. (In the field, flow would be diverted to lower perm zones containing oil, however in these proof-of-concept tests we sought to divert flow from the high perm brine-saturated core to the lower permeability brine-saturated core.)

First, a pair of sandstone cores was selected. Core properties are presented in Table 10.7.1.

Core:	Berea and Carbon Tan Sandstones		
Brine:	4% KCl	Berea Sandstone	Carbon Tan Sandstone
Temperature:	25°C	$K_{w(Berea)} = 80.8 \text{ mD}$	$K_{w(Carbon Tan)} = 22.6 \text{ mD}$
Pore Pressure:	3,000 psi	$\Phi_{Berea} = 20.20\%$	$\Phi_{Carbon Tan} = 17.53\%$
Confining Pressure:	5,000 psi	$PV_{Berea} = 70.21 \text{ cc}$	$PV_{Carbon Tan} = 60.90 \text{ cc}$
Flow Rate:	0.25 cc/min	$S_{wi(Berea)} = 44.66\%$	$S_{wi(Carbon Tan)} = 57.03\%$
Total PV:	131.11 cc		
$S_{wi/Total}$ :	50.40%		

**Table 10.7.1 Properties of the dual sandstone cores used in dual parallel core conformance control studies and experimental conditions**

Figure 10.7.1 illustrates the configuration of the equipment at SCAL used to conduct these tests.



### **Control test**

1. Saturate cores with brine; flow brine through core
2. In some cases, CO<sub>2</sub>-flood only the high perm core to replicate years of CO<sub>2</sub> flooding of the thief zone
3. Inject CO<sub>2</sub> into the core/cores; measure brine production and pressure drop;
4. Continue until steady state brine production ceases

### **Effect-of-polymer test**

1. Saturate cores with brine
2. Inject CO<sub>2</sub>+PFA solution into the isolated thief zone, or into both cores;
3. Inject CO<sub>2</sub> into both cores and measure brine production and pressure drop; continue until steady state  $S_{w,ir}$  achieved

**Figure 10.7.1. Configuration of dual cores and test strategy for mobility control or conformance control studies**

The objective of the first set of dual core displacement tests was to assess the efficacy of PFA-CO<sub>2</sub> solutions for mobility control. First a “control” CO<sub>2</sub> flood (no PFA) of parallel brine-saturated sandstone cores was conducted. In the second test, the PFA-CO<sub>2</sub> solution would be simultaneously injected into both cores in an attempt to displace more brine using less CO<sub>2</sub> without prohibitive pressure drop increases.

The control results of brine recovery as a function of PVI CO<sub>2</sub> is presented in Figure 10.7.2. PVI is based on the combined volume of the two cores. CO<sub>2</sub> breakthrough occurs at 0.04 PVI. Up to 0.35 PVI CO<sub>2</sub>, water recovery is primarily from the high permeability Berea. Thereafter brine recovery from the lower permeability Carbon Tan sandstone increases. Ultimately 48% of the total amount of brine that originally resided in both cores was recovered

### Injection of pure CO<sub>2</sub> into dual parallel brine-saturated sandstone cores

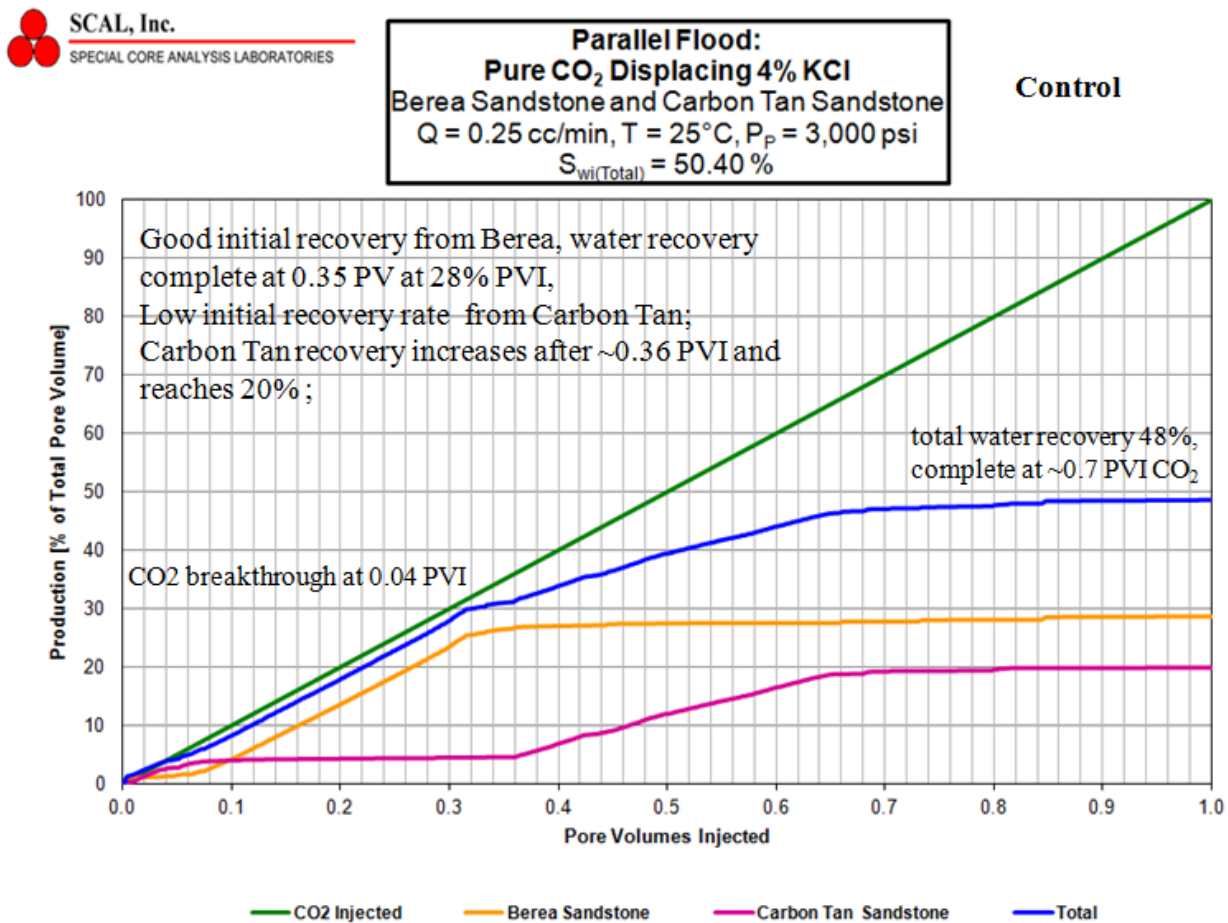


Figure 10.7.2. Mobility control results for the displacement of brine by CO<sub>2</sub> in dual parallel sandstone cores; CO<sub>2</sub> is injected into both cores simultaneously through this experiment

Figure 10.7.3 presents the pressure drop data for the same experiment. A spike in pressure drop occurs when a significant amount of  $\text{CO}_2$  begins to enter the lower permeability core at about 0.35 PVI. Note that after water recovery is complete, the pressure drop across the parallel cores is about 0.1 psi.

### Injection of pure $\text{CO}_2$ into dual parallel brine-saturated sandstone cores

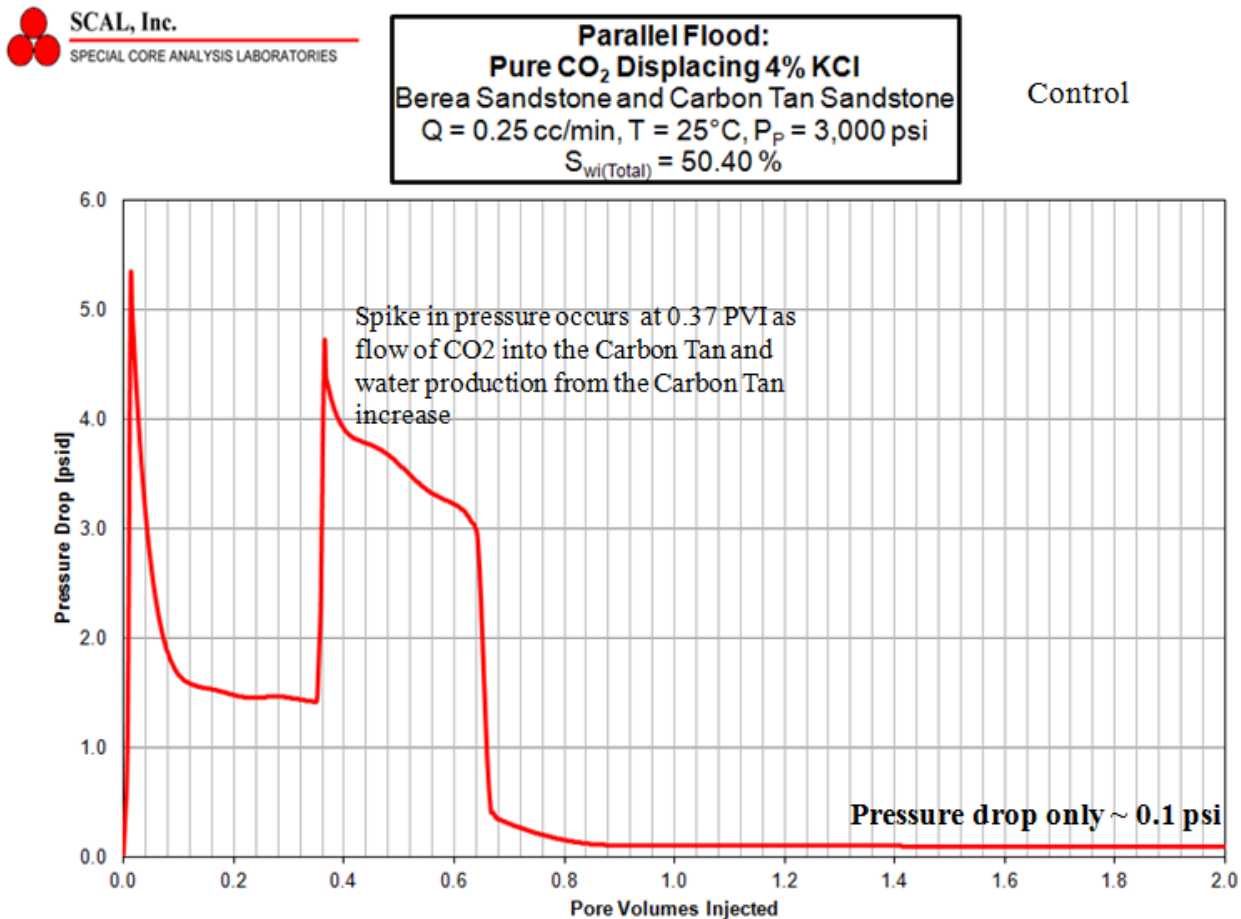


Figure 10.7.3. Pressure drop for mobility control test for the displacement of brine by  $\text{CO}_2$  in dual parallel sandstone cores;  $\text{CO}_2$  is injected into both cores simultaneously through this experiment

The experiment was then repeated, but with thickened  $\text{CO}_2$  (1 wt% PFA in  $\text{CO}_2$ ). These results in Figure 10.7.4 demonstrate improved mobility control, as evidenced by a delayed  $\text{CO}_2$  breakthrough (~0.47 PVI vs. 0.04 PVI for pure  $\text{CO}_2$ ); and a much smaller PVI requirement for complete recovery (~0.5 PVI vs. 0.7 PVI for pure  $\text{CO}_2$ ). The same ultimate displacement of brine from the parallel cores (50%) was realized in the cores. (Note that there was some scatter in the data that resulted in the blue curve rising above the green line at 0.28 PVI, then falling below the green line before rising back to the green line at 0.47 PVI; a small amount of  $\text{CO}_2$  may have been produced during this interval.)

### Injection of 1wt%PFA in $\text{CO}_2$ into dual parallel brine-saturated sandstone cores

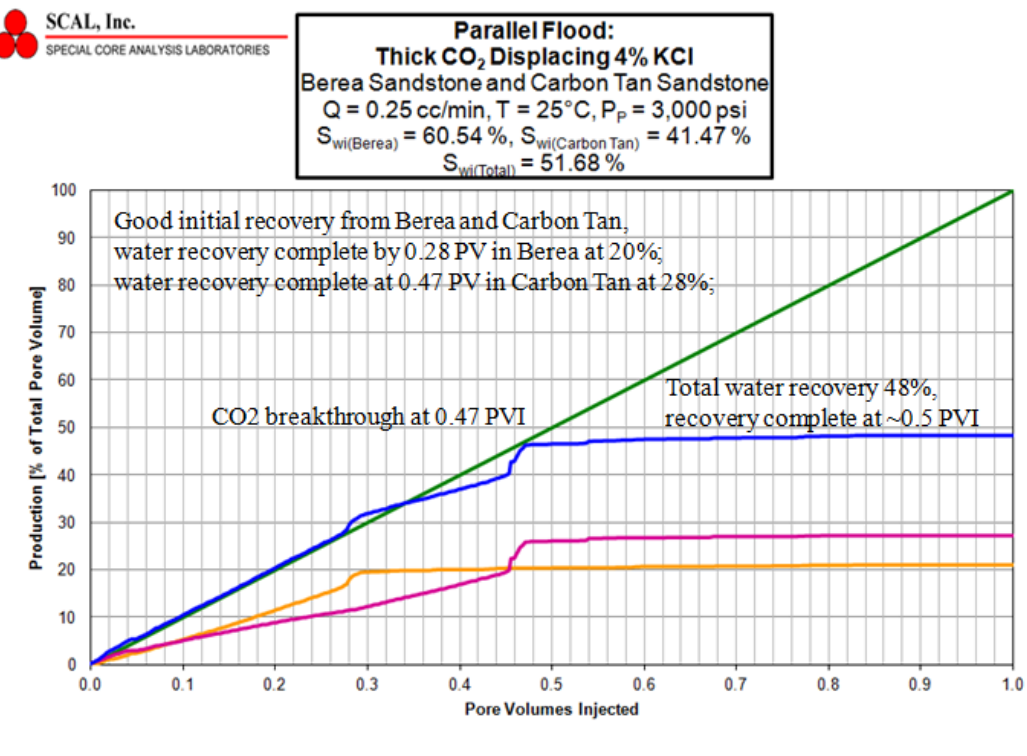
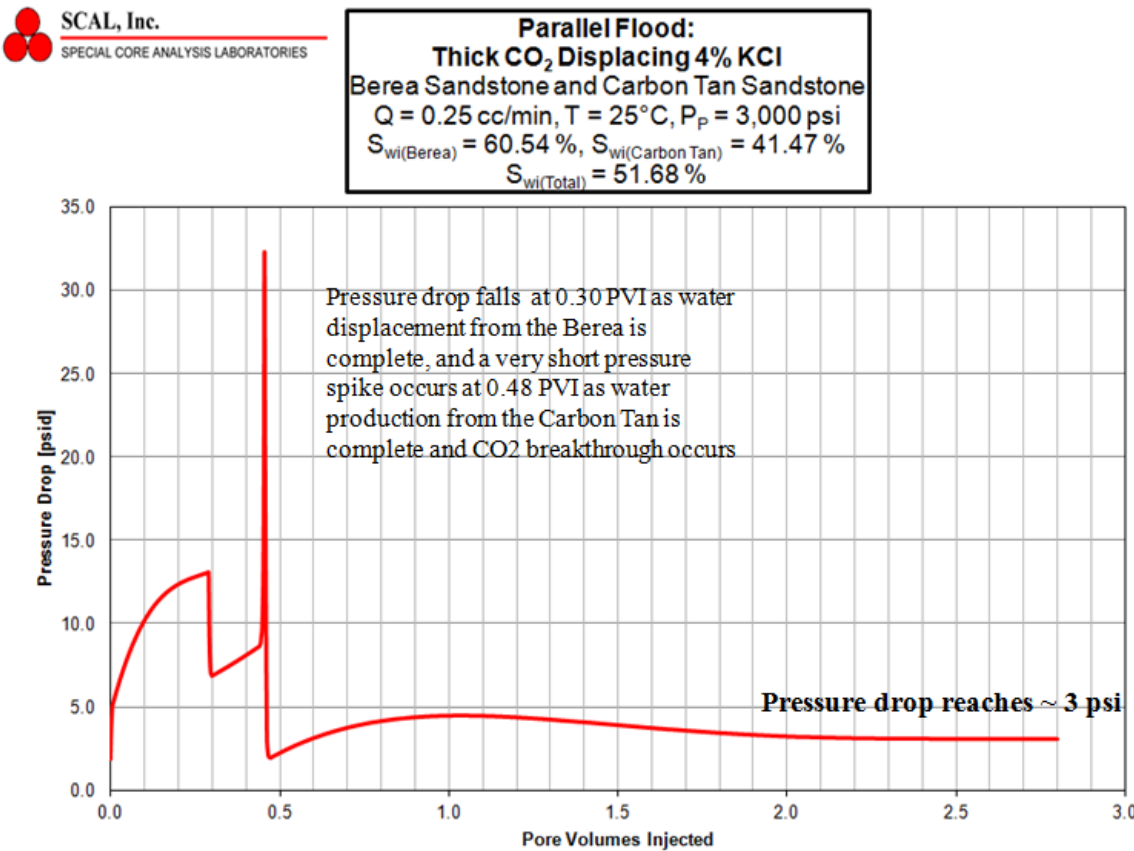


Figure 10.7.4. Mobility control results for the displacement of brine by thickened  $\text{CO}_2$  in dual parallel sandstone cores; thickened  $\text{CO}_2$  is injected into both cores simultaneously through this experiment

The pressure drop for this displacement of water from dual Berea cores is shown in the Figure 10.7.5. Compared to the pressure drop results for the displacement using pure CO<sub>2</sub>, Figure 10.7.3, the pressure drops are roughly 10 times greater prior to breakthrough and 30 times greater (3 psi vs. 0.1 psi) after the displacement of water was complete.

### Injection of 1wt%PFA in CO<sub>2</sub> into dual parallel brine-saturated sandstone cores



**Figure 10.7.5. Pressure drop for mobility control test for the displacement of brine by thickened CO<sub>2</sub> in dual parallel sandstone cores; thickened CO<sub>2</sub> is injected into both cores simultaneously through this experiment**

Therefore, these two experiments demonstrate that if CO<sub>2</sub> is injected simultaneously into both cores, CO<sub>2</sub> breakthrough is delayed and more prior to breakthrough more water is displaced using less thickened CO<sub>2</sub>. However, the ultimate recovery of water was comparable in both tests. Although this is a somewhat promising mobility control result, the pressure drop required for the displacement of thickened CO<sub>2</sub> was roughly 10-30 times greater than that required for pure CO<sub>2</sub> even though the thickened CO<sub>2</sub> was only about 3.5 times more viscous. This is another indication that the PFA is altering the rock properties leading to undesirable large pressure drop increases for mobility control.

The next two experiments were similar in nature to the prior two, but they were conducted with parallel limestone cores; a high permeability Indiana limestone and a low permeability Edwards Yellow limestone. The results are shown in Figure 10.7.6. It is apparent that both cores likely had a very high permeability streak in that  $\text{CO}_2$  breakthrough occurs very soon after the injection of  $\text{CO}_2$ . Recovery of brine from the Indiana limestone is complete at about 0.46 PVI, and the displacement of brine from the Edwards Yellow is complete at about 3 PVI. Ultimately, 43% of the brine initially present in both cores was recovered.

### Injection of pure $\text{CO}_2$ into dual parallel brine-saturated limestone cores



**Parallel Flood:**  
**Pure  $\text{CO}_2$  Displacing 4% KCl**  
**Indiana Limestone and Edwards Yellow Limestone**  
 $Q = 0.25 \text{ cc/min}$ ,  $T = 25^\circ\text{C}$ ,  $P_p = 3,000 \text{ psi}$   
 $S_{wi(\text{Total})} = 57.45 \%$

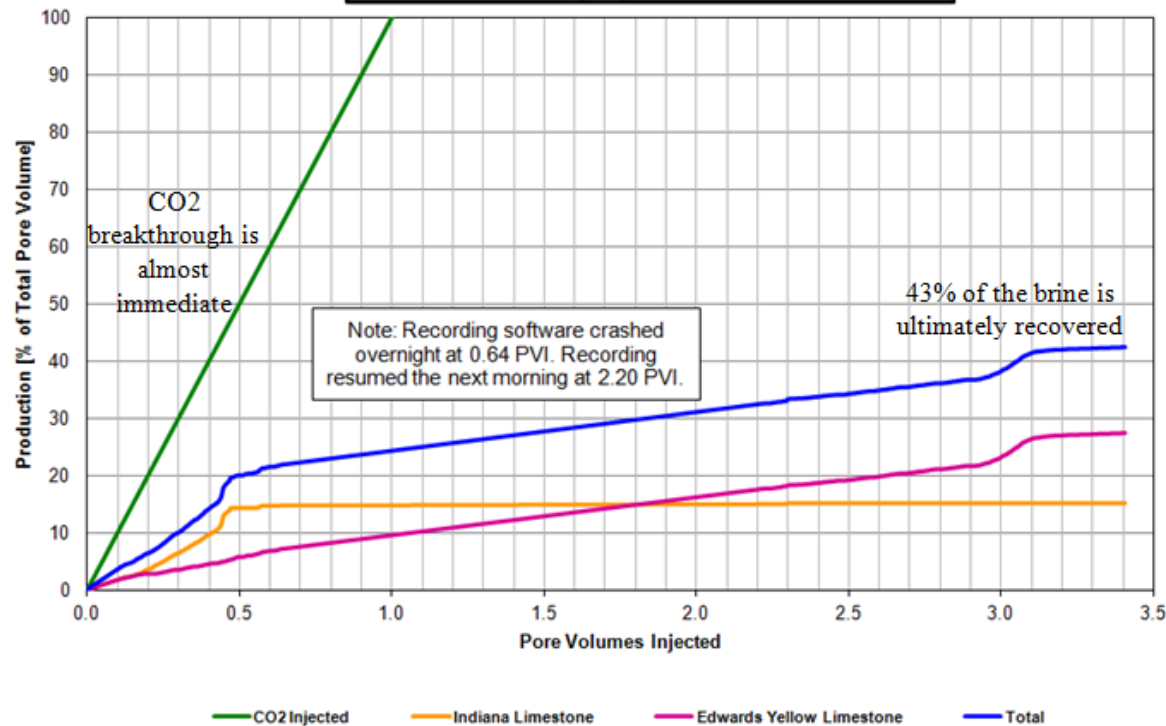


Figure 10.7.6. Mobility control results for the displacement of brine by  $\text{CO}_2$  in dual parallel limestone cores;  $\text{CO}_2$  is injected into both cores simultaneously through this experiment

The corresponding pressure drop results are shown in the Figure 10.7.7; the pressure drop for this experiment was rough 1.2 psi,  $\pm 0.2$  psi.

### Injection of pure CO<sub>2</sub> into dual parallel brine-saturated limestone cores

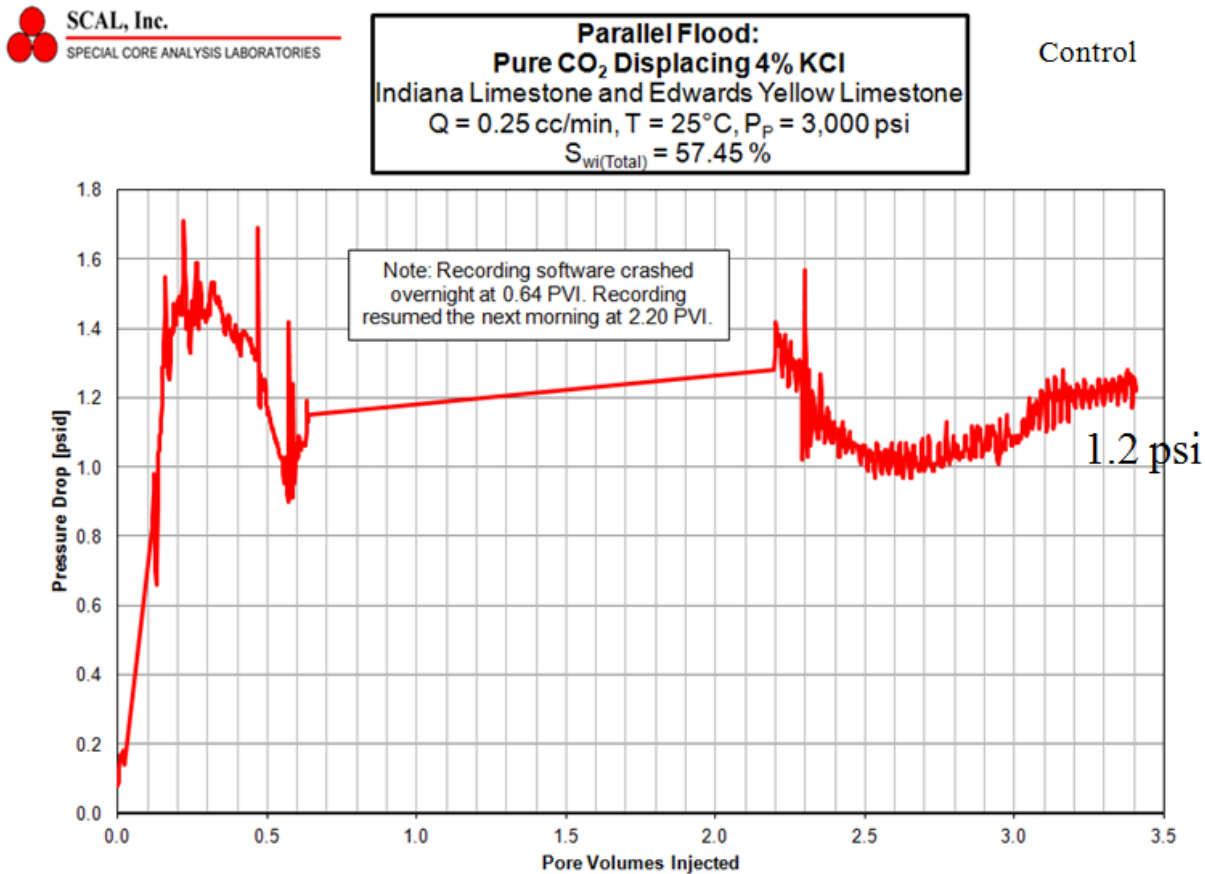


Figure 10.7.7. Pressure drop for mobility control test for the displacement of brine by CO<sub>2</sub> in dual parallel limestone cores; CO<sub>2</sub> is injected into both cores simultaneously through this experiment

Then the displacement of brine from dual parallel limestone cores was repeated using thickened  $\text{CO}_2$  (1 wt% PFA in  $\text{CO}_2$ ).  $\text{CO}_2$  breakthrough was delayed to about 0.05 PVI, and little  $\text{CO}_2$  production occurred until 0.25 PVI. Much less  $\text{CO}_2$  was needed to displace the brine than pure  $\text{CO}_2$ , and the ultimate amount of brine recovered (55%) was much greater than that recovered with pure  $\text{CO}_2$  (43%). The results are shown in Figure 10.7.8. With respect to recovery, this was a promising mobility control result.

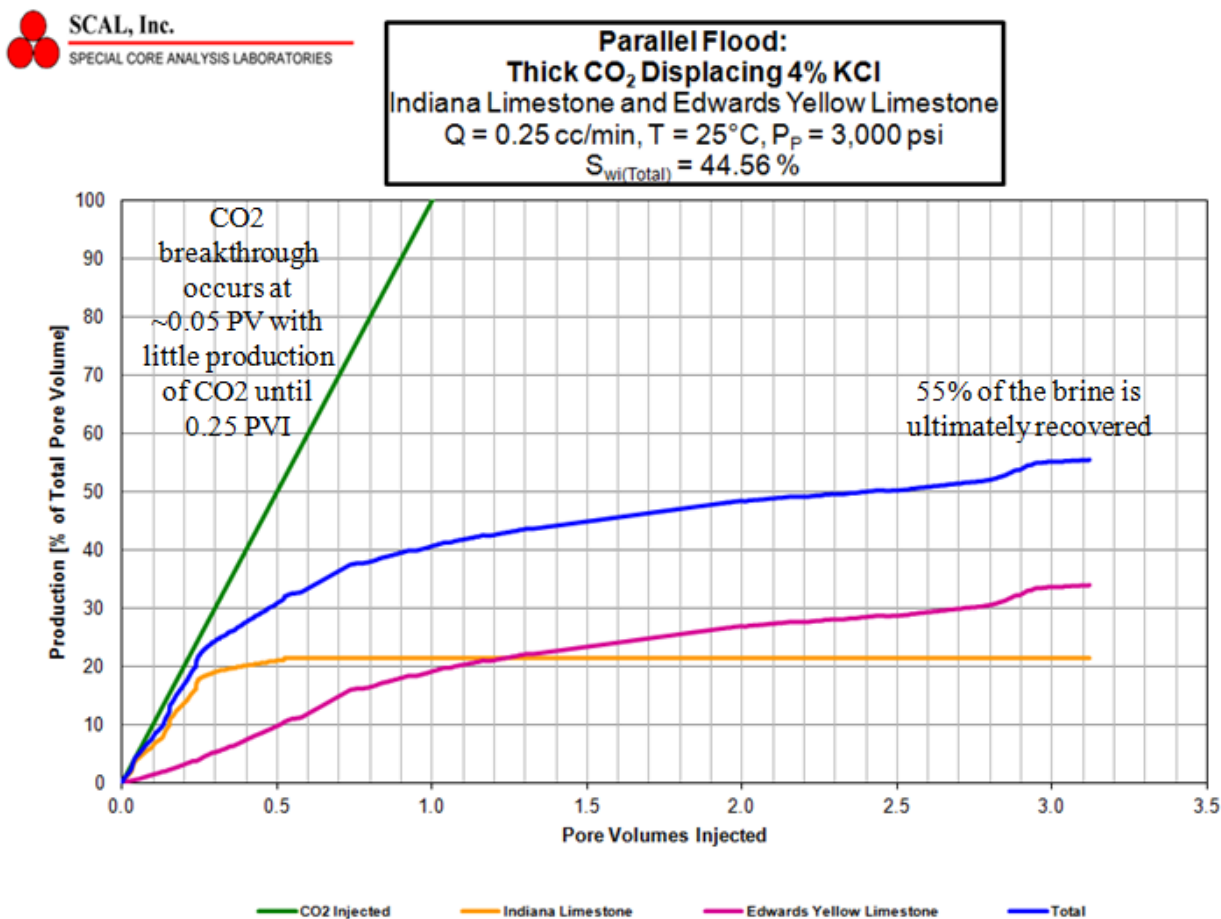


Figure 10.7.8. Mobility control results for the displacement of brine by thickened  $\text{CO}_2$  in dual parallel limestone cores;  $\text{CO}_2$  is injected into both cores simultaneously through this experiment

There was a tremendous increase in the pressure drop, however, as shown in the Figure 10.7.9. Pressure drop climbed steadily, reaching values as high as 70 psi at 3 PVI. Once again, it appears the PFA is significantly altering the permeability of the cores, leading to unacceptably large 60-fold pressure drop increases even though the PFA-CO<sub>2</sub> solution is no more than 4 times as viscous as pure CO<sub>2</sub>.

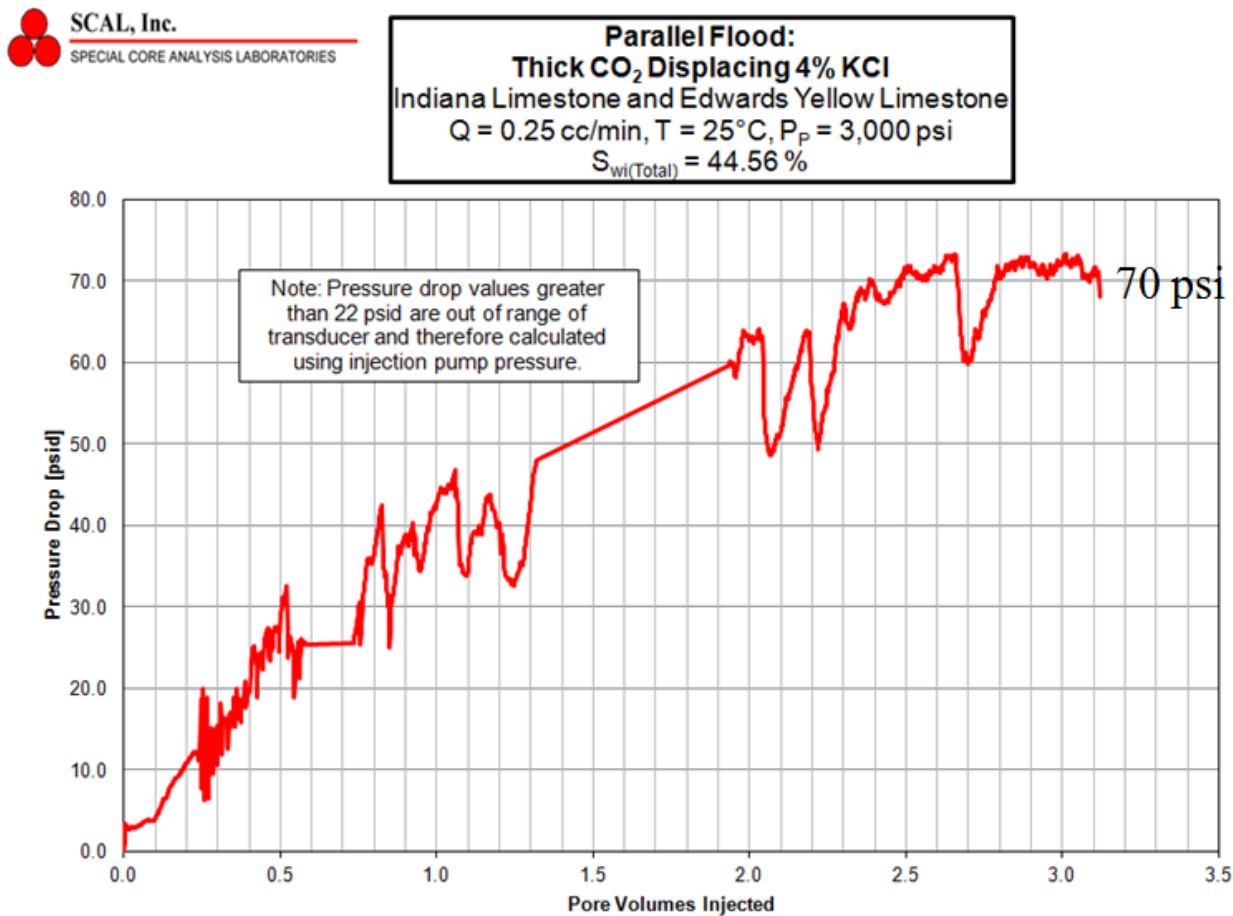


Figure 10.7.9. Pressure drop for mobility control test for the displacement of brine by CO<sub>2</sub> in dual parallel limestone cores; CO<sub>2</sub> is injected into both cores simultaneously through this experiment

The next tests were intended to more carefully represent a high permeability thief zone that has been both waterflooded extensively and CO<sub>2</sub> flooded extensively. After brine-saturating both cores, the high permeability core was isolated and then flooded with CO<sub>2</sub> to simulate the long-term preferential flow of CO<sub>2</sub> into that high perm thief zone. At that point, CO<sub>2</sub> (or thickened CO<sub>2</sub>) was introduced to both cores simultaneously. This comparison was mostly related to mobility control because the thickened CO<sub>2</sub> was injected into both cores.

First a “control” experiment was conducted using CO<sub>2</sub> (no PFA). As shown in the Figure 10.7.10, no water production resulted from the Carbon Tan core; all of the CO<sub>2</sub> entered only the Berea core and only the brine. 30% of the total brine from both cores was recovered, and all of it came from the Berea sandstone.

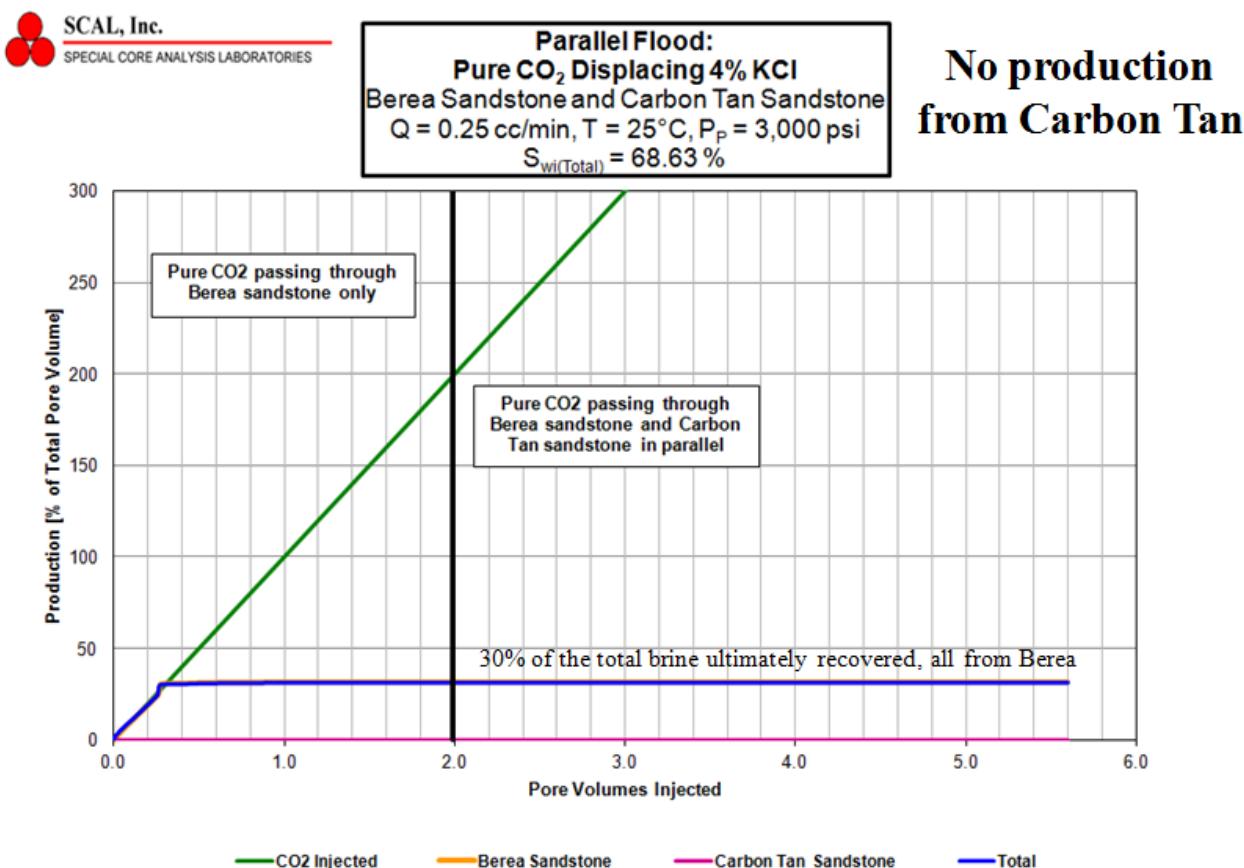


Figure 10.7.10. Mobility control results for the displacement of brine by thickened CO<sub>2</sub> in dual parallel sandstone cores; the high perm core was isolated and flooded with pure CO<sub>2</sub>, then CO<sub>2</sub> was injected into both cores simultaneously through this experiment

The corresponding pressure drop results for this test are shown in the Figure 10.7.11. The pressure drop was initially about 4 psi, and dropped to about 2 psi after 0.3 PVI, and then steadily dropped to about 1 psi after 5.6 PVI.

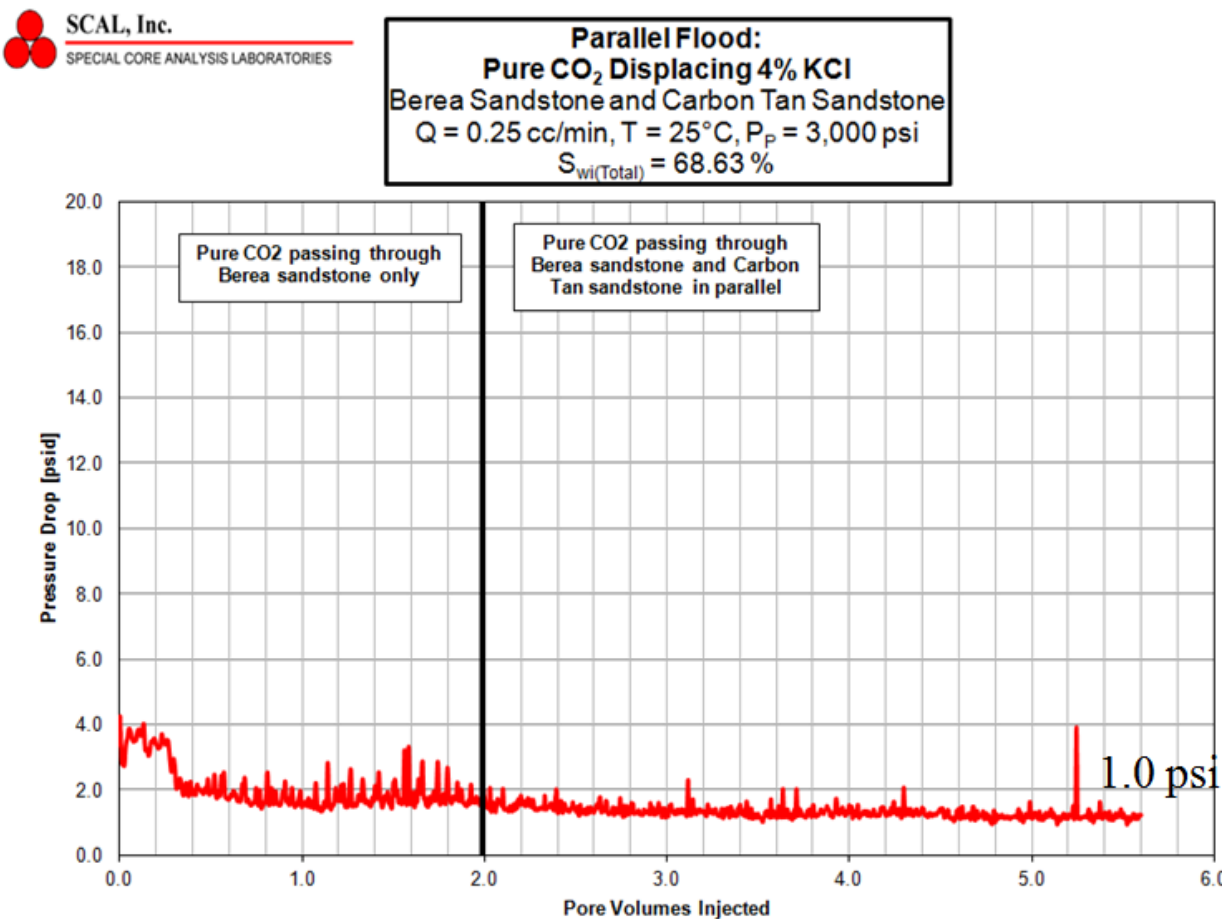


Figure 10.7.11. Pressure drop results for the displacement of brine by thickened CO<sub>2</sub> in dual parallel sandstone cores; the high perm core was isolated and flooded with pure CO<sub>2</sub>, then CO<sub>2</sub> was injected into both cores simultaneously through this experiment

In the following test, both cores were initially brine-saturated. As in the prior test, the high perm Berea core was then isolated and flooded with pure CO<sub>2</sub>, with CO<sub>2</sub> breakthrough occurring at 0.3 PVI, until brine production ceased as shown in Figure 10.7.12. However, in this test thickened CO<sub>2</sub> (1 wt% PFA in CO<sub>2</sub>) was then simultaneously injected into both the Berea and carbon tan sandstone cores. Improved mobility control is evident because CO<sub>2</sub> entered the Carbon Tan during this test resulting in a very large increase in water production (ultimately 62%) from both cores, as opposed to the 30% value when pure CO<sub>2</sub> was used and brine was only recovered from the Berea core. Both cores showed incremental brine displacement after the introduction of thickened CO<sub>2</sub>.

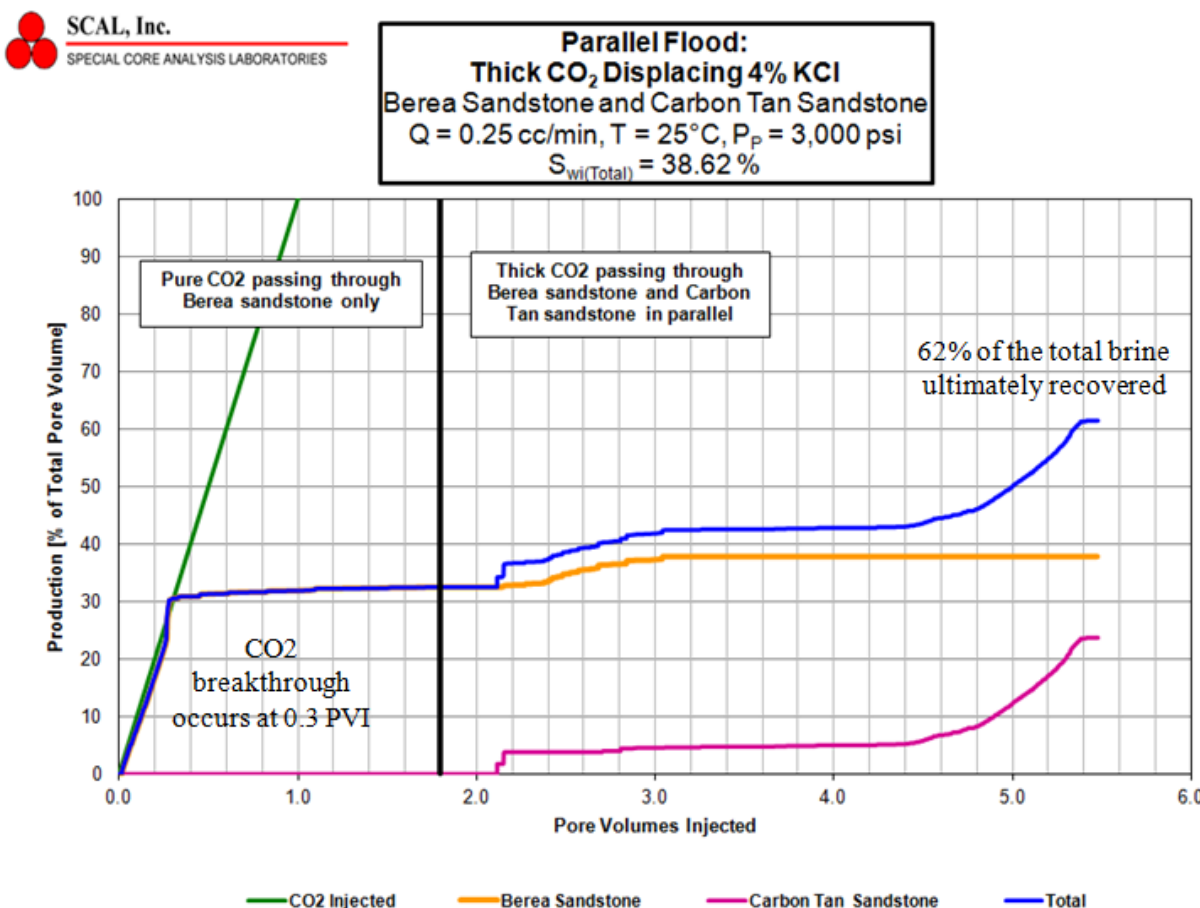


Figure 10.7.12. Mobility control results for the displacement of brine by thickened CO<sub>2</sub> in dual parallel sandstone cores; the high perm core was isolated and flooded with pure CO<sub>2</sub>, then thickened CO<sub>2</sub> was injected into both cores simultaneously through this experiment

The following results shown in Figure 10.7.13 indicate that the pressure drop was initially ~ 2 psi (a value consistent with Figure 10.7.11). At 0.3 PVI there was a pressure spike that occurred at CO<sub>2</sub> breakthrough in the Berea sandstone. Although pressure spikes at breakthrough are not uncommon while collecting data for these types of tests, the pressure drop subsequent to the spike reached 6 psi and slowly increased to about 7 psi. It was expected that the pressure drop

would not display such a dramatic distinct increase at 0.3 PVI that was maintained until 1.6 PVI. It is possible that the pressure drop in this period between 0.3 and 1.6 PVI is artificially high, perhaps due to the deposition of PFA within the BPR or tubing in such a manner that it induced a pressure drop. Although thickened  $\text{CO}_2$  was then introduced into both cores at 1.6 PVI, the pressure drop smoothly continued a slow increase from 7 to 8 psi thereafter. Again, this pressure drop behavior is unusual in that in all other tests found in this report that include the sudden introduction of thickened  $\text{CO}_2$ , a distinct pressure drop increase occurs. Although there is a chance that the pressure drop associated with the flow of thickened  $\text{CO}_2$  through the parallel cores just after 1.6 PVI was about the same as the pressure drop associated with the flow of pure  $\text{CO}_2$  through the high perm core only at 1.6 PVI, there is also a chance that the pressure drops reported for this run may not be as accurate as the other experiments in this report. Therefore it appears that this experiment demonstrated very good mobility control with respect to increased brine displacement, however the 4-fold pressure drop reported from 2 to 8 psi may not be as accurate as other pressure drop data in this report.

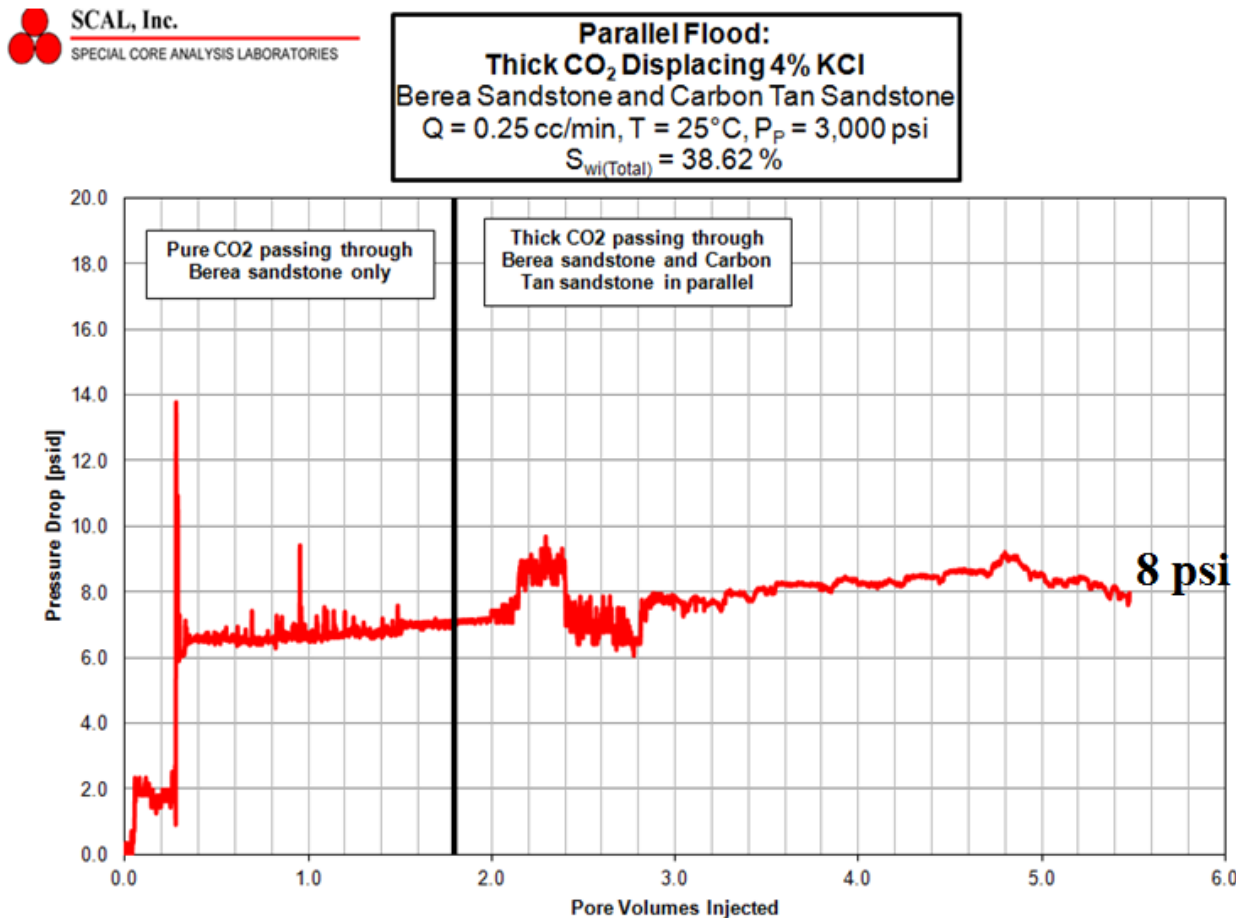


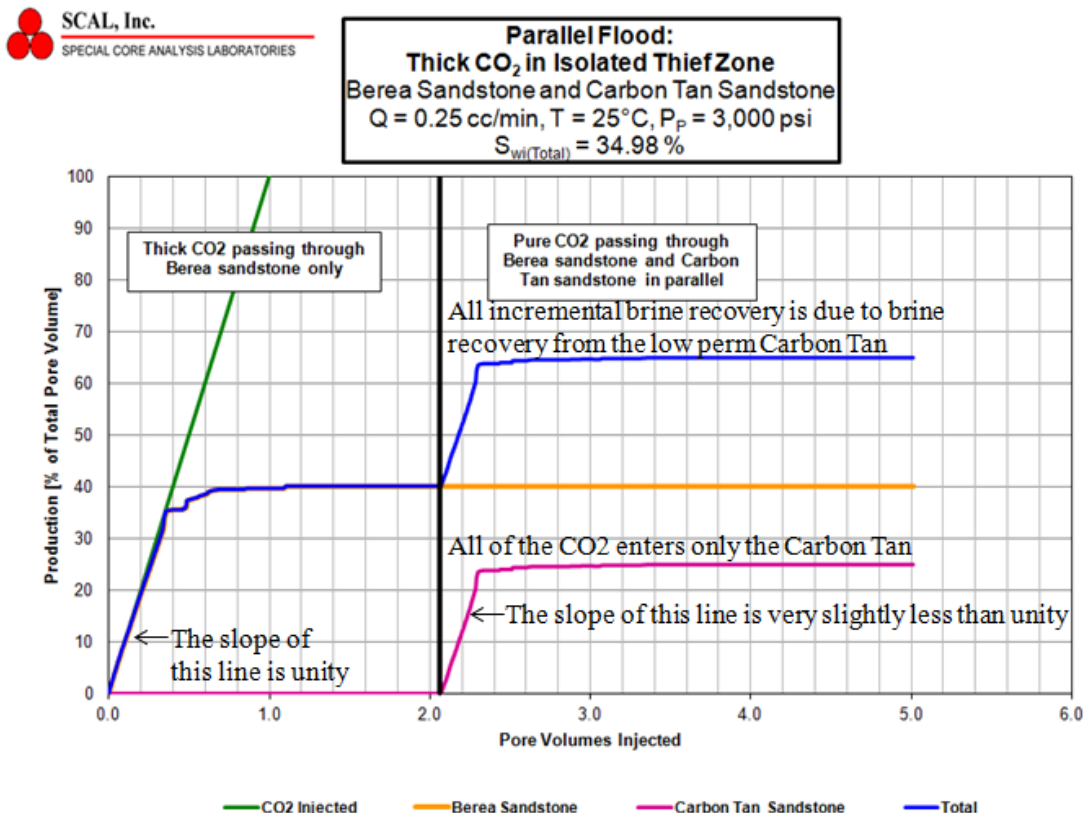
Figure 10.7.13. Pressure drop results for the displacement of brine by thickened  $\text{CO}_2$  in dual parallel sandstone cores; the high perm core was isolated and flooded with pure  $\text{CO}_2$ , then thickened  $\text{CO}_2$  was injected into both cores simultaneously through this experiment

Given that all of the testing to this point seemed to indicate that substantial reductions in rock permeability were occurring due to PFA adsorption or retention within the cores, the following dual core tests were designed to represent conformance control strategies. In other words, the objective of the following sets of dual parallel core tests was to block flow of CO<sub>2</sub> into a thief zone with the hope that it would be diverted to the lower perm core without an unacceptably large pressure drop (because that zone would have never “seen” PFA). This represented a distinct change in the original intent of this project, which was directed at mobility control. However, our team discussed this change in strategy with industrial advisors at Kinder Morgan and Denbury Resources. Both supported this change in emphasis, and the NETL project manager also agreed to the change in direction. Because brine is easier to work with in the lab than crude oil, these conformance tests were conducted with brine-saturated cores (rather than crude oil-saturated cores, or cores in which the entire geologic and secondary flooding history of the sandstone is replicated). In other words, the objective was to divert CO<sub>2</sub> from a thief zone (that was initially brine-saturated and then CO<sub>2</sub>-flooded) toward a lower perm core that contained a displaceable fluid (our team selected brine).

The following sets of tests assess the ability of (PFA-CO<sub>2</sub> solutions as conformance control agents. To the best of our knowledge, these are the first known examples of using a CO<sub>2</sub>-soluble additive for conformance control – and the results were very promising.

In the conformance control results shown below in Figure 10.7.14, both cores (high permeability Berea sandstone and the low permeability Carbon Tan sandstone) were initially saturated with brine. The high perm Berea core was then isolated and thickened  $\text{CO}_2$  was used to displace all of the recoverable brine from that core alone. After that, the valves leading to the low perm sandstone core were opened allowing the subsequently injected pure  $\text{CO}_2$  access to both cores. As shown in Figure 10.7.14, the ideal conformance result occurred. None of the  $\text{CO}_2$  entered the PFA-treated thief zone; all of the  $\text{CO}_2$  entered only the lower perm Carbon Tan core. Further, the rate of brine recovery between 2.1 to 2.3 PVI before  $\text{CO}_2$  breakthrough is only slightly less than unity (the injection rate of  $\text{CO}_2$ ), meaning that very little  $\text{CO}_2$  was being produced from this core until 2.1 PVI, when a substantial increase in the rate of  $\text{CO}_2$  production occurred. This high rate of brine production was expected, however, because no  $\text{CO}_2$  had been previously given the opportunity to flow into the lower permeability Carbon Tan core.

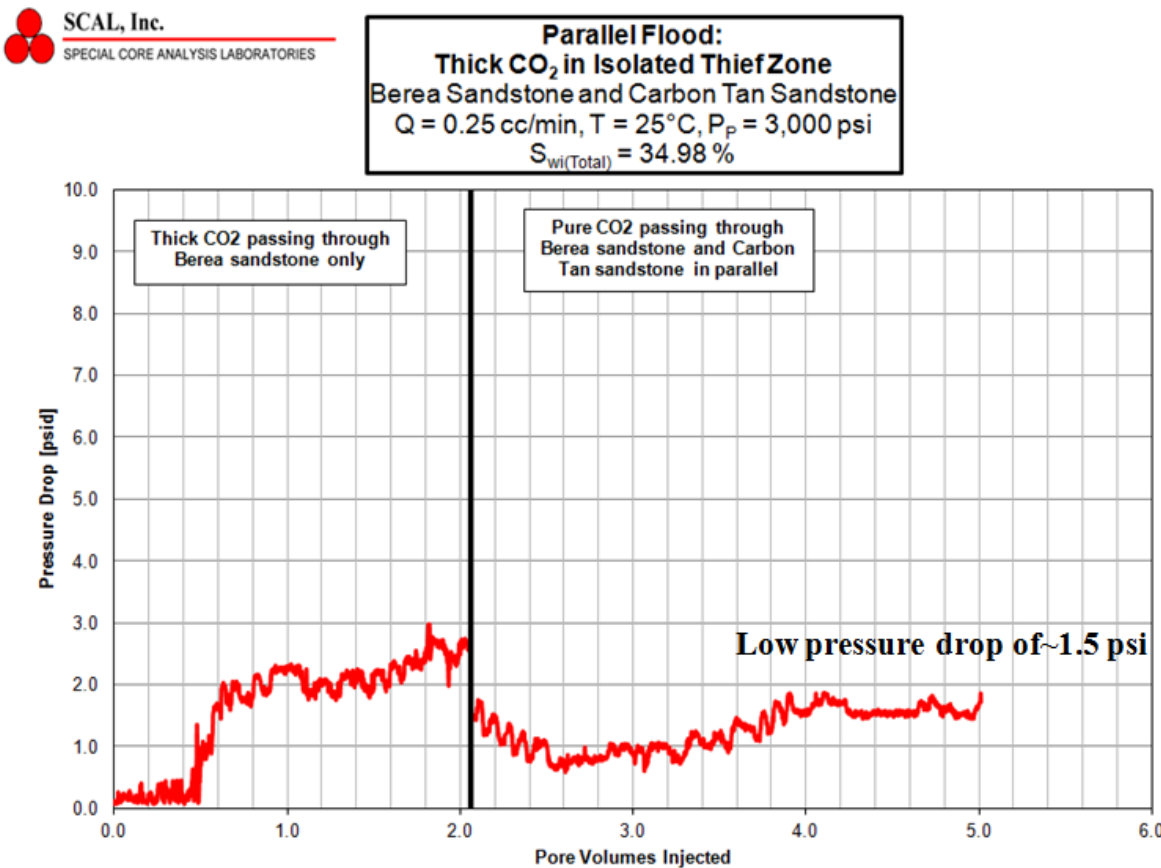
### **Sandstone cores, injection of 1%PFA in $\text{CO}_2$ into thief zone alone, then injection of $\text{CO}_2$ into thief zone core and low perm cores**



**Ideal conformance control result achieved; all  $\text{CO}_2$  diverted to Carbon Tan; only Carbon Tan produced brine after the Berea was treated**

Figure 10.7.14. Conformance control results for dual parallel brine-saturated sandstone cores; the high perm core was isolated and flooded with thickened  $\text{CO}_2$ , then pure  $\text{CO}_2$  was injected into both cores simultaneously

Because the lower perm Carbon Tan zone was isolated when the PFA-CO<sub>2</sub> solution was introduced to the higher perm Berea thief zone, it was not expected that the dramatic pressure drops would be observed. This was the case as shown in Figure 10.7.15; the pressure drop remained between 1-2 psi through this test.



### Reasonable pressure drop maintained for displacing brine from Carbon Tan

Figure 10.7.15. Pressure drop results for the dual parallel sandstone core conformance control test. The high perm core was isolated and flooded with thickened CO<sub>2</sub>, then pure CO<sub>2</sub> was injected into both cores simultaneously.

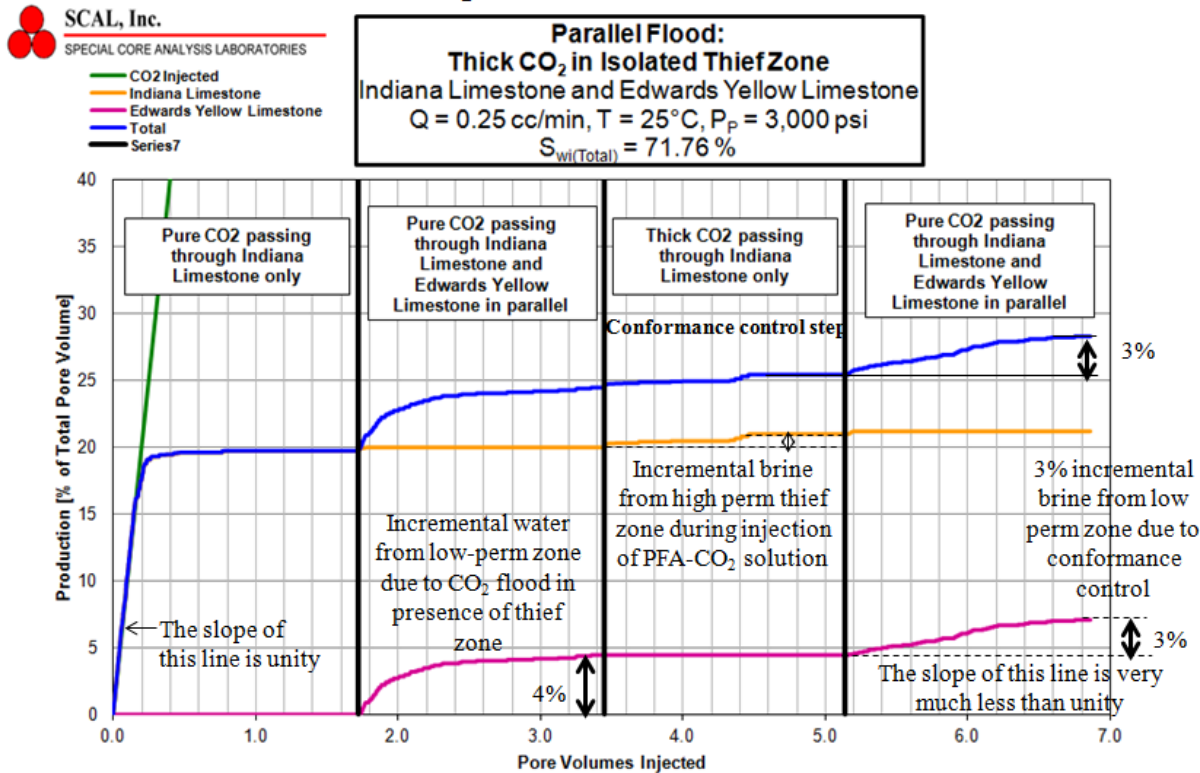
Figures 10.7.14 and 10.7.15 represent ideal conformance control results in that all of the CO<sub>2</sub> was diverted away from the PFA-treated thief zone, and because the low perm zone never “saw” PFA, the pressure drops associated with the diverted flow were commensurate with values expected for pure CO<sub>2</sub> flowing through a Carbon Tan core that did not have its permeability reduced by PFA.

In the following set of tests, the ability to achieve conformance control in dual parallel limestone cores was assessed. In an attempt to better simulate geologic history, the generation of a thief zone, CO<sub>2</sub> EOR prior to conformance control, the introduction of a conformance control agent, and the subsequent injection of CO<sub>2</sub> after conformance control,

- (a) both cores were initially saturated with brine,
- (b) CO<sub>2</sub> was injected only into the isolated high perm core until water production ceased to represent prolonged CO<sub>2</sub> flooding in a thief zone,
- (c) CO<sub>2</sub> was then injected into both cores simultaneously until water production ceased to represent CO<sub>2</sub> EOR with two parallel cores one of which was a watered-out, CO<sub>2</sub>-out thief zone,
- (d) thickened CO<sub>2</sub> (1 wt% PFA in CO<sub>2</sub>), which acts as a conformance control agent, was then injected into only the isolated high perm core, and
- (e) CO<sub>2</sub> was injected into both parallel cores until water production ceased.

The results are shown in Figure 10.7.16. After flooding the high perm Indiana limestone with brine-saturated core with  $\text{CO}_2$  until water displacement from that core was complete at 20% of the PV recovered, the subsequent  $\text{CO}_2$  flood of the parallel cores yielded an addition 4% PV brine recovered from the low perm Edwards yellow limestone (far left, Figure 10.7.16). During the subsequent conformance control step, the PFA- $\text{CO}_2$  solution was injected into the isolated Indiana core, yielding an addition 1% PV brine recovery. At the end of the conformance agent application step, brine recovery was at 25% PV. The subsequent injection of  $\text{CO}_2$  into the parallel cores yielded 3% additional PV recovery, all of which came from the low perm Edwards Yellow core. Both brine and  $\text{CO}_2$  were being produced from the Edwards yellow during this step. This two-phase flow was expected because (unlike the prior experiment with the dual sandstone cores), the parallel cores were both flooded with  $\text{CO}_2$  prior to the introduction of thickened  $\text{CO}_2$ .

### Injection of 1%PFA in $\text{CO}_2$ into thief zone alone, then injection of $\text{CO}_2$ into dual parallel limestone cores



Very good conformance control result achieved;  
only Edwards Yellow Limestone produced brine after the Berea was treated

Figure 10.7.16. Conformance control results for dual parallel brine-saturated limestone cores; the high perm core was isolated and flooded with pure  $\text{CO}_2$ , then both cores were flooded with pure  $\text{CO}_2$ , then only the isolated high perm core was flooded with thickened  $\text{CO}_2$  (PFA in  $\text{CO}_2$ ), and then both parallel cores were flooded with  $\text{CO}_2$

As was the case in the sandstone core test of conformance control via application of PFA- $\text{CO}_2$  to the isolated thief zone, the pressure drops associated with this test, shown in Figure 10.7.17, were reasonable because PFA had never entered the lower perm core into which the  $\text{CO}_2$  was diverted.

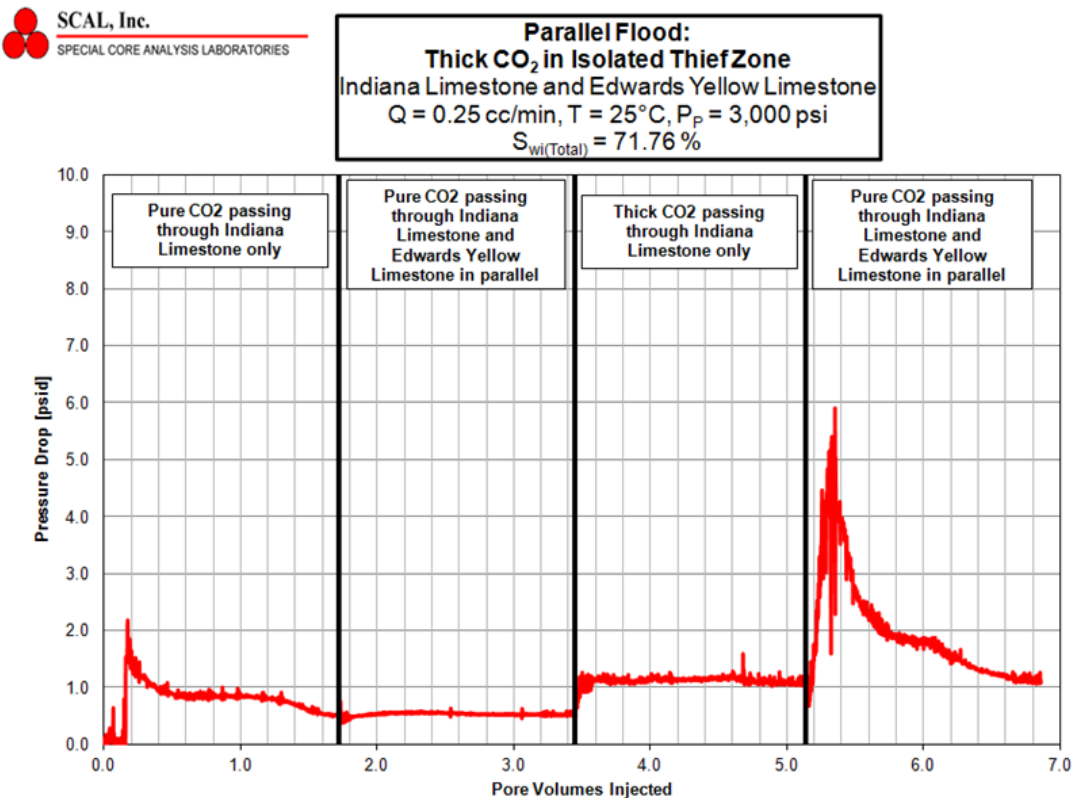


**Figure 10.7.17. Pressure drop results for dual parallel brine-saturated limestone cores; the high perm core was isolated and flooded with pure  $\text{CO}_2$ , then both cores were flooded with pure  $\text{CO}_2$ , then only the isolated high perm core was flooded with thickened  $\text{CO}_2$  (PFA in  $\text{CO}_2$ ), and then both parallel cores were flooded with  $\text{CO}_2$**

Figures 10.7.16 and 10.7.17 also represent very good conformance control results. 3% PV of incremental brine was displaced from the low perm core (from which only 4% PV brine had been previously recovered prior to conformance control), and the pressure drops associated with the diverted flow were commensurate with values expected for pure  $\text{CO}_2$  flowing through a low perm Edwards Yellow limestone core that did not have its permeability reduced by PFA.

Lesson learned from these dual core tests:

These results convincingly demonstrate that the best use for PFA is for near-wellbore conformance control. The PFA should be dissolved in  $\text{CO}_2$ , and the (PFA- $\text{CO}_2$ ) solution should be injected solely into the isolated thief zone. After this treatment neat  $\text{CO}_2$  can be injected into all of the layers, and the PFA treatment is likely to divert most of the  $\text{CO}_2$  that was formerly flowing into that thief zone toward the other layers.

## **10.8 Improved wellbore integrity via sealing small cracks with CO<sub>2</sub>-soluble polymers that block water, oil and gas**

### **Introduction**

Domestic petroleum resources that are vital to U.S. energy needs must be produced while effectively addressing environmental concerns. Therefore maintaining wellbore integrity is critically important, especially as wells are drilled in more complex environments like thin shale formations that require complicated multiple lateral horizontal wells that penetrate miles into the formation, and the ultradeep wells in the deepwaters of the Gulf of Mexico. Petroleum from these formations must be produced while preventing reservoir fluids from flowing anywhere other than into the production casing or liner. Traditionally, cement is pumped into the annulus between the casing and the rock layers to provide production zone isolation, casing support, and a barrier that prevents produced fluids from migrating into the annulus or into high permeability thief zones. Despite careful placement of cement or cement alternatives, cracks and fractures may still occur.

Typically, a cement squeeze is used for remediation of these defects; although well suited for the largest openings, the presence of small particles (1-100 microns) within the cement prevents it from sealing cracks with widths that are comparable in size to the particles. Solids-free epoxy resins (~100-1000 cp when fresh, prior to curing) are better suited for flowing into smaller cracks. Another option is the use of an emulsion (~100 - 500 cp) of polymerizing chemicals suspended in a carrier liquid; when displaced toward a small crack the carrier fluid passes through the crack while the emulsified droplets accumulate at the crack entrance and polymerize into a seal.

*The objective of the work conducted in this NETL project is to use an extremely low viscosity fluid for sealing cracks in casing cement.* The fluid is a single-phase, transparent solution of carbon dioxide (CO<sub>2</sub>) and a high molecular weight, amorphous, elastic, sticky, thermally stable polymer that is water-, oil-, and natural gas-repellant. Polyfluoroacrylate (PFA) is a unique polymer in that it is extremely hydrophobic and oil-phobic, yet soluble up to ~20wt% carbon dioxide (CO<sub>2</sub>) at ambient temperature and pressures at or above the “cloud point pressure”; for example the about 1450 – 1500 psi is required to dissolve PFA in CO<sub>2</sub> at 21°C. The viscosity of the CO<sub>2</sub>-PFA solutions containing up to several percent of PFA is in the 0.1 – 1.0 cp range; which is 2-5 orders of magnitude less viscous than cement, resin, or polymerizing emulsions. Therefore the CO<sub>2</sub>-PFA solution can enter and flow into and through extremely small cracks that are big enough to provide a pathway for natural gas leaks but small enough to hinder the use of the much more viscous cements, resins and emulsions. The CO<sub>2</sub>-PFA solution is not intended to seal very large cracks or voids.

Although the PFA polymer is very soluble in liquid or supercritical CO<sub>2</sub> as observed in a high pressure phase behavior cell, PFA exhibits a very strong tendency to adsorb onto cement and rock surfaces even at temperature and pressure conditions where one would otherwise expect it to remain in solution. Therefore in small cracks, where the ratio of area to volume is high, the effects of adsorption can be significant. Of course, if the pressure of the solution does drop below its cloud point value, then the PFA will begin to come out of solution in the crack via precipitation (in addition to the adsorption that is occurring).

Two proof-of-concept experiments have shown that when a CO<sub>2</sub>(99%)-PFA(1%) solution flows through an impermeable cement plug that has been cracked in half, exhibiting a permeability of only 81 nanoDarcy (in the first experiment) or 89 microDarcies (in the second experiment), the PFA strongly adsorbs on the *entire* surface area of the cement crack (not just the inlet to the crack) and seals it even though the fluid pressure within the entire crack remains above the cloud point. PFA also adsorbs onto sandstone or limestone surfaces, even if the surfaces are initially wet with water or oil. Because PFA is an amorphous, sticky polymer, it effectively flows into the rough surfaces of the crack and essentially glues the pieces of cement together; even if one attempts to remove the PFA with CO<sub>2</sub> after it has adsorbed, preliminary results have shown that the adsorbed polymer is unlikely to re-dissolve. The proposed technology of injecting CO<sub>2</sub>-PFA solutions into small cracks is *not* intended to replace the cement, resin, or polymerizing emulsions; rather the low viscosity CO<sub>2</sub>-PFA solutions are intended to provide operators with another wellbore integrity tool for sealing the smallest cracks that can degrade wellbore integrity.

If this concept is successful, it would provide oilfield operators with another vital tool for enhancing wellbore integrity that has been diminished by the formation of tiny cracks associated with the cement in the well annulus. Because the proposed solutions of 1-10wt% high molecular weight polymer in a low viscosity supercritical fluid solvent will retain a viscosity that is several orders of magnitude less than currently-used alternatives, this technology is best suited for the remediation of the smallest problematic cracks, while the remediation of the largest cracks and voids in cement can remain adequately addressed with cement, solid-free resin and emulsions.

### **Statement of the Problem**

Domestic petroleum resources that are vital to U.S. energy needs must be produced while effectively addressing environmental concerns. Therefore, maintaining wellbore integrity is critically important, especially as wells are drilled in more complex environments like thin shale formations that require complicated multiple lateral horizontal wells that penetrate miles into the formation, and the ultradeep wells in the deepwaters of the Gulf of Mexico. Petroleum from these formations must be produced while preventing reservoir fluids from flowing anywhere other than into the production casing or liner perforations. Traditionally, cement is pumped into

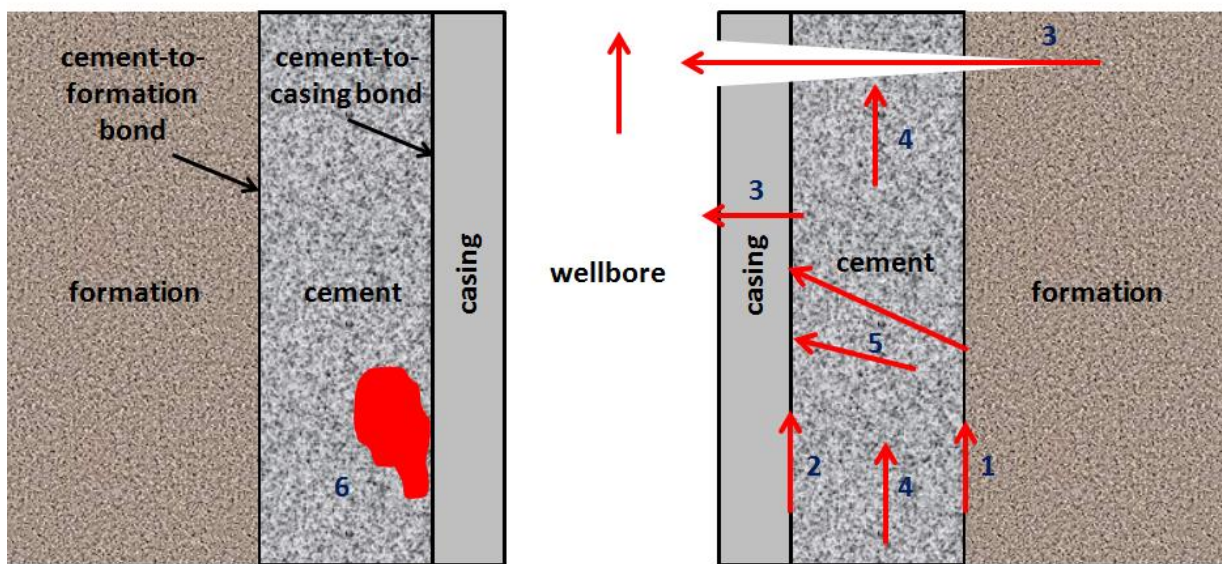
the annulus between the casing and the rock layers to provide production zone isolation, casing support, and a barrier that prevents produced fluids from migrating into the annulus or into high permeability thief zones or from generating a sustained casing pressure (SCP) at the wellhead. Ideally, after hardening the cement provides a resilient seal that does not contain any cracks or fractures. The cement should maintain its integrity throughout the annular column and there should not be any pockets where the cement did not flow. Further, the bond between the inner surface of the annular column of cement and the outer surface of the casing should be strong and free from gaps or cracks. Likewise, there should be a strong, leak-free adherence of the outer surface of the annular cement column with the rock formations that were drilled through.

In an effort to maintain the highest levels of wellbore integrity that provide a critical line of defense against uncontrolled releases of hydrocarbons into the environment, every effort is made to carefully place the cement in the annulus between the casing and rock formations as the well is being completed. There have also been new cement formulations that are designed to prevent the formation of cracks. For example, Schlumberger has developed several “self-healing” cements (Schlumberger 2010, Engelke et al. 2017) that provide enhanced protection against cracks that cause leaks and SCP at the wellhead. One of these self-healing products, referred to as FUTUR (Schlumberger 2010); if cracks form in the FUTUR, the subsequent flow of hydrocarbons through the crack will “activate” components within the cement to close the crack, thereby stopping the leak.

As an alternative to cement, various resins (epoxies, phenolics, furans) with resilient mechanical properties have been used to fill the annular gap between the casing and the rock. For example, due to the poor compatibility between traditional aqueous-based cements and synthetic-based drilling fluids (SBF’s) that may lead to poor casing-to-cement and formation-to-cement bonds, Halliburton developed an epoxy resin with tunable density and rheology and high compressive strength for deepwater well environments (Morris, et al. 2012). Hyperbranched epoxy resins have also been proposed (Teixeira et al. 2014). Halliburton has even developed modifications in well logging technology aimed at assessing the integrity of the resin based cement behind the production casing (Foianini et al. 2014). Given the attributes of cement and resin, it is not surprising that cement-resin blends have also been proposed, such as the ultralightweight cement slurry (90%) that was mixed with an epoxy resin (10%) used by Halliburton to reduce downhole losses during cementing while enhancing the mechanical properties of the set cement sheath (Bhaisora et al. 2015).

Despite these efforts, there are cases where defects can occur that reduce the integrity of the wellbore. A few of the pre-production problems that degrade wellbore integrity (Carey 2010) include incomplete cement placement that results in voids, cement shrinkage, failure to establish good casing-cement and cement-formation bonds, and contamination of the cement by drilling mud or reservoir fluids. During production, mechanical stresses can result in fractures, the

formation of a micro-annulus at the casing-cement interface, or the disruption of the bond between the cement and the formation that was drilled through. Geochemical-based reactions can result in corrosion of the metal casing and the degradation of the cement (Carey 2010). As a result, problematic pathways for the migration of reservoir fluids can form as depicted in Figure 10.8.1 [Carey 2010, Global CCS Institute 2017, Teodoriu et al. 2012], including poor cement-formation bonds, a micro-annulus adjacent to the exterior surface of the casing, openings that penetrate the casing, cracks within the cement itself, and fractures that extend completely through the cement.



Undesirable flow paths include (1) gaps between the formation and the cement; (2) the micro-annulus between the cement and outside of the casing; (3) fractures passing through the wall of the casing into the wellbore ; (4) cracks within the cement itself; (5) radial fractures in the cement that extend to the formation; and (6) voids or pockets where the cement did not flow. (this figure is not drawn to scale)

Figure 10.8.1 Cement defects that can lead to wellbore integrity failures (after After Carey et al. 2010)

There are several technologies that are used to deal with these problems, as illustrated in Figure 10.8.2.

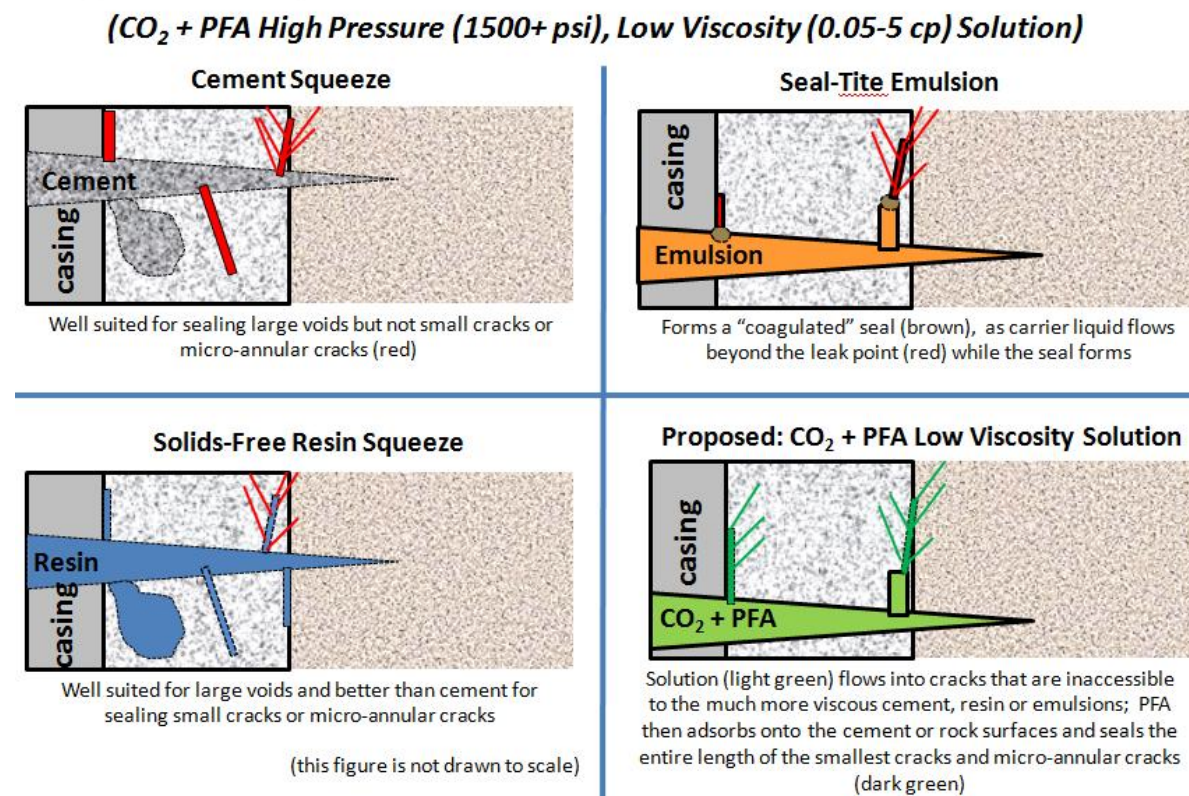


**Figure 10.8.2 Unique role for new sealant for cracks**

A cement squeeze is the most common remedial method used to restore wellbore integrity, especially for voids and cracks that are significant in size (Figure 10.8.2, upper left). Typically, the problematic area is identified by cement logs, and cement slurry is pumped through an opening in the casing (either a corrosion defect, casing split, or a perforation) into the voids using a Bradenhead technique or a squeeze that uses packers to isolate a short length of the casing. With respect to the properties of the fresh cement, it has a density of roughly 1.9 g/ml and contains particles in the 1 – 100 micron size range (Ferraris 2004; Dahl et al. 1993). The rheology of cement slurries is highly dependent on temperature, water/cement ratio and the type of admixture used, but in general they commonly exhibit Bingham plastic viscosities of roughly 10 – 100 cp at 23°C as measured in rheometers with large gaps (Shahriar, 2011; Nehdi, 2012; Odiete, 2015 ; Memon 2014, Abbas 2014); obviously these slurries harden to form solids. Cement squeezes are particularly well suited for large holes and voids, but the slurry is unable to flow into micro-channels primarily due to particle bridging and filter cake formation. The amount of cement that is squeezed into the voids is approximately the same volume as the void space that can be filled.

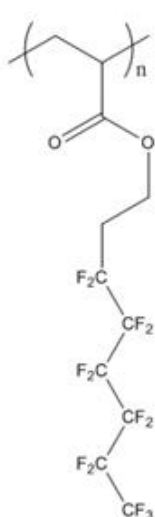
Another remediation technology is a resin squeeze (Figure 10.8.2, lower left). The approach is similar to that used in cement squeezes, but in this case a liquid hydrocarbon-based epoxy is injected. In addition to the favorable mechanical properties of the cured epoxy, the fresh, liquid epoxy can be formulated to be solids-free, therefore facilitating its flow into smaller cracks and crevices that could not be filled with cement. With respect to the properties of the fresh epoxide resin, it has a density of about 1.1 g/ml and contains hardening agents. The epoxide resin may also contain optional accelerating and weighting agents, and typically exhibits a viscosity of roughly 100 cp to several thousand cp. In general, one injects a volume of resin that corresponds to the volume of targeted openings and the resin cures when in place, forming a resilient solid.

Another option for improving wellbore integrity that is designed to stop leaks of hydrocarbon fluids passing through small cracks has been developed by Seal-Tite (Figure 10.8.2, upper right). Although the exact composition of their product is proprietary, their literature (Rusch et al. 1999, 2004a,b,c, 2005; Mendoza et al. 2000; Offshore Source 2006; Oil & Gas Tech. 2006; Chivvis et al. 2009) provides a general description. Seal-Tite's product for micro-annular repairs is composed of a liquid resin and liquid curing agent that, when mixed, form an opaque emulsion (~1.3 g/ml) of suspended droplets of monomers, oligomers, polymers, and polymerizing chemicals (initiators and crosslinkers) carried in a liquid. If the emulsion is flowing through large openings where there is little pressure drop and the width of the crack is greater than the size of the droplets, the emulsion simply flows through. However, at the leak site associated with very small cracks, the carrier liquid passes through the crack while the suspended droplets, which are comparable in size to the size of the opening are retained. This results in the monomers, polymers and polymerizing agents accumulating to a high enough concentration for polymerization and crosslinking to occur, forming a flexible solid seal. Because a relatively large pressure drop occurs at the leak site where the components are forming the flexible polymeric seal, the emulsion is referred to as "pressure activated". For smaller cracks that yield gas leaks a solution with a viscosity of ~100 cp at 23°C is prepared, while a more viscous solution of 200 – 500 cp is prepared for liquid leaks. Injection of slightly more than one pore volume of the emulsion occurs ("pore volume" is the estimated volume of the void up to the restriction where the leak occurs) because some of the carrier liquid leaks past the point where the seal is forming until the seal cures and blocks the opening.

### **Novel Crack-sealing Technology Presented in this Quarterly Report**

The objective of the preliminary tests conducted during this project was to conduct only two proof-of-concept tests for a new technique for sealing cracks in cement. The solution is a high pressure, low viscosity solution of the polyfluoroacrylate polymer shown in Figure 10.8.3 dissolved in CO<sub>2</sub>.

## PFA, Polyfluoroacrylate, a CO<sub>2</sub>-soluble polymer



**Polyfluoroacrylate (PFA) – a CO<sub>2</sub>-soluble (1500+ psi) high molecular weight, completely amorphous, elastic, extremely sticky polymer that is water-repellant, and oil-repellant; Tg 6°C**

Figure 10.8.3. The PFA polymer structure, appearance, and properties

This new technique is intended to complement cement squeezes by providing a method that is effective for sealing very small cracks, where other methods, such as resin squeezes and the application of polymerizing emulsions, may not be very effective. Therefore, this CO<sub>2</sub>-polymer solution could be ideally suited for the remediation of extremely small cracks in casing cement; cracks so small that the other remediation solutions may not be capable of accessing them, yet large enough to provide pathways for undesirable natural gas or crude oil migration.

Figure 10.8.2 (lower right) illustrates that a dilute solution (1 – 20wt%) of the polymer would be injected into large openings in the casing; the CO<sub>2</sub> – polymer solution is not intended to block or seal these large voids. However, because the viscosity of this fluid can be as low as 0.05 cp, the CO<sub>2</sub> – polymer solution will flow into even the smallest cracks. Although the polymer is soluble in liquid CO<sub>2</sub> that is at a pressure of about 1500 psi or more, the polymer strongly partitions into an extremely viscous polymeric coating phase as it adsorbs onto the surfaces of sandstone, limestone or cement regardless of what fluid (if any) was originally residing in the opening. The adsorption of this polymer is most effective in the closure of cracks with very small gaps.

Two proof-of-concept tests (which will be described in the remainder of this report) conducted in a core apparatus shown in Figure 10.8.4 demonstrated that a PFA seal is deposited within the

crack; as this seal is forming the polymer-depleted CO<sub>2</sub> leaks farther into the crack. In these experiments, the cement crack was sealed via the injection of a few “pore volumes” a dilute solution (1wt%) of the polymer in CO<sub>2</sub> (the “pore volume” is the volume of the crack). The sticky polymer is highly hydrophobic and oil-phobic, and the sealed crack is impermeable to natural gas, crude oil or brine. *Therefore, this new technology may be ideally suited for the remediation of cracks with substantial permeability to natural gas and/or liquids but which are too small to be plugged using rapidly-pumped materials with viscosities that far exceed those of the formation fluids.* Hence, developing and demonstrating the use of the proposed plugging material is a significant advance in the enhancement of wellbore integrity.

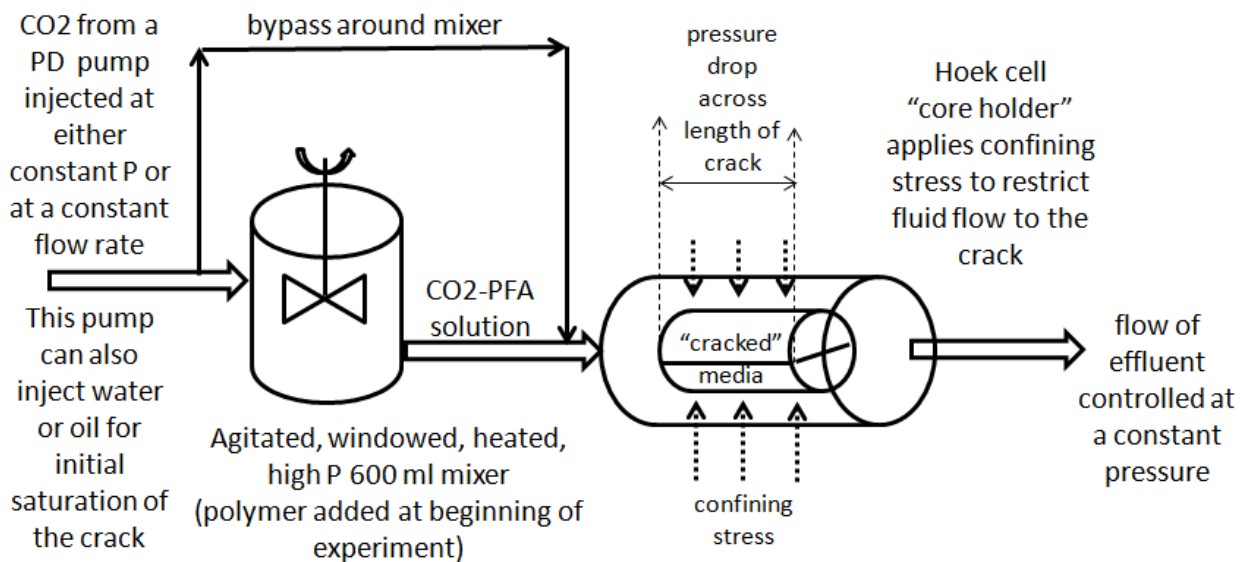


Figure 10.8.4. Experimental apparatus used to conduct crack-sealing proof-of-concept experiments

### Proof-of-Concept Results

Two proof-of-concept tests were conducted at SCAL using the same core flooding apparatus that was used for the experiments with sandstone and limestone cores, as illustrated in Figure 10.8.4. Each proof-of-concept experiment was conducted at 23°C to determine if a CO<sub>2</sub>-PFA solution could penetrate cracked cement with an extremely low apparent permeability and seal the crack. It was hypothesized that if PFA adsorption onto cement occurred, then the deposited PFA layer could actually seal the crack along its length (rather than just at the entrance to the crack).

In the first test, a 6” long, 2” diameter Portland cement plug was made, and its permeability was determined to be below the detection limit of the equipment. The cement cylinder was then sawn in half, and the two halves were carefully placed together and inserted into the rubber

sleeve of a high-pressure core holder. After applying a confining pressure of 5000 psi, pure CO<sub>2</sub> was injected using an inlet pressure of 4500 psi and outlet pressure of 3000 psi, and a steady-state flow rate of 0.0075 ml/min was established, as shown in Figure 10.8.5. This indicates a permeability of 0.000081 mD (0.081 micro Darcy, 81 nano Darcy) based on the entire cross-sectional area of the plug. A solution of CO<sub>2</sub> – 1%PFA was then introduced to the cracked cement at the same conditions. After injection of only 2 ml of the solution (containing about 0.02 gr PFA) at a constant pressure drop of 1500 psi, the flow through the cracked cement became immeasurably small indicating a seal had been formed (Figure 10.8.5).

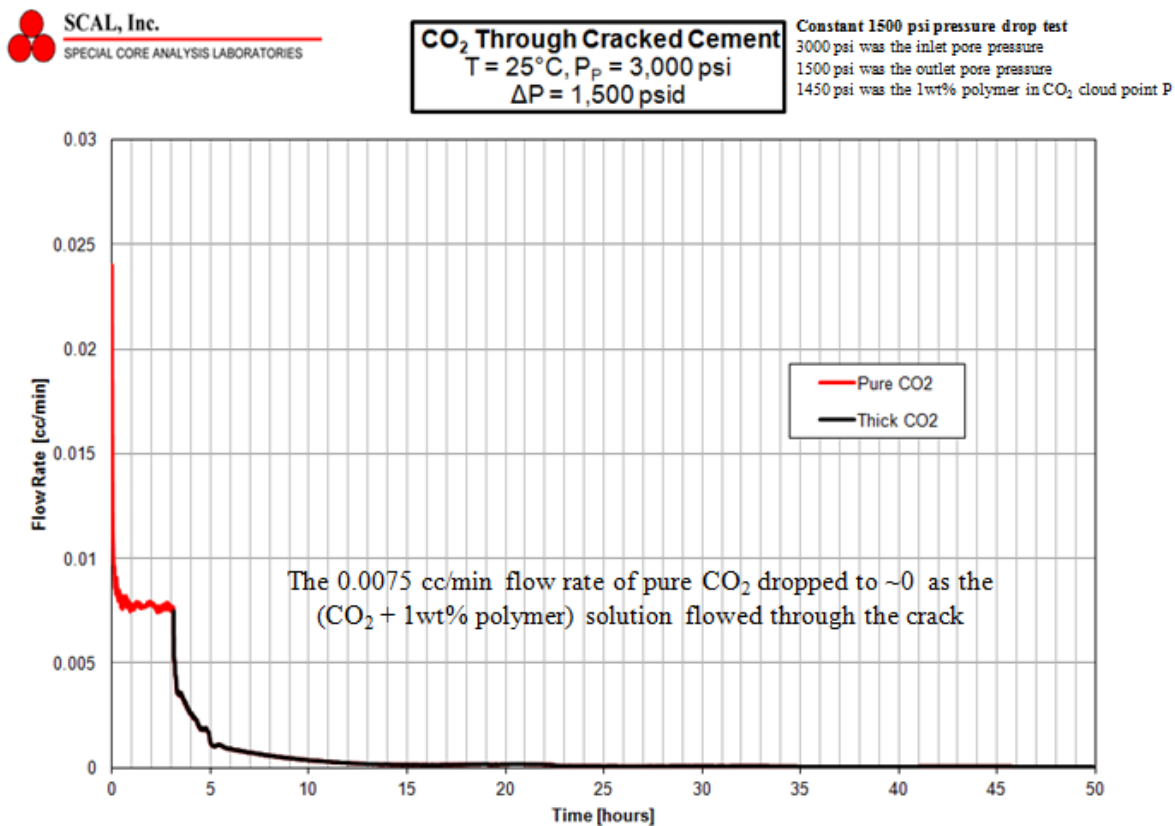


**Figure 10.8.5. Flow rate vs time data for the injection of the CO<sub>2</sub>+PFA solution into the 81 nanoDarcy crack at a constant pressure drop of 1500 psi (outlet P maintained at 1500 psia)**

After the experiment, it was observed that the cement halves were “glued” together by the adsorbed PFA. After prying the halves apart (Figure 10.8.6), it was noted that water “beaded up” anywhere a droplet was placed on the flat surfaces. Further, the relatively thicker portions of the PFA film appeared as a sticky white or yellow coating over most of the cement crack surfaces, as seen in Figure 10.8.6.

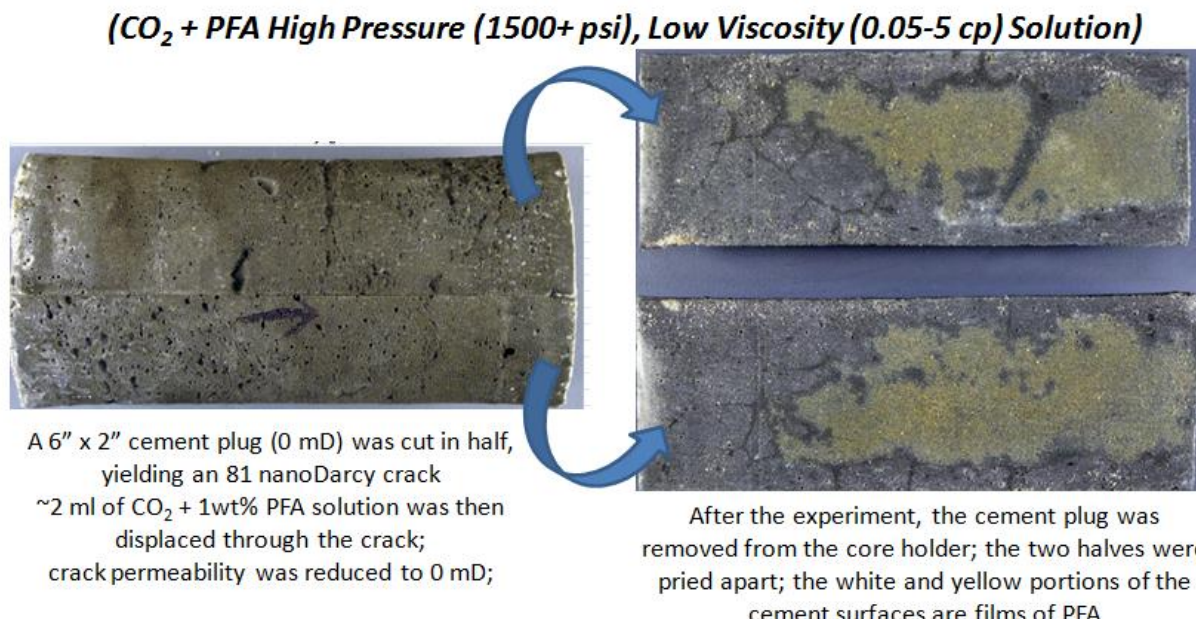


**Figure 10.8.6. Appearance of the (81 nanoDarcy cracked cement after the test before (left) and after being pried apart**

In the second test, a 6" long, 2" diameter Portland cement plug was made, and its permeability was determined to be below the detection limit of the equipment. The cement cylinder was then sawn in half, and the two halves were carefully placed together with a thin layer of unconsolidated 100 mesh sand between the halves and inserted into the rubber sleeve of a high pressure core holder. After applying a confining pressure of 5000 psi, pure CO<sub>2</sub> was injected at a constant flow rate of 0.25 ml/min with the core outlet pressure maintained at 1500 psi. A steady-state flow rate pressure drop of 60 psi was established for pure CO<sub>2</sub>, as shown in Figure 10.8.7. This indicated a permeability of 0.089 mD (89 micro Darcy) based on the entire cross-sectional area of the plug. A solution of CO<sub>2</sub> – 1%PFA was then introduced to the cracked cement at the same conditions. After injection of only 2.5 ml of the solution (containing about 0.025 gr PFA), the pressure drop attained the highest permitted level of 1500 psi (at which point the inlet pressure attained 4500 psi, which was 500 psi less than the overburden pressure, Figure 10.8.7), therefore the test was stopped. At this point the permeability of the crack had been reduced 25-fold to a value of 3.25 microDarcies.

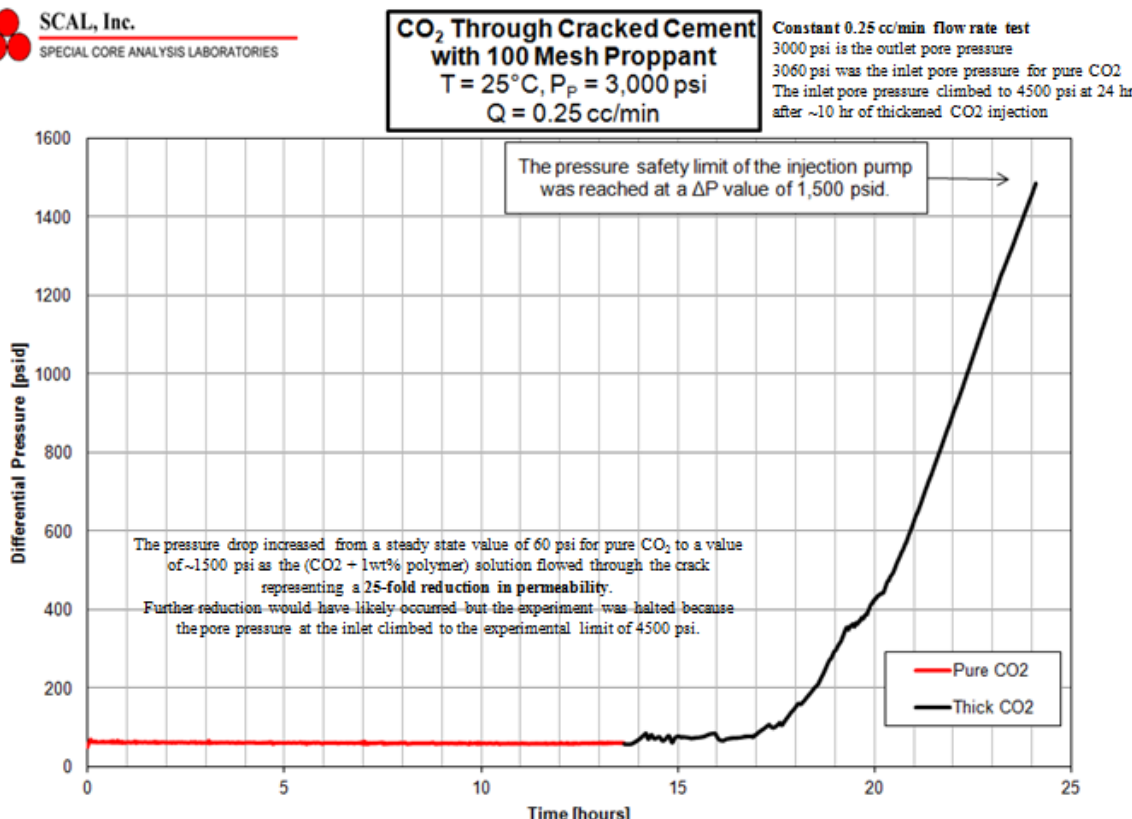


**Figure 10.8.7.** Flow rate vs time data for the injection of the CO<sub>2</sub>+PFA solution into the 89 microDarcy crack at a constant flow rate of 0.25 ml/min (outlet P maintained at 1500 psia)

After the experiment, it was observed that the cement halves were “glued” together by the adsorbed PFA, as seen in Figure 10.8.8. After prying the halves apart, the sand was attached to one of the two halves by a thin film of PFA.

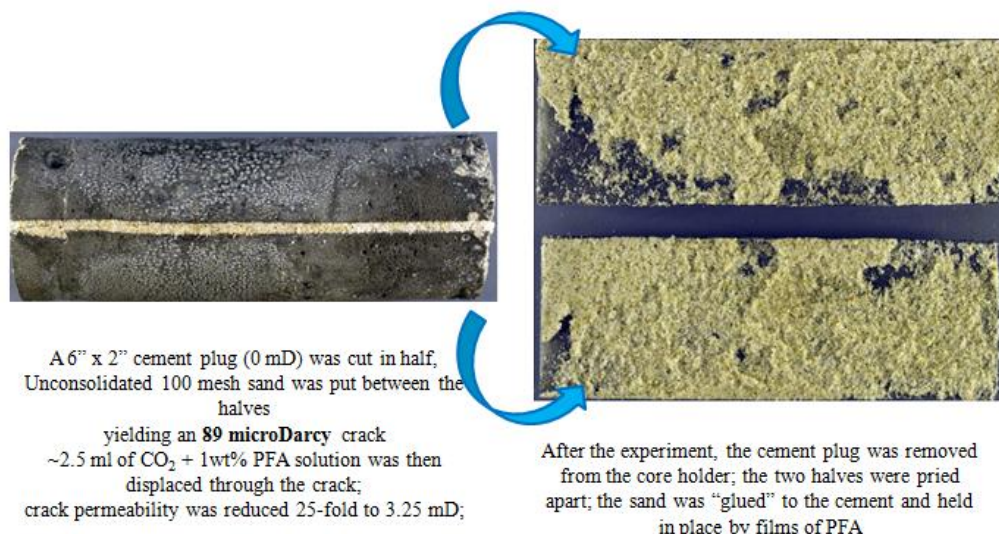


**Figure 10.8.8.** Appearance of the (89 microDarcy) cracked cement after the test before (left) and after being pried apart

No PFA adsorption proof of concept test has been performed on cracks between cement and steel (analogs to microannular cracks). However, none of the 1/8" stainless steel tubing or fittings through which the CO<sub>2</sub>-PFA solution passed during the proof-of-concept tests described in the previous paragraphs became clogged by PFA. All metal surfaces *were* coated with a thin film of PFA, however, as evidenced by the high degree of hydrophobicity of these surfaces after the experiment was complete.

### Potential Benefits of this Technology

If future studies on this topic are promising, it could lead to the new technique for sealing very small cracks, as illustrated in Figure 10.8.9. The defective portion of the casing would need to be isolated with a packer straddle system and then the CO<sub>2</sub> + polymer solution would have to pass through either (1) a defect/hole in the casing or (2) a perforation made for remediation in order to flow into the cracks associated with the cement. The polymer would adsorb onto the rock surface while forming a seal.

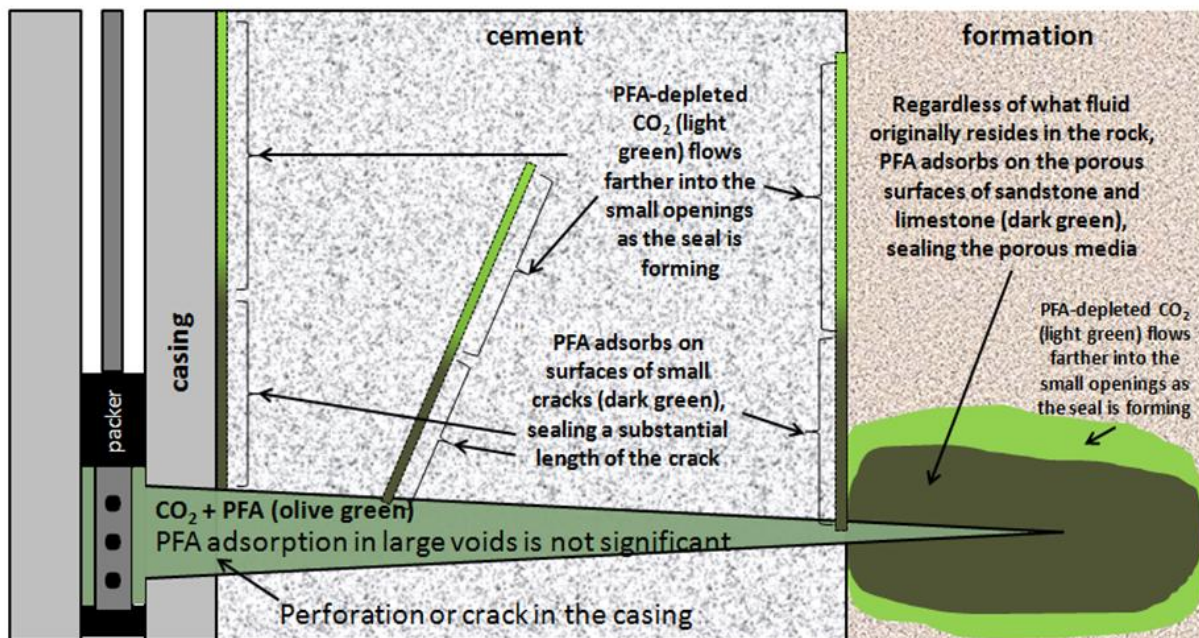


**Figure 10.8.9. Conceptual diagram for application of the CO<sub>2</sub>+PFA solution to seal cracks or reduce permeability of porous media for conformance control**

In the following section the potential merits (i.e., impacts/benefits) of the proposed research in comparison to current state of knowledge or technology or current commercial and emerging technologies related to *deepwater well integrity technologies* will be summarized.

*Enhanced wellbore integrity:* The injection of a supercritical solution of a PFA-based polymer in CO<sub>2</sub> will certainly provide the oil industry with a remarkably low viscosity fluid for sealing small cracks. This fluid is not designed or intended to fill large gaps or voids in cement; conventional cement squeezes and resin squeezes are more appropriate. However, because the proposed “CO<sub>2</sub> squeeze” fluid is orders of magnitude less viscous than any of the conventional treatments (cement, resins, polymerizing emulsions), it will have the ability to not only block the entrance to small cracks, but it will also be able to penetrate deep within these cracks and seal them completely.

*Remarkable polymer properties:* The proposed polymer has remarkable properties that make it an excellent choice for sealing cracks, namely it is sticky, highly hydrophobic, highly oil-phobic and uniquely CO<sub>2</sub>-soluble.

*Resolving environmental barriers:* Polymers such as those in this proposal made using the -C<sub>6</sub>F<sub>13</sub> fluorinated side chain chemistry enjoy global regulatory approval in a wide variety of applications and are safe and effective replacements for the older C<sub>8</sub>F<sub>17</sub>-based water repellent articles especially because data in non-human primates indicate that they have substantially shorter half-lives in these animals than the PFOA degradation products associated C<sub>8</sub>F<sub>17</sub>-based products and are less toxic than long-chain PFCA chemicals. Therefore in 2013 the EPA affirmed that compounds containing C<sub>6</sub>F<sub>13</sub> groups would not be targeted by EPA’s 2009 Long-Chain Perfluorocarbon Action Plan Proposal (Poston and Connell 2013).

*High polymer cost is offset by low polymer amount:* PFA and similar polymers are expensive because the fluorinated monomers used to form them are expensive. For example, bulk quantities of the fluoroacrylate monomer can be expected to cost \$40/lb. An order-of-magnitude estimate of the polyfluoroacrylate polymer made from this monomer would be roughly \$100/lb. However, the proposed research is likely to demonstrate that a relatively small amount of polymer will be required to seal these cracks. For instance our only proof-of-concept result (Figures 10.8.5-8), demonstrated that in order to seal a 12 in<sup>2</sup> crack, 0.02 gr of PFA was required. This corresponds to about 0.00025 gr PFA/cm<sup>2</sup> crack area, or 2.5 gr/m<sup>2</sup>, or \$0.50 of PFA/m<sup>2</sup> crack area.

### **Uniqueness of this concept**

The topic of sealing cracks in cement with supercritical fluids containing dissolved polymers was searched in the Society of Petroleum Engineers OnePetro database, the Web of Science, SciFinder, Google and Google patent. As directed in the FOA, the offshore portfolio of 2008-2016 Ultra-Deepwater Program research projects was reviewed, along with the Dept. of Interior Bureau of Safety and Environmental Enforcement website. No references were found. In

addition, all of the members of our proposed advisory team have already been contacted and none of them knows of a comparable wellbore integrity technology to the one that we have proposed. There are several references for prior work that bear some similarities to our proposed work, but these older projects remain fundamentally different than our CO<sub>2</sub>-PFA solutions and are inferior for the proposed application of sealing cracks. For example, there is a 2001 DuPont patent (Tuminello and Wheland 2001) in which amorphous fluorinated polymers like PFA were described as having the potential to dissolve in CO<sub>2</sub>, and to then be sprayed through a (pressure-reducing) nozzle that causes the CO<sub>2</sub> to evaporate as a vapor while a mist of fine fluoropolymer droplets falls upon building stone surfaces to provide a weather- and pollution-resistance barrier for preservation. This technology can only be applied via spray to a surface of a rock exposed to a de-pressurized CO<sub>2</sub>-polymer mixture; our proposal involves the high pressure adsorption of PFA onto rock surfaces deep within cement cracks. Another example is a Feb 14, 2011 article in “The Engineer”, a UK electronic journal, which describes (in no meaningful detail) an effort led by Mehran Sohrabi of Heriot-Watt University to dissolve an additive in the CO<sub>2</sub> that “will automatically precipitate as a sealant when the gas density drops”. No other peer-reviewed, non-peer-reviewed, or patent documents could be found related to this technology. This technology was intended to provide a self-sealing way to stop leaks of CO<sub>2</sub> into the caprock during sequestration. However, there is no indication that this additive is a sticky, high molecular weight, amorphous polymer that can effectively adsorb onto and into the irregular surfaces of small cracks. Further, the article is described the “additive” coming out of solution due to a pressure drop that causes the CO<sub>2</sub>-additive solution to fall below its cloud point. Our own research team has identified a *dozen* highly CO<sub>2</sub>-soluble solid additives that will come out of solution due to a pressure drop, mostly tert-butylated benzene compounds and sugar acetates, and precipitate as solids upon pressure reduction. (Enick, et al. 2005; Miller et al. 2012). *None* of these compounds is a sticky, high molecular weight, amorphous polymer, however; each is a high melting point granular solid that would have difficulty sealing cracks. In our proposed work, the high molecular weight sticky polymer sealant will come out of solution *even at and above its cloud point* due to its strong tendency to interact thermodynamically with the cement surface. Of course, the PFA-based polymers would also come out of solution and seal the cracks if the pressure falls below the cloud point pressure.

## 11. References

**Abbas**, G.; Irawan, S.; Kumar, S.; Memon, K.; Khalwar, S.; J of Ap. Sciences 14 (11) 2014, 1154-1160

**Bhaisora**, D.; Aly, A.; Morsy, A.; Shamma, H.; EI Nashar, R.; Eldin, S.; Karim, E.; IPTC-18504-MS, 2015.

**Carey**, B., Los Alamos National Laboratory, 2010,

**Chivvis**, R.; Julian, J.; Cary, D.; SPE 120978, SPE Western regional meeting, March 24-26, 2009

**Dahl**, J.; Harris, K.; Leinan, A.; The Journal of Canadian Petroleum Technology, Nov 1993, 32(9) 25-27

**DeSimone**, J.M.; Guan, Z.; Elsbernd, C.; Science, 1992, 257 (14), 945-947

**Doherty**, M., Lee, J.; Dhuwe, A.; Cummings, S.; O'Brien, M.; Perry, R.; Beckman, E.; Enick, R.; Energy and Fuels, 2016, IF 2.8, 30, 5601-5610, IF 2.8

**Enick**, R., Hong, L., Thies, M., Journal of Supercritical Fluids Vol 34/1, 11-16, 2005

**Engelke**, B.; de Miranda, C.; Daou, F.; Peterson, D.; Aponte, S.; Oliveira, F.; Ocando, L.; Conceicao, A.; Guillot, D.; SPE/IADC 184641, 2017, SPE/IADC Drilling Conference, March 14-16, The Netherlands

**Foianini**, I.; Frisch, G.; Jones, P.; SPWLA 55<sup>th</sup> Annual Logging Symposium, May 18-22, 2014.

**Global CCS Institute**, Generic failure models for well integrity under exposure to CO<sub>2</sub>, accessed 2017,

**Huang**, Z.; Shi, C.; Kilic, S.; Xu, J.; Beckman, E., Enick, R., Macromol. 33, No. 15, 2000, 5437-5442.

**Jones**, P.; Karcher, J.; Ruch, A.; Beamer, A.; Smit, P.; Hines, S.; SPE 167759, 2014.

**Jones**, P.; London, B.; Tennison, L.; Karcher, J.; SPE 165699, 2013.

**Luna-Barcenas**, G.; Mawson, S.; Takishima, S.; DeSimone, J.; Sanchez, I.; Johnston, K. Fluid Phase Equilibria 146, 1998, 325-337

**Mawson**, S.; Johnston, K. P.; Combes, J. R.; DeSimone, J.M.; Macromolecules, 1995, 28, 3182-3191

**McClain**, J.B.; Betts, D.E.; Canelas, D.A.; Samulski, E.T.; DeSimone, J.M.; Landona, J.D.; Wignall, G.D.: proceedings of the 1996 Spring meeting of the ACS, Division of Polymeric Materials, New Orleans, LA: Science and Engineering, Vol. 74, pp. 234–235.

**Memon**, K.; Shuker, M.; Memon, M., Lashari, A.; Abbas, G.; J of Ap Sciences 14 (11) 2014, 1204-1209

**Mendoza**, M.; Hernandez, J.; Rusch, D.; SPE 59026, SPE Int Pet Conf and Exhibition, Feb 1-3., 2000

**Miller**, M.; Wei, B., Luebke, D., Enick, R., JSCF, 61, 212-220, Jan 2012

**Morris**, K.; Deville, J.; Jone, P.; SPE 155613, 2012.

**Nehdi**, M.; Shahriar, A., Construction Materials 165(1) 25-44, Feb 2012

**NIST webbook**, Thermophysical properties of fluid systems, accessed March 2017, Michael J. O'Brien, Robert J. Perry, Mark Doherty, Jason Lee, Aman Dhuwe, Eric Beckman, Robert Enick, *Anthraquinone Siloxanes as Thickening Agents for Supercritical CO<sub>2</sub>*, Energy & Fuels, April 2016, 30, 5990-5998, IF 2.8

**Odiete**, W.; Iyagba, E.; Int J Curr Sci 2015 (14) 70-73

**Offshore Source**; April 2006, page 30

**Oil & Gas Technology**, pressure-activated sealants, Sept 11, 2006, 28-31

**Poston**, T.; Connell, K.; Daikin presentation, October 2013

**Rusch**, D.; Ellis, B.; SPE 55996, SPE Western regional Meeting, May 26-28, 1999

**Rusch**, D.; Romano, M.; SPE 91400, SPE Eastern Regional Meeting, Sept 15-17, 2004

**Rusch**, D.; Sabins, F.; Aslakson, J.; SPE 91399, SPE Eastern Regional Meeting Sept. 15-17, 2004.

**Rusch**, D.; SPE 88566, SPE Asia Pacific Oil and Gas Conference, Oct 18-20, 2004

**Rusch**, D.; Slezak, M.; Spring Conf of the Soln Mining Research Inst, April 17-20, 2005, Syracuse, NY

**Schlumberger**; FUTUR Self-healing cement technology for long-term zonal isolation, 2010

**Shahriar**, A.; PhD thesis, Univ. of Western Ontario, 2011

**Shen, Z.**, McHugh, M., Xu, J., Belardi, J., Kilic, S., Mesiano, A., Bane, S., Karnikas, C., Beckman, E., Enick, R.; Polymer 44, 2003, 1491-1498

**Teixeira G.**; Lomba, R.; Fontoura, S.; Melendez, V.; Ribeiro, E.; SPE-170266-MS, 2014

**Teodoriu, C.**; Kosinowski, C.; Amani, M.; Schubert, J.; Shadravan, A.; Int J Eng Ap Sc, 2013, 2(2) 1-13

**Tuminello, W.**, Wheland, R. US Patent 6,767,626,

**Washington, J.**, Jenkins, T., Environmental Science & Technology, 2015, 49, 14129-14135.

**Washington, J.**, Jenkins, T., Rankin K., Naile, J., Env. Science & Technology, 2015, 49, 915-923.

**Xu, J.**; Wlaschin, A.; Enick, R.; SPE Journal 8(2) June 2003, 85-92

**Zhang, D.**; Advances in Petroleum Exploration and Development, 8(2) 2014, 29-32